# UNIVERSITY OF PADUA


## Department of Clinical and Experimental Medicine

**International PhD in Arterial Hypertension and Vascular Biology**
**in collaboration with the Charité Universitätsmedizin Berlin**
**and the Medical University Gdansk**
**XXI CICLE**


# ROLE OF INFLAMMATION IN THE DEVELOPMENT OF LUNG FIBROSIS AND IN THE PATHOGENESIS OF PULMONARY HYPERTENSION


**Coordinator: Ch.mo Prof. Gianpaolo ROSSI, MD**

**Tutor: Ch.mo Prof. Carlo AGOSTINI, MD**

**PhD student: Dott.ssa Cristina GATTAZZO**


**March 2009**

# INDEX

# ABBREVIATIONS

| | |
|---|---|
| **AMs** | Alveolar Macrophages |
| **APC** | *Adenomatous polyposis coli* protein |
| **ANA** | Anti-Nuclear Antibody |
| **APC** | Antigen Presenting Cell |
| **BCR** | B Cell Receptor |
| **BLM** | Bleomycin |
| **CBP** | CREB Binding Protein |
| **CI** | Confidence Interval |
| **CK2** | Casein Kinase 2 |
| **CCR** | Chemokine Receptor |
| **COPD** | Chronic Obstructive Pulmonary Disease |
| **CTGF** | Connective Tissue Growth Factor |
| **CXCL** | CXC chemokine |
| **CXCR** | Chemokine CXC Receptor |
| **CXR** | Chest X Radiograph |
| **DLCO** | Diffusing capacity of the Lung for Carbon Monoxide |
| **ECM** | Extracellular Matrix |
| **EMT** | Epithelial–Mesenchymal Transition |
| **FGF-2** | Fibroblast Growth Factor 2 |
| **FRAT/GBP** | Frequently Rearranged in advanced T-cell lymphomas/GSK-3 binding protein |
| **FVC** | Forced Vital Capacity |
| **FXA** | Activated Factor X |

| | |
|---|---|
| **GATA-3** | GATA Binding Protein 3 |
| **GM-CSF** | Granulocyte-Macrophage Colony-Stimulating Factor |
| **GSK-3** | Glycogen Sintetase Kinase 3 |
| **HP-NAP** | Neutrophil-activating protein of *Helicobacter pylori* |
| **HRCT** | High Resolution Chest Radiography |
| **IFN-γ** | Interferon γ |
| **Ig** | Immunoglobulin |
| **i.p.** | Intraperitoneally |
| **i.v.** | Intravenously |
| **IIPs** | Idiopathic Interstitial Pneumonias |
| **IL** | Inter Leukin |
| **ILDs** | Interstitial Lung Diseases |
| **IPF** | Idiopathic Pulmonary Fibrosis |
| **IRF1** | Interferon Regulatory Factor 1 |
| **LD** | Lethal Dose |
| **MAPK** | Mitogen-Activated Protein kinase |
| **MCP** | Monocytes Chemoattractant Protein |
| **MHC-II** | Major Histocompatibility Complex II |
| **MIP-2** | Macrophage Inflammatory Protein 2 |
| **MMPs** | Matrix Metallo Proteinases |
| **MNC** | Mono Nucleate Cells |
| **LPS** | bacterial Lipopolysaccharides |
| **NK** | Natural Killer cells |
| **OVA** | Ovalbumin |
| **PAH** | Pulmonary Arterial Hypertension |

| | |
|---|---|
| **PAI-1, PAI-2** | Plasminogen Activator |
| **PH** | Pulmonary hypertension |
| **P(I)3K/Akt** | Phosphatidylinositol 3-Kinase |
| **$PGE_2$** | Prostaglandin E2 |
| **PDGF** | Platelet-Derived Growth Factor |
| **PKA** | Protein Kinase A |
| **PKC** | Protein Kinase C |
| **STAT** | Signal Transducer and Activator of Transcription protein |
| **TCF/LEF** | T-Cell Factor/ Lymphoid Enhancer-binding Factor-1 |
| **TCR** | T Cell Receptor |
| **T-bet** | T box expressed in T cells |
| **TGF- β** | Transforming Growth Factor- β |
| **Th1/Th2** | T helper type1 and T helper type 2 lymphocytes |
| **TLRs** | Toll like receptors |
| **TDZD** | Thiadiazolidinones |
| **TIMPs** | Tissue Inhibitors of Metallo Proteinases; |
| **TNF-α** | Tumor Necrosis Factor-α |
| **TNF-β** | Tumor Necrosis Factor-β |
| **TNFR** | Tumor Necrosis Factor Receptor |
| **UV** | Ultraviolet radiation |
| **VEGF** | Vascular Endothelial Growth Factor |

# ABSTRACT

**Background:** The bleomycin is a glycopeptide with antitumor and antiviral activity utilized in clinical for chemotherapeutic treatment of several neoplasms. Unfortunately the 10% of treated patients develops interstitial pneumonia that progresses to fibrosis. The fibrogenesis is linked to develop of a Th2 cellular response with proinflammatory chemokines release.

Glycogen Synthase Kinase 3 (GSK-3) is a pivotal element for the control of immune response because modulates the inflammatory cytokines production. Since lung injury caused by bleomycin is characterized by an inflammatory response followed by a fibrotic degeneration, we postulated that blocking GSK-3 kinase activity with a specific inhibitor could affect the bleomycin-induced pulmonary inflammatory and pro-fibrotic cytokine network. Moreover it has been demonstrated that the develop of pathologies which elicit a Th2 inflammatory response could be mitigated by agents able to induce a Th1 immune response. Indeed administration of Neutrophil-Activating Protein of *Helicobacter pylori* (HP-NAP) was found to be able to down modulate the Th2 immune response in a asthma ovalbumin-induced model mouse by eliciting a Th1 immune response and resulted effective in preventing allergic asthma in the model mouse.

**Purpose of the study:** We investigated the effects of the specific and selective ATP-competitive GSK-3 inhibitor, SB216763, and the effects of HP-NAP administration on the onset and development of inflammation and fibrosis in a bleomycin-induced lung fibrosis mouse model.

**Methods:** We differently randomised cohorts of C57BL6 mice to receive intratracheal instillation of inhibitor SB216763, HP-NAP, bleomycin, bleomycin plus SB216763 or bleomycin plus HP-NAP and followed their health status for 28

days. Bronchoalveolar lavage (BAL) was performed and mice were sacrificed at different interval times (2, 7, 14 and 28 days). Histopathological analysis of the lungs, flow-cytometry studies and Cell Sorting of BAL pulmonary monocytes were then performed. Finally we examined cytokines gene expression levels in lung monocytes trough Real Time PCR analysis.

**Results:** SB216763 and HP-NAP administration prevented lung inflammation and the subsequent fibrosis when co-administrated with bleomycin. BALF analysis of mice revealed a significant reduction in bleomycin-induced alveolitis. SB216763 treatment was associated with a significantly lower production of inflammatory cytokines (TNF-α and CCL12) by macrophages. Moreover we observed that HP-NAP administration downmodulated the Th2 inflammatory response bleomycin-induced by eliciting a Th1 phenotype (downmodulating IL-4 chemokine and upregulating the IFN-γ).

**Conclusions:** These findings suggest that GSK-3 inhibition induces a protective effect on lung fibrosis triggered by bleomycin and candidate GSK-3 as a potential therapeutic target for preventing pulmonary fibrosis. Furthermore our results suggest that also HP-NAP, preventing lung fibrosis develop, might be a possible new tool for therapeutic strategies aimed to redirect Th2 into less aggressive Th1 response.

# RIASSUNTO

**Background:** La bleomicina è un glicopeptite con attività antitumorale e antivirale utilizzata in clinica come chemio-terapico per il trattamento di diversi tumori. Sfortunatamente il 10% dei pazienti trattati sviluppa polmonite interstiziale che progredisce in fibrosi. La fibrogenesi è collegata allo sviluppo di una risposta immunitaria di tipo Th2 accompagnata dal rilascio di chemiochine pro-infiammatorie.

La Glicogeno Sintetasi Chinasi 3 (GSK-3, Glycogen Synthase Kinase 3) è un fattore centrale per il controllo della risposta immunitaria poiché modula la produzione di citochine infiammatorie. Visto che il danno polmonare è caratterizzato da una risposta infiammatoria seguita da una degenerazione fibrotica, noi abbiamo ipotizzato che l'inibizione dell'attività di GSK-3, tramite uno specifico inibitore, potrebbe influenzare l'infiammazione del polmone ed il *network* di citochine pro-infiammatorie indotti dalla bleomicina. Recentemente è anche stato visto che lo sviluppo di patologie sostenute da un'infiammazione di tipo Th2 possono essere mitigate da agenti in grado di indurre una risposta infiammatoria di tipo Th1. In accordo con questi risultati la proteina attivante i neutrofili, prodotta dal batterio *Helicobacter pylori* (HP-NAP), stimolando una risposta immunitaria di tipo Th1, si è dimostrata capace di modulare la risposta immunitaria di tipo Th2 indotta dall' ovalbumina in un modello murino di asma, risultando quindi efficace nel prevenire lo sviluppo dell'asma allergica.

**Scopo dello studio:** In questa ricerca abbiamo investigato gli effetti della somministrazione dell'inibitore SB216763, specifico per GSK-3, e della somministrazione della proteina HP-NAP nello sviluppo dell'infiammazione e della fibrosi nel modello murino di fibrosi polmonare indotta da bleomicina.

**Metodi:** Differenti coorti di topi C57BL6 sono state randomizzate per ricevere instillazione di SB216763, HP-NAP, bleomicina, bleomicina più SB216763 o bleomicina più HP-NAP, ed il loro stato di salute è stato monitorato per 28 giorni. I topi sono stati sacrificati ed i lavaggi broncho alveolari (BALs) eseguiti a diversi intervalli di tempo (a 2, 7, 14 e 28 giorni). Quindi sono stati eseguiti l'analisi istopatologia dei polmoni e valutazioni citoflurimetriche del BAL. Infine sono stati esaminati, tramite Real Time PCR, i livelli di espressione genica delle citochine nei monociti di polmone purificati dai BALs tramite sorting.

**Risultati:** La somministrazione dell'inibitore SB216763 e della proteina HP-NAP, quando co-somministrati con la bleomicina, sono stati in grado di prevenire l'instaurarsi dell'infiammazione e il conseguente sviluppo di fibrosi nel polmone. L'analisi dei BALs ha infatti rivelato una significativa riduzione dell'alveolite indotta dalla bleomicina. Il trattamento con l'SB216763 si è associato con una ridotta produzione, da parte di macrofagi, di citochine infiammatorie (TNF-α and CCL12), mentre la somministrazione di HP-NAP ha *down*-modulato la risposta infiammatoria di tipo Th2 indotta dalla bleomicina, stimolando il tipo Th1(diminuendo il livello di espressione delle chemiochina IL-4 ed aumentando invece quello di IFN-γ).

.**Conclusioni**: I risultati ottenuti in questo progetto di ricerca suggeriscono che l'inibizione di GSK-3 ha un effetto protettivo nella fibrosi polmonare indotta dalla bleomicina e candidano GSK-3 come potenziale *target* terapeutico per prevenire la fibrosi polmonare; inoltre suggeriscono che la proteina HP-NAP, prevenendo lo sviluppo della fibrosi polmonare tramite l'induzione di una risposta di tipo Th1, potrebbe essere una nuova strategia terapeutica per ridirezionare la risposta infiammatoria dal fenotipo Th2 verso quello meno aggressivo Th1.

# 1. INTRODUCTION

## 1.1 INTERSTITIAL LUNG DISEASES

Interstitial lung diseases (ILDs) are a diverse group of lung diseases that are characterized by chronic inflammation and progressive fibrosis of pulmonary interstitium. The interstitium is defined as the alveolar walls (including epithelial cells and capillaries), septae, and the perivascular, perilymphatic and peribronchiolar connective tissues.

There are over 200 ILDs (Figure 1.1). They can be broadly classified into the following categories: ILDs with a known etiology, such as those due to occupational/environmental factors, drugs, hypersensitivity reactions and infections; ILDs associated with systemic disorders, such as sarcoidosis and collagen vascular disorders; and rare miscellaneous conditions, such as eosinophilic granuloma and the idiopathic interstitial pneumonias (IIPs).

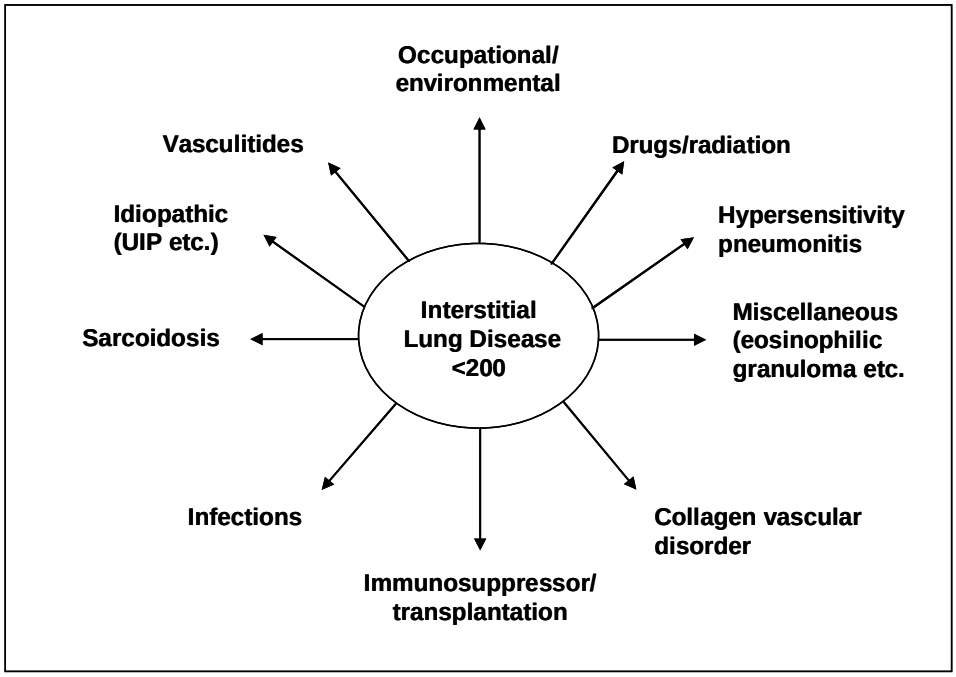


**Figure 1.1 Classification of ILDs.**

The fibrosing ILDs have certain clinical and pathologic features in common. The common clinical features include progressive dyspnea on exertion, nonproductive paroxysmal cough, abnormal breath sounds on auscultation, abnormal findings on chest radiograph (CXR) or high-resolution CT (HRCT) scan, restrictive pulmonary physiology with decreased vital capacity and diffusing capacity of the lung for carbon monoxide (DLCO) and widened alveolar-arterial oxygen pressure difference[1].

## 1.2 THE IDIOPATHIC PULMONARY FIBROSIS

The Idiopathic Pulmonary Fibrosis (IPF), the most common form of IIPs (55-60%)[2], is a chronic disease characterized by scar tissue within the lungs, in the absence of known provocation. Exercise-induced breathlessness and chronic dry cough are the prominent symptoms.

### 1.2.1 Epidemiology

The incidence and prevalence of IPF are difficult to determine because uniform diagnostic criteria have only recently been defined[3] (Table 1). The data from around the world demonstrates that IPF favours no particular race, ethnic group or social environment. It is estimated that IPF effects at least 5 million persons worldwide, with an incidence of approximately 10.7 *per* 100,000 persons for men and 7.4 *per* 100,000 persons for women[4,5]. The incidence increases with age. Most commonly the symptoms appear between the fifth and the seventh decades of life, with two-thirds of all cases arising in patients over 60 years of

age, in fact the mean age at presentation is 66 years old[2]. It also appears that, during the last decade, the incidence of IPF was on the rise[6].

**Table 1. IPF classification**

| | | |
|---|---|---|
| 1. | UIP (Usual Interstitial Pneumonia) | 55% |
| 2. | NSIP (Non Specific Interstitial Penumonia) | 25% |
| 3. | COP (Cryptogenic Organizing Pneumonia) | 3% |
| 4. | AIP (Acute Interstitial Penumonia) | <1% |
| 5. | RBILD (Respiratory bronchiolitis-associated Interstitial Lung Disease) | 15% |
| 6. | DIP (Desquamative Interstitial Pneumonia) | <1% |
| 7. | LIP (Lymphoid Interstitial Pneumonia) | 1% |

Familial cohorts of IPF are described, though sporadic cases constitute the majority of disease. Clinical features of familial IPF are indistinguishable from those of sporadic form, excepting for an earlier age of onset[7]. Familial IPF is defined as two or more verified cases within a group of relatives belonging to a primary family unit. Familial IPF accounts for 0.5 to 2% of all cases of IPF and lung inflammation has been identified in unaffected members of families with IPF[8].

### 1.2.2 Clinical description

IPF patients experience breathlessness upon exertion and are often bothered by a dry cough. The onset of symptoms is low, but symptoms became progressively worse over time. Retrospective analysis of IPF patients suggests that symptoms precede diagnosis by a period of 6 months to 2 years[9]. Symptoms such as weight loss, fever, and athralgias are unusual in IPF, whereas gastro-oesophageal acid reflux is present in close to 90% of patients, but often occurs without symptoms[10]. Auscultation of the lungs reveals early inspiratory crackles, predominantly located in the lower posterior lung zones upon physical exam. These rales have a fine acoustic character reminiscent of

the sound made by *velcro*. Clubbing is found in approximately 50% of patients with IPF. There are no other physical manifestations, unless cor pulmonale has developed in association with end-stage disease. In that case, classic signs of right heart failure may be present. The examination of patients with IPF should attempt to identify those signs suggesting an alternative diagnosis such as systemic sclerosis or polymyositis that can be associated with secondary pulmonary fibrosis. To that end, the examiner should look for sclerodactily, scleroderma, proximal muscle weakness and telangiectasias[11].

There are no specific laboratory abnormalities in IPF. However, mild elevation of the erythrocyte sedimentation rate, a low-positive titer of anti-nuclear antibody (ANA) and/or low-positive rheumatoid factor can be seen and are thought to represent a general state of inflammation. In advanced disease, blood counts may reveal polycythemia. The natural history of IPF is incompletely known. IPF usually assumes a course of relentless physiologic deterioration. However, some patients remain stable for extended periods and individual outcomes can be highly variable[9]. Still, long-term survival with biopsy proven IPF is not expected. The median survival time, demonstrated in recent studies using the modern definition of IPF, is between 2 and 5 years, counting from the time of diagnosis[12-15]. New insight into the natural history of IPF has been gleaned from secondary analysis of the placebo groups assembled for recent multi-center clinical trials[16-18]. It appears that three potential clinical courses exist: a) slowly progressive disease (the most common); b) disease marked by episodic acute exacerbations; and c) rapidly progressive disease[9]. At present, there are no means for accurately predicting the clinical course. Nevertheless, acute exacerbations deserve special attention.

Noteworthy pulmonary hypertension has been reported to occur in 32 to 84% of patients with IPF. The exact prevalence remains unclear because triggers for the evaluation of pulmonary pressures and the best method to detect pulmonary hypertension in IPF remain unsettled[19]. Diffusion capacity is strongly correlated with pulmonary hypertension, being inversely related[20,21]. However, the severity of restrictive physiology has little bearing on the prevalence or degree of pulmonary hypertension. Several studies have demonstrated a lack of correlation between pulmonary artery pressure and forced vital capacity (FVC)[20-22]. Right-heart catheterization is the best diagnostic test for pulmonary hypertension but the implementation of such invasive testing is difficult to justify in the absence of data demonstrating a benefit to treatment of pulmonary hypertension in IPF. Still it is clear that the presence of pulmonary hypertension in IPF adversely affects survival[23].

### 1.2.3 Etiology

The term "idiopathic" suggests there are no known causes for IPF. However, an environmental etiology for IPF is supported by evidence from several sources[24]. In fact a relationship between environmental exposures and IPF is plausible, has been consistently demonstrated by case-control studies and is analogous to known disease, such as asbestosis, in which environmental material is associated with pulmonary fibrosis. Indeed cigarette smoking is consistently associated with IPF. A recent study of familial pulmonary fibrosis looked at 309 affected individuals and after adjusting for age and sex, this cohort demonstrated a strong association between smoking and IPF (odds ratio [OR], 3.6; 95%

confidence interval [CI], 1.3–9.8)[25]. Several intriguing reports suggest also the involvement of herpes virus and/or hepatitis C virus in the etiology of IPF[26-28]. However, another study demonstrated viral infection limited to IPF patients receiving corticosteroids, suggesting that infection is simply a marker of immunosuppression rather than an etiologic agent of fibrosis[29].

### 1.2.4 Pathogenesis

The pathogenesis of pulmonary fibrosis is complex and not well characterized. The currently accepted paradigm proposes that injury to the alveolar epithelium is followed by a burst of pro-inflammatory and fibro proliferative mediators that invoke responses associated with normal tissue repair. For unclear reasons, these repair processes never resolve, a chronic inflammation stimulates an aberrant damage repairing response and a progressive fibrosis ensues (Figure 1.2).

Repair of damage tissue is a normal and fundamental biological process that allows the ordered replacement of dead or injured cells during inflammatory response, a mechanism that is crucial for survival. Tissue damage can result from several acute or chronic stimuli, including infections, autoimmune reactions and mechanical injury. The repair process involves two distinct stages: a regenerative phase, in which injured cells are replaced by cells of the same type and there is no lasting evidence of damage; and a phase known as fibroplasia or fibrosis, in which connective tissue replaces normal parenchymal tissue[30].

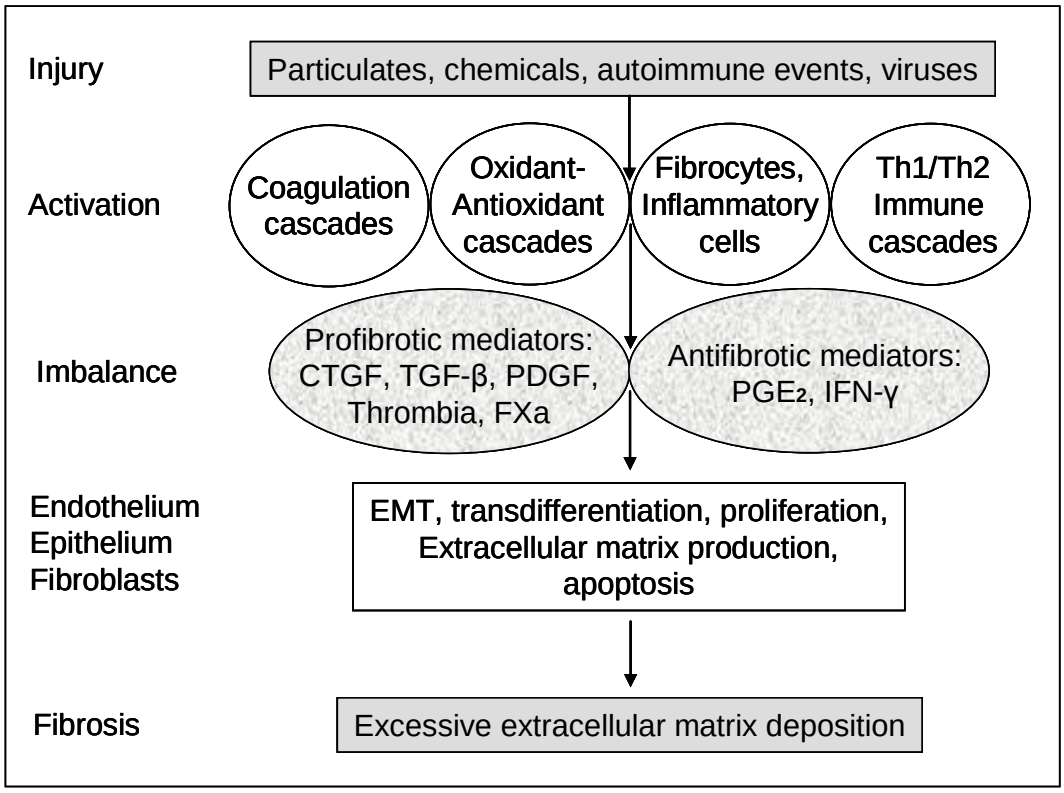


**Figure 1.2 A new model for the pathogenesis of idiopathic pulmonary fibrosis**. Injury activates multiple inflammatory, cell signalling and repair pathways. Activation of these cascades causes an imbalance in pro- and antifibrotic mediators. In turn, these mediators activate multiple cell types, causing changes in cellular functioning and cell–cell interactions that ultimately result in progressive fibrosis. Th: T-helper cell; CTGF: connective tissue growth factor; TGF-ß: transforming growth factor-ß; PDGF: platelet-derived growth factor; FXa: factor Xa; PG: prostaglandin; IFN-γ: interferon-γ; EMT: epithelial–mesenchymal transition.

In most cases, both stages are required to slow or reverse the damage caused by an injurious agent. However, although initially beneficial, the healing process can become pathogenic if it continues unchecked, leading to considerable tissue remodelling and the formation of permanent scar tissue. In some cases, it might ultimately cause organ failure and death. Fibrotic scarring is often defined as a wound-healing response that has gone away[30].

Crucial in this process are the complex interactions among the immune system cells, the cells of alveolus-capillary membrane and cells of pulmonary interstitium (epithelial cells, endothelial cells and fibroblasts). The interaction among these different cell populations and their mediators culminate in a damage of the pulmonary parenchyma, in a persistent deposit of extra cellular matrix and

finally in fibrosis. However the initial stimulus for the recruitment of inflammatory cells, the mechanism responsible of the chronic inflammation and fibrosis are not well understood. Inhaled agents, such as virus or toxins, may induce an excessive inflammatory response which primes the extravasations of activated lymphocytes and ends in a pulmonary damage.

An aberrant expression of MHC-II proteins from alveolar epithelial cells, endothelial cell and alveolar macrophages could promote an exuberant antigenic presentation and the activation of immune system cells could lead to perpetuation of the chronic inflammation. With the proceeding of the chronic inflammation, occur the apoptosis of epithelial cells, the neo angiogenesis and an important increasing of fibroblasts, which infiltrate the interstitium and cause an accumulation of granulation tissue due to excessive production of the extracellular matrix[30].

## 1.3 THE ROLE OF INFLAMMATION IN THE PULMONARY FIBROSIS

The role of inflammation in the pulmonary fibrosis is still debated, even if several data suggest that the inflammation plays a pivotal role in the genesis of this pathology.

Some studies, *in vitro* on murine lung, proposed that IPF likely results from an aberrant activation of alveolar epithelial cells after injury that provokes the migration, proliferation, and activation of mesenchymal cells with the formation of fibroblastic/myofibroblastic foci, leading to the fibrotic reaction without inflammation[31] (Figure 1.3).

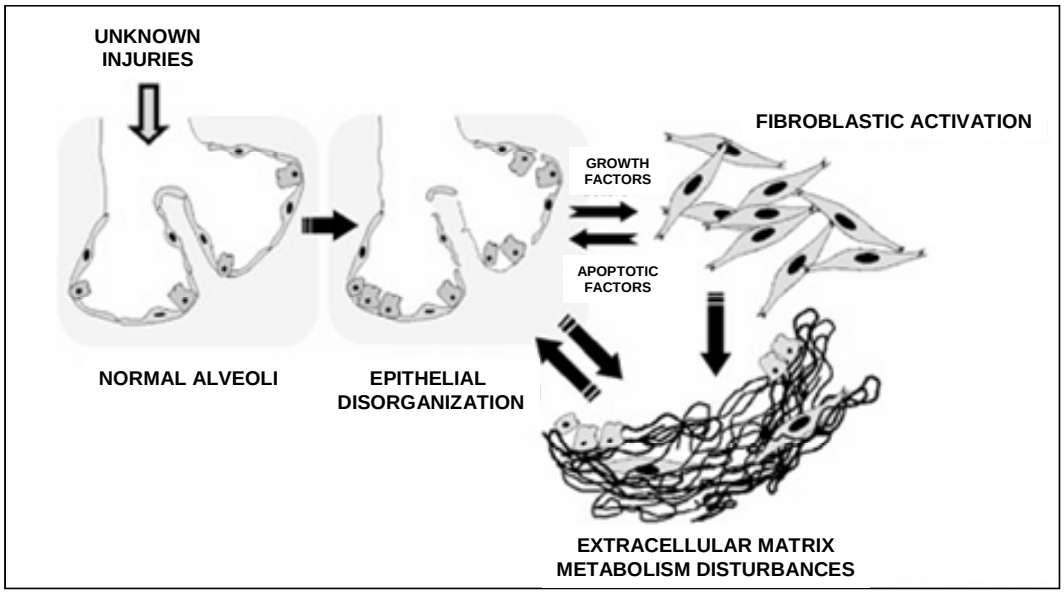


**Figure 1.3 Hypothetical scheme of the abnormal wound healing model for idiopathic pulmonary fibrosis.** Hypothetical scheme of the main pathogenic events in IPF/UIP. Unknown insults provoke multiple microscopic foci of epithelial damage and stimulation. Activated alveolar epithelial cells release factors inducing fibroblast migration and proliferation and changes in cell phenotype. In the microenvironment of the lesion, myofibroblasts can induce epithelial cell apoptosis and basement membrane disruption, thus contributing to abnormal re-epithelialization and perpetuation of a vicious circle. Finally, fibroblasts/myofibroblasts secrete excessive amounts of extracellular matrix components and a disequilibrium between MMPs and TIMPs means that matrix degradation does not occur. The final result is an aberrant remodeling of the lung parenchyma[31].

In this model the final result of IPF is an aberrant tissue remodelling, characterized by excessive deposition of connective tissue with the consequent progressive destruction of the lung parenchyma to form fibrotic honeycomb lesions. The molecular mechanism behind this abnormal remodelling are poorly understood, but the lost of a regulated turnover involves, at least, two families of proteins: the matrix metalloproteinases (MMPs) and tissue inhibitors of metalloproteinases (TIMPs). Recent evidence suggests that profound changes in MMP and TIMP expression and localization take place in the IPF lung microenviroment[31,32]. These studies demonstrate an upregulation of collagenase-1 (MMP-1) and both gelatinases (MMP-2 and MMP-9), as well as the four TIMPs.

However, several studies suggest that fibrosis is the end result of chronic inflammatory reactions induced by a variety of stimuli including persistent infections, autoimmune reactions, allergic responses, chemical insults, radiation,

and tissue injury[32]. Inflammation is also recognized to be a contributor to the pathogenesis of idiopathic pulmonary hypertension (PH), that occurs to 80% of patients with IPF[19,33]. Perivascular inflammatory cell infiltrates are found in lungs from patients with PH and Compared to healthy controls, patients with idiopathic or associated PH exhibit higher circulating levels and pulmonary expression of various inflammatory cytokines and chemokines including interleukin-1beta (IL-1β), IL-6 and monocyte chemoattractant protein (MCP-1)[9,34,35]. In recent studies of patients with COPD, we found that pulmonary artery pressure correlated positively with the circulating levels of two cytokines, namely, IL-6 and MCP-1[36]. Moreover, a close relationship was found between the G(-174)C polymorphism of the IL-6 gene and the severity of PH in patients with COPD[37].

Moreover studies on model mouse of bleomycin-induced pulmonary fibrosis underlighted that an active inflammatory response invariably precedes the fibrotic response[38] and that fibrogenesis is strictly connected to the development of a response mediated by T CD4+ Th1 type cells[39]. Finally the analysis of lung tissue of patients with IPF revealed an increased expression of Th2 type inflammatory cytokines/chemokines with respect to the Th1 type mediators.

### 1.3.1 The Th1/Th2 system

The immune system developed to protect against infection of pathogens and self alteration such as neoplastic transformation. The immune system is organized in Innate Immune System and Adaptive Immune System. The innate immune system is the first defence against microorganisms that are recognised in a non-specific way by macrophages, polymorfonucleates cells and the

complement system. The activation of innate immune system determines the release of inflammatory cytokines. Adaptive immune responses are antigen-specific and develop when the innate immune response is unable to control the infection. The adaptive immune system is composed of highly specialized systemic cells and processes that eliminate or prevent, in a specific way, pathogenic challenges. Important mediators of adaptive immune system are B and T cells which recognize through specific receptor (BCR, TCR) the antigens. Depending on the type of infection, is activated a cell-mediated immune response or an humoral immune response[40]. The lymphocyte T helper (Th) target the immune response *versus* the adaptive or innate cascade. When the T cells interact the first time with the Ag are induced to differentiate in a Th1 or Th2 way, so far activating a specific chemo-cytokine network (Figure 1.4)[41]. The Th1 lymphocytes stimulate IFN-γ, IL-2, and TNF-β, mediate the defence against intracellular microorganism (Th1 type immunity) and favour the isotopic switch to the IgG2-α immunoglobulins.

Differently, the Th2 lymphocytes secrete IL-4, IL-13, IL-15, IL6, IL-10 and IL-9 and are necessary to stimulate an humoral immune response against extracellular pathogens (Th2 immunity), stimulating the isotopic switch to IgG1 and IgE immunoglobulins[42]. The most important factors involved in the Th1 and Th2 differentiation are the IL-12 and IL4. IL-12 induces the phosphorylation of transcriptional factor STAT-4, inducing its activation, and in turn promoting the develop and differentiation *versus* Th1 response. The activation of transcriptional factor STAT-6, downstream IL-4, instead, is essential for differentiation in Th2 response. In fact, model mouse knock-out for STAT-4 and STAT-6 resulted impaired respectively in the develop of Th1 and Th2 immune response[43].

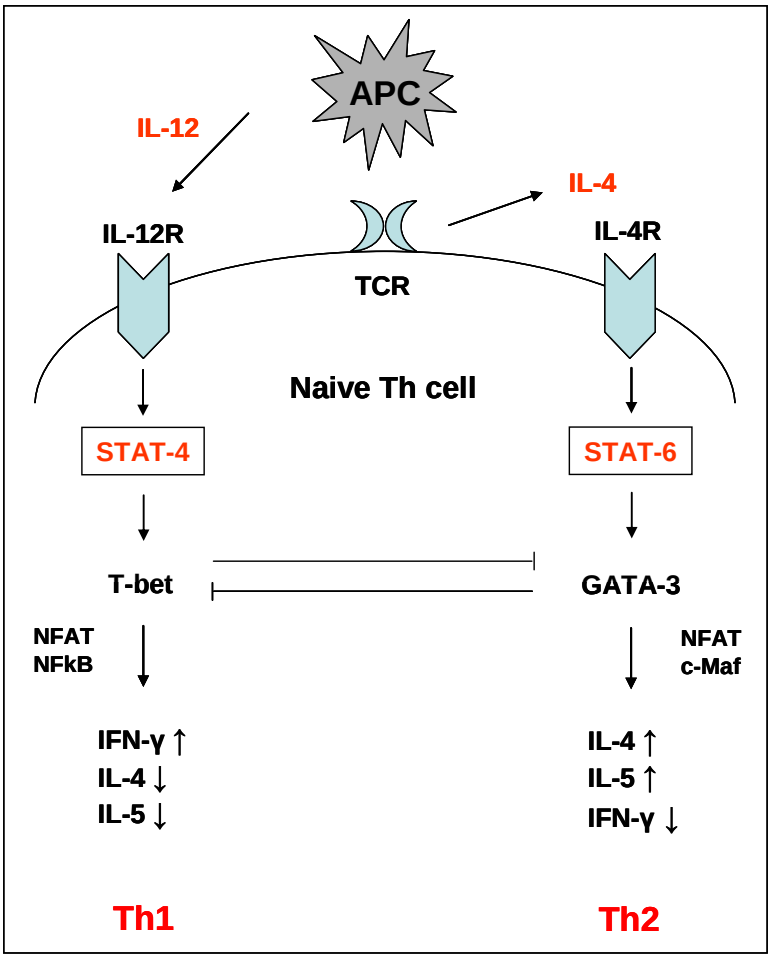


**Figure 1.4 Th1/Th2 differentiation.** The interaction between the IL-12 or IL-4 with the specific receptor, induce the activation respectively of STAT-4 ("Signal Transducer and Activator of Transcription 4") and STAT-6. STAT-4 stimulates T-bet to promote the differentiation in Th1. STAT-6 preferentially activates GATA-3, that modulates the Th2 differentiation. The mutually exclusive expression of T-bet and GATA-3 could reflect the ability of these factors to antagonise each other. APC= antigen-presenting cell; MHC= major histocompatibility complex; TCR= T-cell receptor.

Anyway, the molecular mechanisms that regulate the switch Th1/Th2 are still not well understood. Two transcription factors, define "markers switches", have been recently described, that seem to have a pivotal role in this mechanism: T-box, expressed in T cells (T-bet) and the GATA binding protein 3 (GATA-3). T-bet is a transcriptional factor able to promote the Th1 differentiation, down regulating the Th2 pattern. GATA-3 instead is a member of GATA zinc finger proteins family, so called because binds the DNA consensus (A/T)GATA(A/G), and plays a pivotal role in the development of Th2 phenotype, down modulating the differentiation of Th1 lymphocytes[44].

### 1.3.2 Pathogenetic role of Th2 response in pulmonary fibrosis

In the field of T helper lymphocytes differentiation, several quoted studies demonstrated that the fibrogenesis is linked to develop of a Th2 cellular response, and to the consequent increased expression of Th2 type cytokines, as IL-4, IL-5, IL-10 and IL-13[45]. On the contrary a Th1 immune response resulted able to inhibit the deposition of fibrotic tissue during the flogistic processes. Moreover these studies underlighted as the entity of fibrosis was tightly regulated by the Th phenotype of immune response, more than by the intensity or period of inflammatory stimulus[39]. The model mouse, knockout for different cytokines/chemokines, allowed to investigate the role of Th2 inflammatory network in the pathogenesis of IPF. Transgenic mice for IL-13 have a eosinophilic pulmonary inflammation and develop a more marked fibrosis with respect to the control mice[46]. More ambiguous is instead the role IL-4 that in different model mouse of pulmonary fibrosis showed contrasting results. Some authors, in fact, in a IL-$4^{-/-}$ mouse, demonstrated a duplex role of this cytokine in the inflammatory/fibrotic process, underlighting, in the earlier phase, a role in the prevention of T lymphocytes recruitment in the sites of inflammation. In the last phase, instead they demonstrated a pro-fibrotic role in development of bleomycin induced fibrosis[47]. In agreements with the Th2 hypothesis, in the model mouse of IPF, knockout for the chemokine CXCR3 (C57BL6 $CXCR3^{-/-}$), CXCR3 resulted to have a non-redundant role in the prevention of fibrogenetic process development[48]. Moreover, mice treated with IL-2, a potent IFN-γ inducer, present an important reduction of fibrotic lesions in the lung, confirming the pivotal role of Th2 lymphocytes and cytokines pattern in the IPF[49]. Nevertheless, still remain

some studies that support different hypothesis about the profibrotic role of IFN-γ, demonstrating that the process is still not well characterized.

### 1.3.3 Cytokines and chemokines in pulmonary fibrosis

In the natural immune response, beyond the activation of the alternative complement pathway, other soluble molecules are involved in the immune processes, such as cytokines and chemokines. Several experimental evidences support the pivotal role of chemokines and cytokines in alveolitis development. Probably the expression of these factors, and then the evolution of the lesions through the fibrosis, is locally modulated by cell-cell and cell-matrix interactions. The important role of these molecules is confirmed by the significant influence that the over expression of chemokines and cytokines and/or the down regulation of their receptors could have on the regulation of pulmonary inflammation.

Cytokines are a category of signaling proteins and glycoproteins that, like hormones and neurotransmitters, are extensively used in cellular communication. While hormones are secreted from specific organs to the blood, and neurotransmitters are related to neural activity, the cytokines are a more diverse class of compounds in terms of origin and purpose. They are produced by a wide variety of hematopoietic and non-hematopoietic cell types and can have autocrine, paracrine and endocrine effects, sometimes strongly dependent on the presence of other chemicals. The cytokine family consists mainly of small, water-soluble proteins and glycoproteins with a mass between 8 and 30 kDa. Cytokines are critical for the development and functioning of both the innate and adaptive immune response. They are often secreted by immune cells that have

encountered a pathogen, thereby activating and recruiting further immune cells to increase the system's response to the pathogen. Cytokines are also involved in several developmental processes during embryogenesis. The name "cytokine" is derived from the Greek ("cyto" - cell, and "kinos" - movement). Each cytokine binds to a specific cell-surface receptor. Subsequent cascades of intracellular signaling then alter cell functions. This may include the upregulation and/or downregulation of several genes and their transcription factors, resulting in the production of other cytokines, an increase in the number of surface receptors for other molecules, or the suppression of their own effect by feedback inhibition. The effect of a particular cytokine on a given cell depends on the cytokine, its extracellular abundance, the presence and abundance of the complementary receptor on the cell surface, and the downstream signals activated by receptor binding; these last two factors can vary by cell type. Cytokines are characterized by considerable "redundancy", in that many cytokines appear to share similar functions. They have been classified as lymphokines, interleukins, and chemokines, based on their presumed function, cell of secretion, or target of action. Because cytokines are characterized by considerable redundancy and pleiotropism, generalization of functions is not possible with cytokines. Nonetheless, based on position of their cystein residues, they have been classified in 4 families: α-, β-, C- and $CX_3C$- chemokines[50]. The chemokines are also subdivided in chemokines with inflammatory activity and homeostatic activity. The inflammatory chemokines are released in inflamed tissues by resident cells or by cells recruited in the tissue by *pro*-inflammatory cytokines. They are specialized in recruitment of effector cells, as monocytes, granulocytes and T lymphocytes. On the contrary, the homeostatic chemokines are

constitutively expressed in lymphoid and non-lymphoid tissues, as skin and mucosa, and regulate the physiologic traffic and the recruitment of immune system cells during the phases of maturation, differentiation and activation[51].

Among the several chemokines involved in the pathogenesis of IPF, particular importance has been attributed to the IL-1 and TNF-α, member of the CXC family, as IL-8, ENA-78, IP-10, I-TAC. Moreover literature data indicate an important role in the pathogenesis of fibrosis by cytokines belonging to CC family, as MCP-1 (Monocyte Chemotactic Protein-1α), CCL17 and CCL22. Finally also TGF-β (Transforming Growth Factor- β) and PDGF (Platelet Derived Growth Factor) are involved in tissue repair and fibrosis[52].

### 1.3.4 The Th1 cytokine/chemokine

The most important and the most studied Th1 chemokine is without doubt the interferon γ (IFN-γ).

**IFN-γ**:

The IFN-γ is a crucial cytokine during immune response in the lung. It stimulates the ancillary functions of macrophages, the cytotoxic activity of macrophages and lymphocytes and regulates the secretion of several cytokines, lymphokines and chemokines in the surrounding microenvironment. Moreover it activates the phagocytosis in neutrophils and alveolar macrophages. IFN-γ is released by T lymphocytes that infiltrate the lung in most ILDs, included sarcoidosis, tuberculosis and HIV infections. It is also believed that monocytes/macrophages

are a source of IFN-γ in the lung. The pleiotropic effects of this chemokine are also involved in the expression of stimulatory molecules by ancillary cells, in increased cytotoxicity, in growth and differentiation of T lymphocytes. Moreover, stimulating the secretion of chemokines (CXCL9, CXCL10 and CXCL11), IFN-γ plays a pivotal role in recruitment of CXCR3+ T lymphocytes into inflamed tissues. This cytokine has also an important anti apoptotic effect since inhibits the proliferation of endothelial cells and the synthesis of collagen by fibroblasts.

**IL-2**:

This molecule, released by T lymphocytes, stimulates in the lung the growth and activation of T lymphocytes infiltrating the lung tissues in the patients with sarcoidosis, HIV infection, tuberculosis and other ILDs. It is also involved in the regulation of Ig production and in enhancing of cytotoxic T cell activity.

### 1.3.5 The Th2 cytokine/chemokine

Each of the main Th2 cytokines has a distinct role in regulation of tissue remodelling and fibrosis.

**IL-4**

IL-4, released by T lymphocytes, eosinophils and mastocytes, is an important co-factor for fibroblast proliferation. It plays also a pivotal role during activation and differentiation of T and B lymphocytes, especially towards the production of IgG1 and IgE. Its receptor is expressed on fibroblast, that once stimulated, expresses

extra cellular matrix proteins such as I and III type collagen, and fibronectin. Moreover IL-4/IL13 axis is involved in the activation and amplification of inflammation in airways. This chemokine stimulates also the release of chemokines, such as CXCL8/IL-8, in bronchial epithelial cells and plays a pivotal role in the development of pulmonary fibrosis[42].

**IL-13**

This factor is a central profibrotic mediator and share several functions with IL-4, in fact, both proteins interact with the same receptor and operate through the transcription factor STAT-6. Nevertheless, IL-13 has a unique role with respect to IL-4, in fact its over expression causes an important fibrosis in sub epithelial airways, even with out inflammatory stimuli[39].

**IL-5**

In the lung it is the most important cytokine during the eosinophilic inflammation induced by antigens. In human this cytokine is mostly a transcription factor for growth of eosinophils, while in mouse interacts with B lymphocytes too, stimulating their differentiation. Activation of Th2 cells stimulates the production of IL-5 that, in turn, promotes proliferation and differentiation and survival of myelocyte eosinophils and eosinophil degranulation. These effects are mediated by IL-5R, expressed on eosinophil itself.

**IL-6**

This chemokine is mostly expressed by AMs, but it is produced also by B and T lymphocytes, endothelial cells and fibroblasts. It influences the antigen specific

inflammatory response and enhances the inflammatory reaction. Moreover, *in situ* it stimulates fibroblast proliferation.

**IL-9**

IL-9 is produced by T lymphocytes and enhances the inflammatory response recruiting in the airways eosinophils, lymphocytes and mastocytes. Since human fibroblasts express the IL-9 receptor, this cytokine is supposed to be involved in the fibrosis development.

**MCP-1**

This is a signal molecule belonging to super family of C-C chemokine. It is expressed under the appropriate stimuli by endothelial cells, epithelial cells, monocytes, smooth muscle cells and fibroblasts. Identified for its chemotaxis activity *versus* the macrophages, this chemokine plays a pivotal role with MIP-1 (Inflammatory Macrophage Protein 1) during the development of acute and chronic inflammation. MCP-1, besides its role in leucocytes recruitment, plays a stimulatory effects, inducing production of collagen through specific receptors stimulation and expression of TGF-β by fibroblasts[53]. Mouse knockout for MCP-1 (CCR-2) are protected against the bleomycin induced fibrosis, present an altered expression of profibrotic chemokines, have fibroblast less responsive to TGF- β and macrophages impaired in the recruitment and ability of releasing enzymes for extracellular matrix remodelling. Moreover MCP-1 is important for fibrocytes recruitment in the lung.

**IL-10**

It is known as inhibitory factor for the synthesis of chemokines. Actually IL-10 inhibits the production of IFN-γ, IL-1, IL-6 and TNF-α. Finally it has a pivotal role in the regulation of IgE syntesis[54].

**TNF-α**

It is a molecule with pleiotropic effects, mostly expressed by activated monocytes and macrophages, lymphocytes, epithelial and endothelial cells. In neutrophils and macrophages TNF-α induces the release of proteases, stimulates the respiratory burst and induces the expression of adhesions molecules. It plays a pivotal role in lung damage and in fibroblast growth through the stimulation of IL-6. It modulates, directly and/or indirectly, the release of cytokine like IL-1, IL-8, TGF-β, PDGF, and chemokines like CXCL8 and CCL2, and regulates their ability of degrading extracellular matrix. This molecule has been found in lung of patients with IPF and its was found overexpressed in IPF model mouse. Moreover TNF-α knockout mouse do not develop pulmonary fibrosis after treatment with bleomycin[55]. However the role of this chemokine is not so unique: other studies showed a protective effect of TNF-α against the develop of IPF bleomycin-induced and the test of reducing TNF-α activity in patients with IPF were barely effective[52].

### 1.3.6 Other cytokines of pulmonary fibrosis

**IL-1**

IL-1α and β are chemokines abundantly expressed and with strong inflammatory activity. Both molecules are able of stimulating PDGF secretion, fibroblast proliferation and I or III pro-collagen, favouring a pro-fibrotic phenotype. The expression of these chemokines was identified in AMs of patients with IPF. Studies on model mouse confirmed IL-β role in lung damage and tissue repair and demonstrated as a transitory overexpression of this chemokine in alveolar epithelial cells induces acute flogosis and tissue damage, with production of fibro-genetic chemokines as TGF-β and progressive pulmonary fibrosis[56]. The IL-1β profibrotic effect takes place also in alveolar fibroblasts by the induction of osteopontin, a multifunction protein present in the extracellular matrix, up-regulated in IPF patients and in model mouse of bleomycin-induced pulmonary fibrosis. Inhibition of IL-1β in model mouse results into a milder disease[57] and it is in progress the putative use for this pathology of anakinra, a IL-1 inhibitor, already utilized for the treatment of rheumatoid arthritis.

**TGF-β**

This is a cytokine expressed by several cell types and involved in different biological processes, such as cell differentiation, extracellular matrix deposition, embryonic development and healing of wounds. There are 3 different TGF-β isoforms ($\beta_1$, $\beta_2$, $\beta_3$), where the isoforms $\beta_1$ plays a pivotal role in pulmonary fibrosis pathogenesis, as demonstrated by its over-expression in IPF patients and IPF model mouse. The TGF-β over-expression, mediated by Adenovirus or IL-13

causes a severe prolonged fibrosis, that could be inhibited by anti bodies anti TGF-β or soluble receptors. This cytokine modulates the fibrosis by recruitment of fibroblasts and monocytes, stimulating the production of extracellular matrix, the angiogenesis, proliferation of fibroblasts and their differentiation in myofibroblasts[58]. The fibroblasts proliferation seems to be an indirect effect of TGF-β through the induction of FGF-2 (Fibroblast Growth Factor) and the consequent activation of MAP kinase pathway. The production of ECM is regulated by TGF through the promotion of gene transcription (I, III, IV, V collagen, fibronectin, proteoglicans) and the suppression of MMPs activity, with consequent collagen degradation. Moreover it has been demonstrated the important role of intracellular factor Smad3 in the transduction of TGF-β signal.

**Chemokines CXC**

The CXC chemokine family is a group of pleiotropic cytokines, expressed by macrophages, fibroblasts and epithelial cells, involved in the promotion of traffic of several leucocytes, in the regulation of angiogenesis and in vascular remodelling and in mobilization and migration of mesenchymal progenitor cells as fibrocytes. These functions appear fundamental in the pathogenesis of pulmonary fibrosis and other proliferative disorders. These chemokines, depending on the presence or absence of structural domain ELR, are subdivided into 2 groups ($ELR^+$ or $ELR^-$). The $ELR^+$ domain is fundamental for angiogenesis promoting (CXCL2, CXCL3, CXCL8, CXCL5), whereas the cytokines $ELR^-$ (CXCL9, CXCL10, CXCL11), that are up regulated by IFN-γ and Th1 chemokines, have angiogenetic activities. The angiostatic activity of CXC $ELR^+$

chemokines is mostly mediated by CXCR2 expressed on endothelial cells, while the angiostatic activity of CXC ELR$^-$ chemokines is mediated by CXCR3 always expressed on endothelial cells. Several CXCR3 variants, generated by alternative splicing, have been identified. The variant CXCR3A is the receptor most expressed by Th1 effector cells, T CD8$^+$, activated B cells and NK.

**Chemokines CC**

MCP1/CCL2 and MIP-1α/CCL3 are proinflammatory chemokines responsible of monocytes recruiting and of secreting a variety of cell types such as lymphocytes, macrophages, fibroblasts and endothelial cells. Both are significantly up regulated in BALFs of patients with IPF and in the bleomycin-induced IPF model mouse. Data obtained in model mouse confirm the involvement of these chemokines in the pathogenesis of IPF. The pathologic over expression of CCL2 and CCL3 seem to depend, at least in part, by alteration in IL-13 regulation, which results up-regulated in macrophages of patients with IPF.

CCL17 and CCL22 are two chemokines up-regulated by Th2 type cytokines, and their receptors are over-expressed in the areas of fibrotic pulmonary tissue as compared to areas of normal pulmonary parenchyma. In particular it has been demonstrated that CCR4 is prevalently expressed by macrophages in areas of fibrosis. Moreover, neutralization of CCL17 and CCL22 reduces the lung tissue damage[52]. The chemo-cytokine network in the IPF pathogenesis in presented in Figure 1.5.

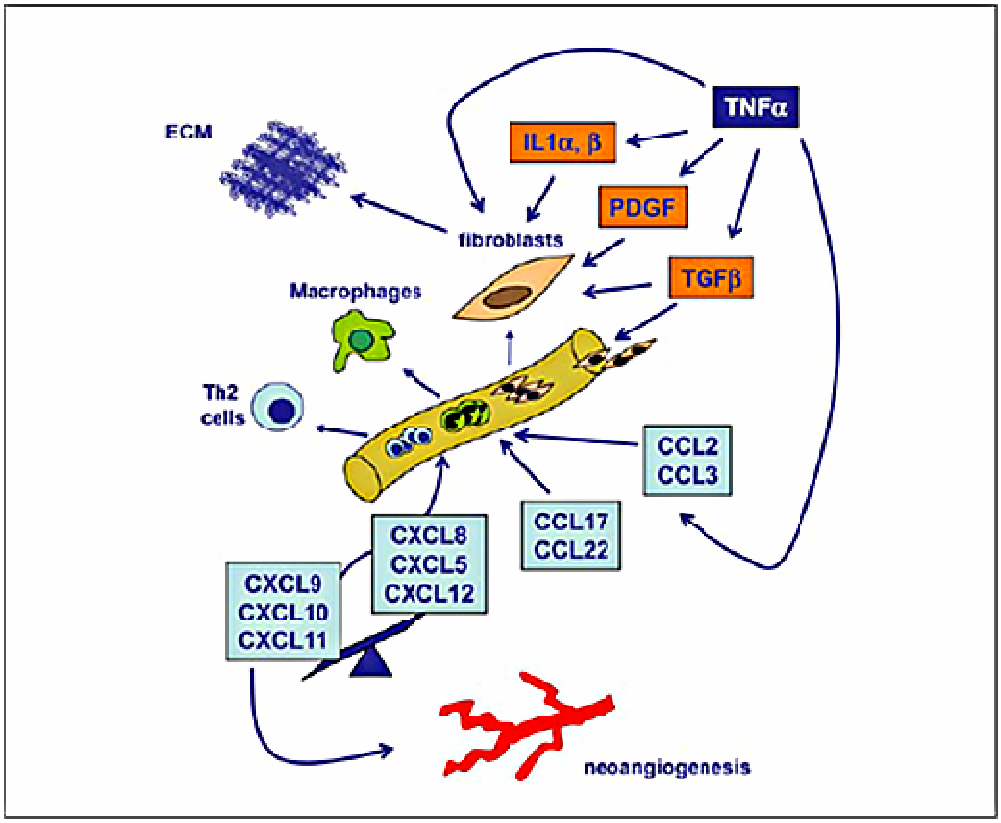


**Figure 1.5. Presentation of chemo-cytokine network involved in the IPF pathogenesis**

## 1.4 PULMONARY FIBROSIS MODEL MOUSE

### 1.4.1 The bleomycin

The bleomycin (Figure 1.6) is a glycopeptide of 1.5 kDa produced by *Streptomyces verticillus*[59]. This molecule has antitumor and antiviral activity and acts mostly by blocking the cell cycle in G2 phase. The bleomycin stimulates the lung damage through its ability to interlayer the DNA every 5 base pairs, inducing a site specific nick (between G-C and G-T bases) and a non-specific nick both in the single and in double helix. Moreover bleomycin is able to inhibit the DNA repair enzymes such as DNA ligase. This compound is usually degradeted by

bleomycin-hydrolyse enzyme, that is expressed in several tissues, except skin and lung. In the extremities this molecule presents a DNA and $Fe^{2+}$ binding regions. The $Fe^{2+}$ binding region is necessary because acts like co-factor able of damaging the DNA with the consequent cytotoxic effect.

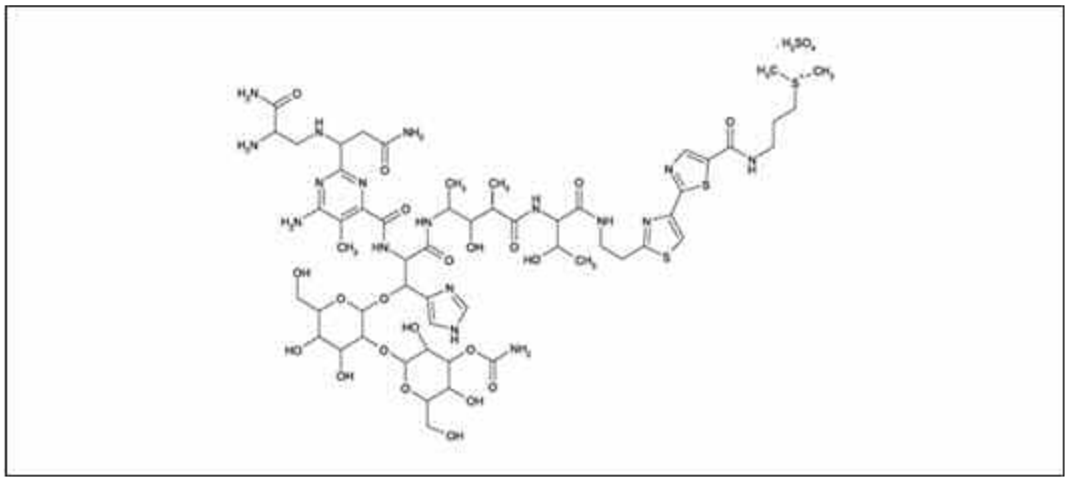

**Figure 1.6 Chemical structure of bleomycin**

This drug is utilized in clinical for chemotherapeutic treatment of neoplasms such as squamous cell carcinoma of the cervix, oesophagus, skin, lung, neoplasms of testis germ cells, Hodgkin and non-Hodgkin lymphoma. Unfortunately the 10% of patients treated with a cumulative dose of bleomycin upper than 200U/$m^2$ develops interstitial pneumonia, that progresses to fibrosis. About the mechanism through which bleomycin induces inflammation, recently it has been demonstrated that the stimulation of Toll-like receptor 2 (TLR2) by bleomycin itself induces the activation of monocytes and proinflammatory chemokine release[60]. The ability of innate immune system to recognize and replay to exogenous agents is largely attributed to the Toll-like receptors family (TLRs). These receptors are mostly expressed on the surface of antigen presenting cells (APC) such as monocytes, macrophages and dendritic cells, and are able of discriminating among separate molecular patterns associated to microbial

elements. The recognition by these receptors of products of pathogens stimulates several transduction signalling pathways that regulate the type, the scope and the duration of inflammatory response. In this context the inability of host itself to regulate the type or duration of inflammatory response is critical, as in the case of inflammatory chronical diseases. The stimulation of TLR2 by bleomycin causes the activation of NF-κB, which in turn induces the transcription of genes for proinflammatory chemokines such as IL-8, IL-1β e TNF-α[60].

### 1.4.2 Pulmonary fibrosis model mouse

The pulmonary dose-dependent toxicity of bleomycin was useful to create experimental models of IPF in animals. Though several studies have highlighted the presence of important differences between the acute and the chronic phase in the pulmonary fibrosis of animals, the model mouse represents an evaluable tool in order to verify, *in vivo*, the proteins and the molecules involved in the pathogenesis of pulmonary fibrosis. Moreover the possibility to manipulate genetically the mice, creating knock out models, is useful to demonstrate the involvement of specific genes in pneumonia characterized by fibrosis development. In the model mouse of bleomycin induced pulmonary fibrosis, the initial event is the damage to epithelial lung cells, that stimulates the migration of granulocytes and fibroblasts into the damaged tissue and the consequent migration of macrophages, lymphocytes and fibroblasts. The development of an acute inflammation is finally followed, within 4 weeks, by interstitial fibrosis.

Only in some cases these mechanisms, instead hesitate in fibrosis, cause a "respiratory distress syndrome" leading to rapid death of animals. The model

mouse of pulmonary fibrosis, induced by bleomycin, draws near some key characteristics of human pulmonary fibrosis, including the damage to alveolar epithelial cells, recruitment of inflammatory cells, proliferation and activation of fibroblasts responsible of extracellular matrix production and deposition in the pulmonary parenchyma. Particularly the anatomic-pathologic characteristic of lung lesions specifically recall the characteristic patterns of UIP, evident in IPF of human pulmonary biopsies. The importance of model mouse in the study of IPF pathogenesis is due to the fact that, in human, this pathology is always diagnosed late, when the function of lung is already reduced and when the early natural history of IPF, its causal factors and pathogenetic mechanism, are not anymore comprehensible. About the study of inflammatory phenomena and mechanisms that lead to the fibrotic tissue deposition, it is not possible to only consider the informations obtained by human pulmonary biopsies. From here emerges the irreplaceable role of an animal model that can reproduce, as faithfully as possible, the characteristics of IPF[38].

## 1.5 THE GLYCOGEN SYNTHASE KINASE 3

The Glycogen Synthase Kinase 3 (GSK-3) was initially identified in 1980 as Serine/Threonine kinase involved in the metabolism of Glycogen[61], able to inactivate, by phosphorylation, the glycogen synthase enzyme, the enzyme rate-limiting in the biosynthetic pathway of glycogen itself.

This kinase is ubiquitously expressed in mammal tissues and it is involved in several cellular process such as stability of cytoskeletal, control of transcription, synthesis of proteins, metabolism of glycogen, cells proliferation

and differentiation, embryonic development, cell motility and apoptosis. This kinase is mostly cytosolic, but it is expressed also in the nucleus and in mitochondria.

### 1.5.1 The GSK-3 structure

This enzyme has 2 isoforms, strictly correlated: GSK-3α, of 51kDa, and GSK-3β, of 47 kDa, codified by 2 different genes but with an homology of 97% in the catalytic syte[62].

Outside the kinase domain, the sequence differs substantially. The homology, in fact, reduces to 36% in the C-terminal region of the protein. The difference in the size is particularly significant in the N-terminal region of protein, where the isoform α presents a portion rich of glycines (Figure 1.7)[63].

The two isoforms do not show the same functions: it has been demonstrated that the mice harbouring the deletion for the exon 2 of GSK-3β do not express the protein and die on the sixteenth day of gestation because of a massive liver degeneration caused by an extended phenomenon of apoptosis. The inability of GSK-3α to substitute GSK-3β in knockout mice, indicates that the degenerative phenotype of liver depends by the β isoform lack[63].

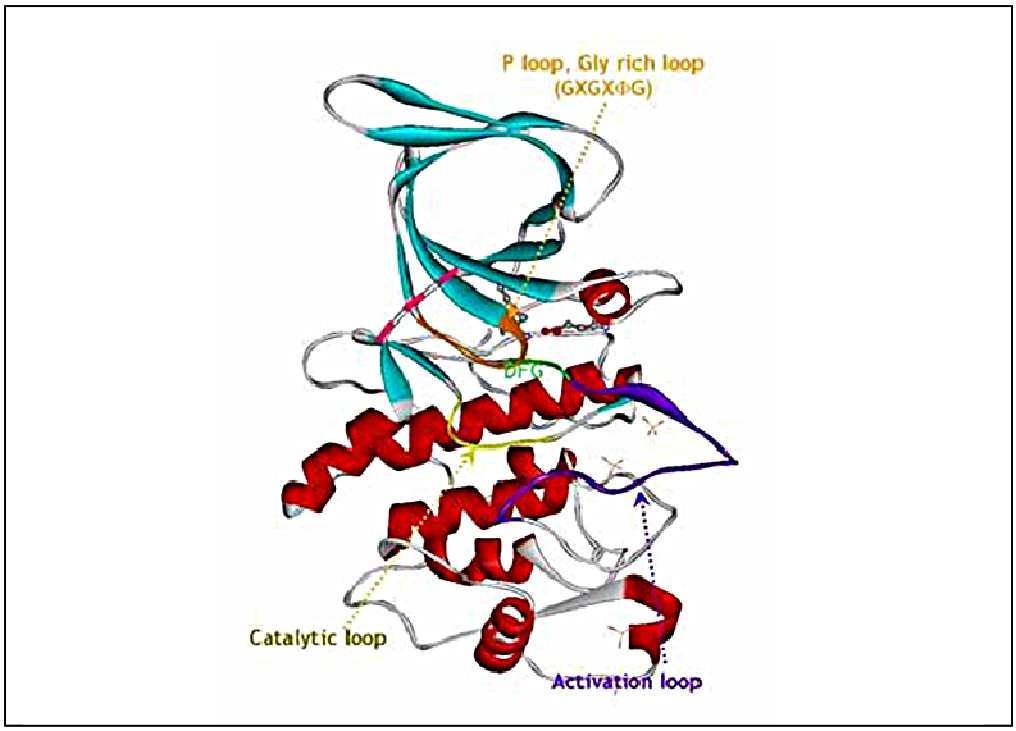


**Figure 1.7 Structure of GSK-3** The structure is similar to that of other kinases, with a small portion N-terminal mostly constituted by β-sheets, and a wider C-terminal portion of α helixes. The site for the ATP binding is localized between the two lobs. The Arg96, Arg180 and Lys205 constitute a small task where bind the phosphate group of the pre-phosphorylated substrate and the pseudo-substrate.

### 1.5.2 Control of GSK-3 activity

The determination of crystalline structure of GSK-3 allowed to identify the different mechanisms of enzyme control and function. It has been demonstrated that GSK-3, because of its kinase activity, needs that some substrates were already phosphorylated on Serine or Threonine residues, in the C-terminal portion close to the phosphorylation site of GSK-3. The consensus sequence involved in this mechanism is Ser/Threonine-X-X-X-Ser-P/Thr-P, where the first Ser or Thr residue represents the target of GSK-3, X represents a generic residue (often a Proline) and the phosphorylated residue (Ser-P/Thr-P) is the preventive phosphorylation site. An example of this mechanism is the activity of GSK-3 on

the glycogen synthase enzyme where, after a first phosphorylation of a Serine residue by the Casein Kinase 2 (CK2), follow to four phosphorylation by GSK-3, thus leading to the inactivation of glycogen synthase (Figure 1.8)[64].

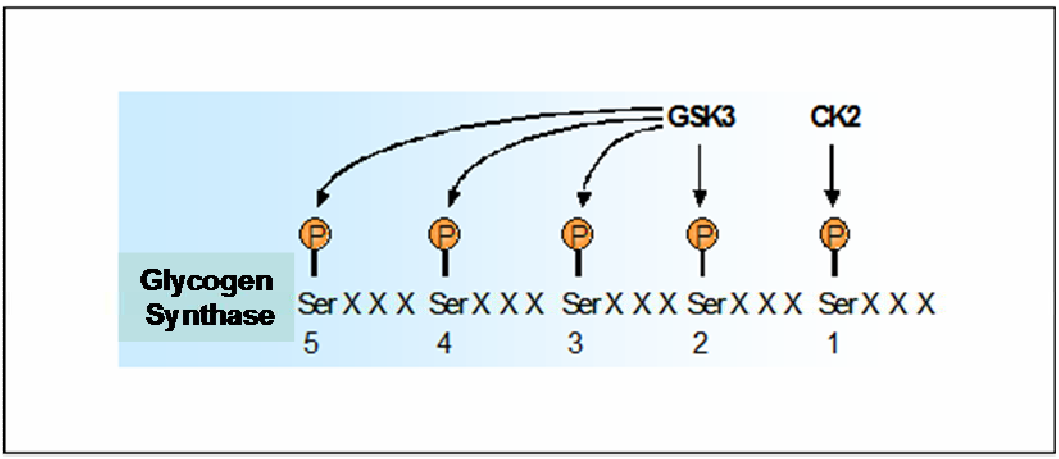


**Figure 1.8 Mechanism of action of GSK-3 on Glycogen Synthase**

The most important inhibitory mechanism of GSK-3, is a site of phosphorylation localized in the N-terminal region of enzyme. Several stimuli, such as insulin or other growth factors, stimulates, through the P(I)3K/Akt axis, the phosphorylation of a Serine residue (Ser21 in GSK-3α and Ser9 in GSK-3β) causing a structural modification of amino-terminal portion of GSK-3 and blocking in this way the catalytic activity. The N-terminal domain, phosphorylated in Ser9 of GSK-3β, acts like pseudo-substrate, blocking the access to the physiologic substrate into the catalytic site. Several kinases can phosphorylate GSK-3, as the protein kinase A (PKA) or C (PKC).

Not all the substrates are subjected to preventive phosphorylation by the catalytic site of GSK-3 and this allows, during a event of inhibitory phosphorylation, to discriminate between different substrates. Opposing to inhibitory phosphorylation (on Serine residues), the activity of GSK-3 is favored by phosphorylation in Tyr216 for the isoform β and Tyr279 for the isoform α[62].

GSK-3 is downstream of several signal pathways, among the most studied is the Wnt/β-catenin one. The Wnt (Wingless-type) proteins are glycoproteins rich in Cystein residues that regulate growth, differentiation, migration and cell destiny[65]. GSK-3 is able to form a complex with Axin, APC (*Adenomatous polyposis coli* protein) and β-catenin. Without a Wnt signal, GSK-3 is activated and can phosphorylate β-catenin on series of terminal Serine residues, creating a recognition site for the F-box βTrCP protein binding. In turn F-box βTrCP protein acts like a subunit of recognition for binding of the E3 ubiquitin-ligase and consequent β-catenin degradation *via* proteasome. The phosphorylation of β-catenin by GSK-3 is facilitated by Axin, that acts like a support binding the different components of the complex (GSK-3, β-catenin and APC). Axin and APC are substrates of GSK-3: the phosphorylation of Axin is important for its stability, whereas the phosphorylation of APC favours the interaction of APC with β-catenin (Figure 1.9). The binding of Wnt to its receptor activates the protein FRAT/GBP (Frequently Rearranged in advanced T-cell lymphomas/GSk-3 binding protein) that, with DVL (disheveled protein), binds the specific site of GSK-3, usually occupied by the protein Axin. In this way is not allowed the formation of the complex GSK-3/Axin/APC/β-catenin, the transcription factor β-catenin is not phosphorylated by GSK-3 and subsequently is not degraded by the ubiquitin-proteasome system[66]. Therefore β-catenin accumulates in the cytoplasm and nucleus, where through the binding to transcription factor of TCF/LEF (T-cell factor/ lymphoid enhancer-binding factor-1) family, activates the transcription of genes target in the Wnt pathway. In this complex β-catenin provides the trans-activation domain, whereas the specificity of binding is determined by the specific member of TCF/LEF family to whose is bound. As already demonstrated by

studies with GSK-3 knockout mice[67], GSK-3 is moreover implicated in the activity modulation of NF-κB signal pathway, pivotal for the control of immune response because modulates the survival, proliferation, differentiation of B and T lymphocytes and cytokine production.

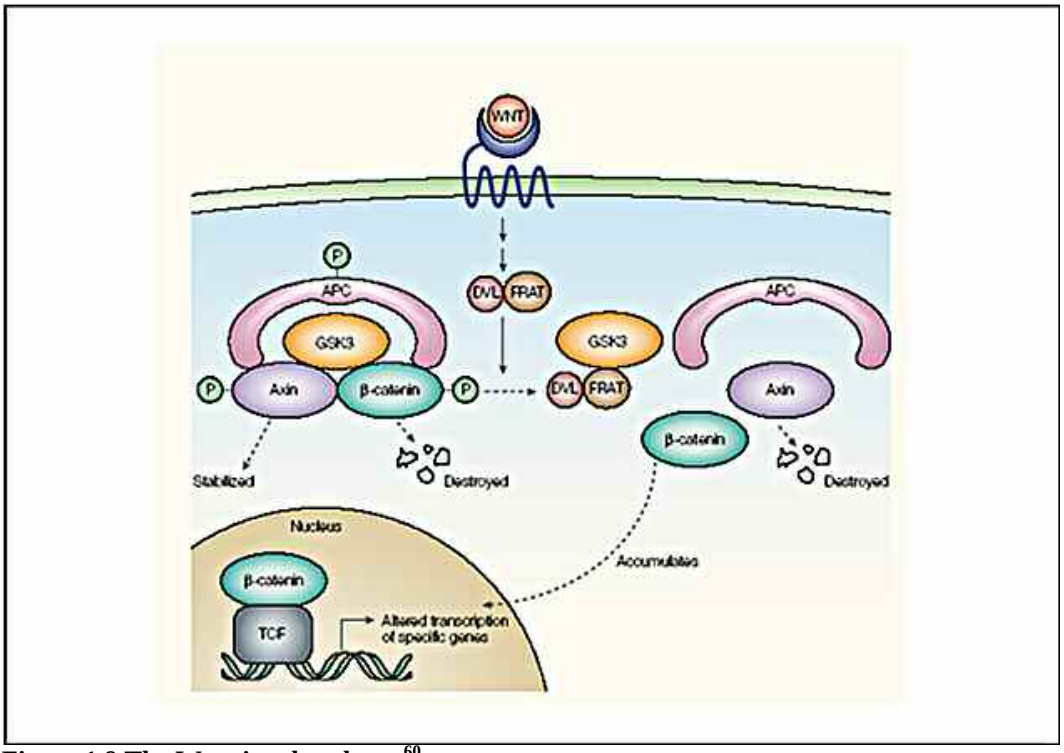


**Figure 1.9 The Wnt signal pathway[60].**

The NF-κB proteins are a family of inducible transcription factors, present on the cytoplasm of the cells, involved in develop, differentiation and oncogenesis: the prototype of NF-κB is a heterodymer composed by p65 and p50. To this family belonging seven proteins: p105, precursor of p50/ NF-κB1, p100, precursor p52/ NF-κB2, RelA/p65, c-Rel and RelB that sharing a N-terminal domain homolog to REL (REL homology domain). The amino-terminal portion of this domain is responsible of interaction with the DNA, whereas the C-terminal domain mediates the dimerization of other elements of family and presents the binding site for the inhibitory elements named IkB, IkB-α and IkB-β. These

inhibitory molecules, binding to NF-κB proteins, block their nuclear localization signal.

Several stimuli, as TNF-α, IL-1, bacterial lipopolysaccharide (LPS), viral proteins, ultra violet radiations (UV) and free radicals, induce the degradation of IkB protein and the translocation to nucleus of NF-κB. After cellular activation IκB-α, associated to NF-κB, is phosphorylated on two Ser residues in the N-terminal domain by the kinase complex of IkB (IKK), constituted by the subunits IKK-α and IKK-β and by the modulatory protein IKK-γ. The consequent degradation of IkB-α releases the heterodimers NF-κB p65/p50 and hides the nuclear localization signal present in RelA/p65, promoting the translocation to the nucleus of NF-κB, where, interacting with other transcriptional factors, induces the expression of the target genes (Figure 1.10)[68].

An important physiologic function of NF-kB has been demonstrated studying the gene expression induced by NF-kB using for example actinomycin D and cicloeximide. The treatment of cells with TNF-α in the presence of these inhibitors, is able to induce massive apoptosis. This result was attributed to the anti-apoptotic activity of NF-kB. TNF-α is usually able to activate both the pro- and the anti- apoptotic pathway and the inhibition of this factor moves the equilibrium in the direction of apoptosis. The consequences of this protective activity are more evident during the embryonic development in p65 knockout mouse. This model dies between the thirteen and fifteen day for massive apoptosis of hepathocytes. But if the mouse is double knockout for p65 and TNF-α or its receptor TNFR1, the mouse survivals. The embryonic fibroblasts of this mouse present defects in NF-kB activation and a high susceptibility to apoptosis

TNF-α-mediated. The same background effects are present also in case of other mutations in the NF-kB pathway [69].

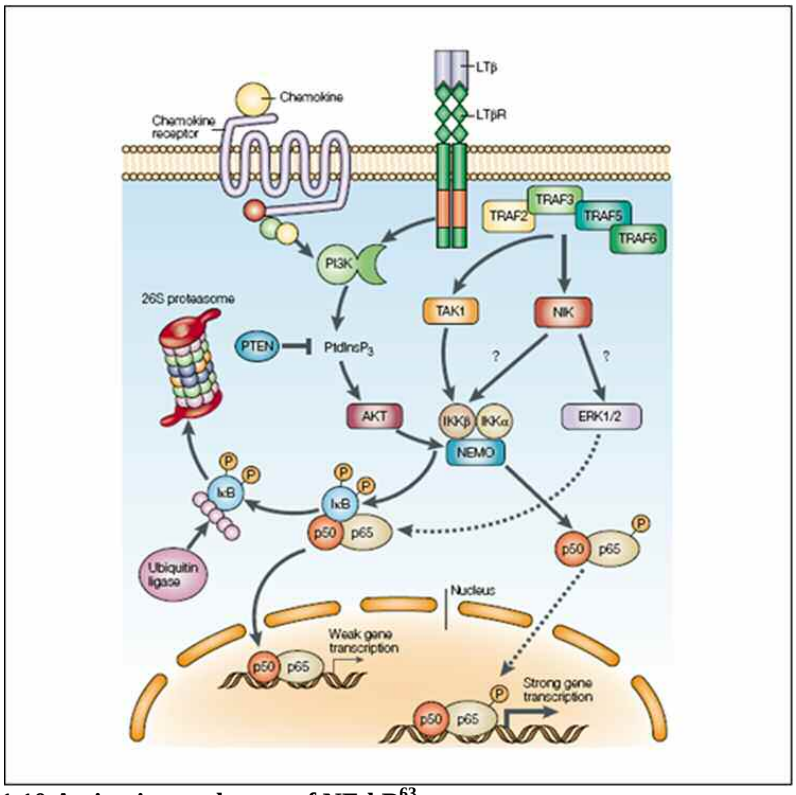


**Figure 1.10 Activation pathways of NF-kB[63].**

The model mouse knockout for GSK-3β undergoes to death during embryogenesis because of massive hepathocytes apoptosis, such as the model mouse knockout for p65, IKK or RelA. The death could be avoid blocking TNF-α activity with a monoclonal anti-body anti TNF-α. In agreement with this result, the cells of this mouse, have a reduced NF-kB activity, suggesting a role of GSK-3β in modulation of FN-kB pathway.

The activity of IkB-kinase, induced by cytokines, and the successive phosphorylation of IkBα, p105 and p65 are not influenced by the lacking of GSK-3β. The accumulation of p65 in the nucleus after TNF stimulation, is not altered by GSK-3 absence. Anyway the ability of NF-kB of DNA binding is reduced in GSK-3β null cells, as in the cells treated with GSK-3 inhibitors. The expression of

some genes under NF-kB control, as IkBα and MIP-2 (Macrophage Inflammatory Protein 2), is minimally influenced by GSK-3 absence. Whereas there is another series of genes NF-kB dependent, as IL-6 and MCP-1, to whose the expression of GSK-3 is indispensable. It has been demonstrated that, for an efficient localization of p65 on IL-6 and MCP-1 promoters after TNF-α treatment, is necessary the presence of GSK-3β. This suggest that GSK-3 has a fundamental role in gene-specific transcription by the promoter specific recruitment of NF-kB. This mechanism is explicated through a direct phosphorylation of p65 by GSK-3β and a conformal modification of chromatin to facilitate the access of transcription factors as NF-kB to specific gene promoters (Figure 1.11)[70].

The role of GSK-3β in NF-kB pathway appears to be specific, since GSK-3α is not able to compensate the lacking of GSK-3β isoform. Whereas the role of GSK-3 in Wnt pathway is not specific because this pathway do not discriminate between the 2 isoforms[69].

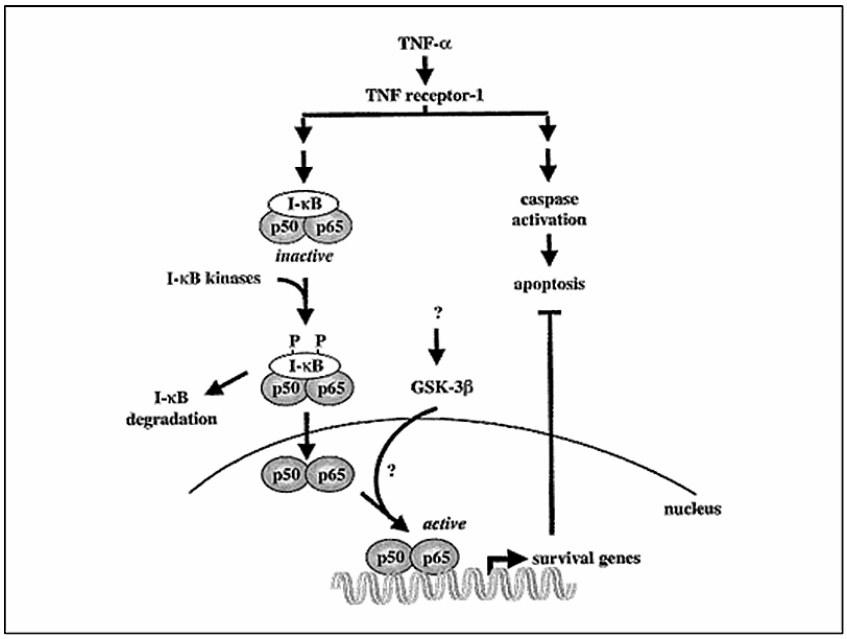


**Figure 1.11 Model of NF-kB control by GSK-3β.** GSK-3 is involved in trans-activation of NF-kB in a way dependent by I-kB-α degradation and its consequent translocation to the nucleus[56].

### 1.5.3 Role of GSK-3 in the inflammation

The cell mechanism that regulates the production of pro- or anti-inflammatory cytokines after TLR stimulation, are not well understood, but some studies have demonstrated that the signal pathway of TLR is able to activate the Phosphatidylinositol 3-Kinase (PI(3)K) to limit the production of TNF and IL-12, stimulating instead the production of IL-10.

PI(3)K is a enzyme organized in a regulatory (p85) and a catalytic (p110) subunit. The activation of PI(3)K is determined by the binding of the regulatory subunit to adaptor proteins. These adaptor proteins are linked to phospho-tyrosine residues present in activated cellular surface receptors. The activation of PI(3)K can mediate the recruitment and successive activation of signal proteins, as the protein kinase Akt, key mediator in this pathway. Once activated by phosphorylation, Akt in turn inactivates by phosphorylation several elements constitutively activated, downstream in PI(3)K pathway, as the Ser/Thr kinases. GSK-3 can modulate, both positively that negatively, a series of transcription factors, that play a pivotal role for the production of pro- and anti-inflammatory cytokines. The exposition of monocytes to bacterial LPS induces the inactivation, in a way PI(3)K-Akt- dependent, of GSK-3β, but not of GSK-3α isoform[71]. This inhibition determines a limited inflammatory cytokine production (IL-12, IL-6, TNF, IL1-β, IFN-γ) and an increased of anti-inflammatory IL-10 cytokine level. Studies with TLR2, TLR4, TLR5 and TLR9 agonists have demonstrated that GSK-3β is able to modulate in a specific manner the production of pro- and anti-inflammatory cytokines in response to multiple TLR signal pathway.

The mechanism responsible of regulating the production of pro- and anti-inflammatory proteins is deeply studied and it has been demonstrated the important role of GSK-3 and NF-kB. The optimal p65 transcriptional activity of NF-kB is mediated by the association with the nuclear co-activator CBP (CREB Binding Protein). For the interaction with CBP, expressed at limiting level, p65 phosphorylated in Ser276 competes with CREB phosphorylated in Ser133 and the binding of CREB with CBP inhibits the activity of NF-kB. Since GSK-3 is able to negatively regulate by phosphorylation the CREB DNA binding activity, the inhibition of GSK-3 by LPS stimulus increases the binding of CREB to the nuclear co-activator CBP, causing damages to the p65 subunit of NFκB. CREB is found to be an important transcriptional factor for the production of IL-10 by human monocytes with contemporary reduction of IL-12 level. Consequently the ability of GSK-3β to regulate the production of pro- and anti- inflammatory cytokines by monocytes stimulated with LPS seems to be dependent by the regulation of CREB activity.

The enhancing of this regulatory mechanism through an GSK-3 inhibitory (SB216763), administered to the mouse 2 hours before or after a lethal dose ($LD_{100}$) of LPS, has been demonstrated able to reduce drastically the mortality, inhibiting efficiently the production of pro-inflammatory cytokines (IL-12, IFN-γ, IL-6) and increasing contemporary the production of the anti-inflammatory cytokine IL-10[71].

Further studies demonstrated that IFN-γ is able to alter the signal transduction induced by TLR2, increasing the level of TNF-α and decreasing the production of IL-10 by macrophages. This last effect is also due by inhibitory activity of IFN-γ on PI(3)K-Akt pathway with subsequent activation of GSK-3

which in turn inhibits CREB and AP-1, both positive regulator of IL-10 production. In agreement with these results, GSK-3 inhibition and IL-10 increasing, demonstrated a protective role during arthritis and peritonitis develop in model mouse[72]. So GSK-3 appears to play *in vivo* a pivotal role in modulation of inflammatory response and results a potential therapeutic target for several inflammatory pathologies[71].

### 1.5.4 GSK-3 inhibitors

The discovery that GSK-3 plays a key role in the regulation of several functions, focused the interest of researchers on this kinase and on develop of pharmacologic inhibitor to verify its putative role as therapeutic target.

The best characterized GSK-3 inhibitor is without doubt the lithium. Even if specific for GSK-3, this element influences the activity of other enzymes and are necessary relatively high amounts to inhibit GSK-3 in cell cultures[63]. The inhibition mechanism is based on competition for $Mg^{2+}$[73]. Moreover it has been demonstrated that also Berillium and the bivalent element of Zn, that mimes the action of insulin, are able to inhibit GSK-3 in cell cultures[74,75].

Several GSK-3 inhibitors have been recently discovered and at the moment more than 30 inhibitors are available, most of them acting with a ATP competitor mechanism[76]. Among ATP competitor GSK-3 inhibitors must remember Aloisines, Hymenialdisines, Indirubins, and Maleimides, among not ATP competitor are the Tiadiozolidinoni (TDZD).

The SB216763 and the SB415286 are two structural distinct maleimides (Figure 1.12), able to pass through the plasma membrane, acting with a ATP

competitor in a way specific and GSK-3α and GSK-3β selective. These two compounds reduced drastically the GSK-3 activity, indeed they were able to induce all the answers induced by GSK-3 inhibition and resulted useful drugs in the study the role of GSK-3 in different signal pathways[3].

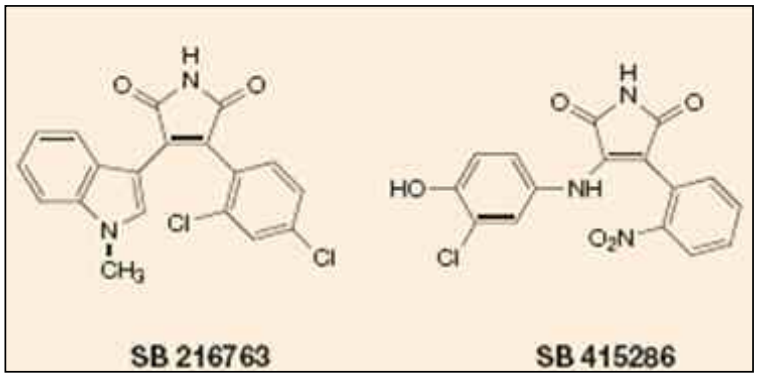


**Figure 1.12 Structure of GSK-3 inhibitors SB216763 and SB415286**

## 1.6 THE NEUTROPHIL-ACTIVATING PROTEIN (HP-NAP) OF *Helicobacter pylori*

*Helicobacter pylori* is a Gram-negative bacterium closely associated with gastric and peptic ulcer disease and with the development of duodenal ulcers[77-79]. Chronic *H. pylori* gastritis is also a major risk factor for development of gastric cancer[80,81]. *H. pylori* infection elicits an inflammatory cell response, and the severity of mucosal injury appears to be directly correlated with the extent of neutrophil infiltration[82,83]. It has been suggested that activated leukocytes may be responsible for some of the tissue damage seen in cases of *H. pylori* gastritis[84,85] and that activated phagocytes, especially in the presence of *H. pylori* products, contribute to carcinogenesis[86,87].

In water extracts of *H. pylori* was identified, by Yoshida's group[88], a neutrophil-activating protein capable of promoting neutrophil adhesion to endothelial cells. This protein was purified as a 150 kDa decamer composed of identical 15 kDa subunits. It was termed HP-NAP because it induces adhesion of neutrophils to endothelial cells and production of reactive oxygen radicals, detected by nitro-benzo-tetrazolium reduction[89] or with the quantitative and sensitive assay based on the peroxidase-mediated oxidation of homovanillic acid[90]. A considerable variation in the level of neutrophil adhesion promoting activity among different *H. pylori* strains was documented[89], suggesting a variable level of expression of the protein, similar to what was found for VacA[77]. HP-NAP is localized in the bacterial cytosol and is released upon autolysis. HP-NAP can bind to the external surface of the outer membrane[91], in a similar manner as urease[92]. In such a location, HP-NAP can mediate the binding of *H. pylori* to the cell surface *via* interaction with carbohydrates[93]. Thus, notwithstanding the possible role of HP-NAP in *H. pylori*–associated diseases and in the human immune response to the bacterium, very little is known about these aspects of HP-NAP activity.

### 1.6.1 The HP-NAP structure

This protein was purified as a 150 kDa decamer composed of identical 15 kDa subunits[88]. Amino acid sequence comparison indicates that HP-NAP belongs to the family of DNA-protecting proteins (Dps) (accession no. PDOC00645 of the PROSITE databank), which has significant structural similarities with the ferritin protein family (accession no. PDOC00181)[94]. A comparison of the available

amino acid sequences of HP-NAP from different strains clearly showed their high similarity, suggesting a defined and important role of this protein in *H. pylori* growth and/or survival.

Homologous sequences presented in databases, suggest that HP-NAP is similar to bacterioferritins (Bfr) and to Dps proteins. The computer-assisted molecular replacement of the amino acid sequence of HP-NAP into the three-dimensional (3D) co-ordinates of Bfr and Dps provided a better fit in the Dps crystallographic structure and suggested that the structure of HP-NAP is closely similar, if not identical, to the model depicted in Figure 1.13.

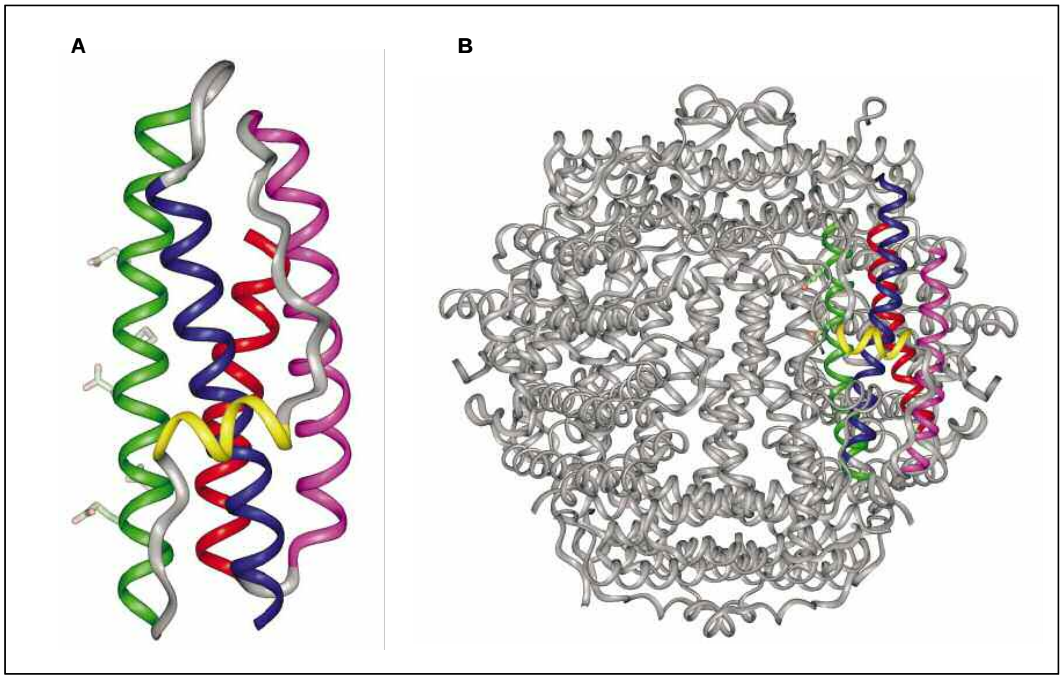


**Figure 1.13 Three-dimensional model of the HP-NAP monomer and oligomer**. **A.** Model of HP-NAP monomer obtained by substitution of the amino acid sequence of HP-NAP into the 3D co-ordinates of *E. coli* Dps (PDB entry 1dps) performed with the SWISS-model server[95]. The carboxylate lateral chains of residues Glu-42, Glu-46, Asp-49, Asp-53 and Glu-56 are highlighted as they are putatively involved in iron binding. **B.** Quaternary structure of Dps showing the position of one monomer in color within the dodecamer with the lateral chains of iron-binding residues pointing into the central cavity. Figures were generated using the program INSIGHT II[96].

Figure 1.13 A shows the HP-NAP monomer and Figure 1.13 B depicts the structure of the putative dodecamer with one monomer coloured; the figure also highlights those residues putatively involved in iron binding, with their lateral

chains pointing into the internal cavity of the oligomer. Moreover the maximum number of iron atoms bound by HP-NAP was estimated to be up to 40 *per* monomer, corresponding to about 500 atoms *per* dodecamer [96].

### 1.6.2 HP-NAP, the Th1-activating protein of *Helicobacter pylori*

During *H. pylori* infection the bacterium induces an inflammatory response in the gastric mucosa characterized by polymorphonucleate and mononucleate cell infiltration. A polarized Th1 response occurs in the stomach of infected individuals and is associated with more serious diseases. A number of factors (related to bacterium, host, environment, age, sex, and other concomitant or previous infections) influence the type of host gastric immune response and HPNAP is a key factor in the gastric inflammation induced by *H. pylori* (Figure 1.14)[91].

HP-NAP could first attract and activate neutrophils to produce IL-12 and IL-23. Then these two Th1-polarizing cytokines, together with HP-NAP and other *H. pylori* factors, stimulate IL-12 and IL-23 production and secretion by macrophages and DCs and drive the gastric T-cell response towards a Th1 type of immune response, characterized by an important IFN-γ production and activation of a cytolytic program with consequent gastric damage. The predominant activation of Th1 cells, with high levels of IFN-γ and TNF-α might result, respectively, in procoagulant activity and an increase in gastrin secretion and pepsinogen release.

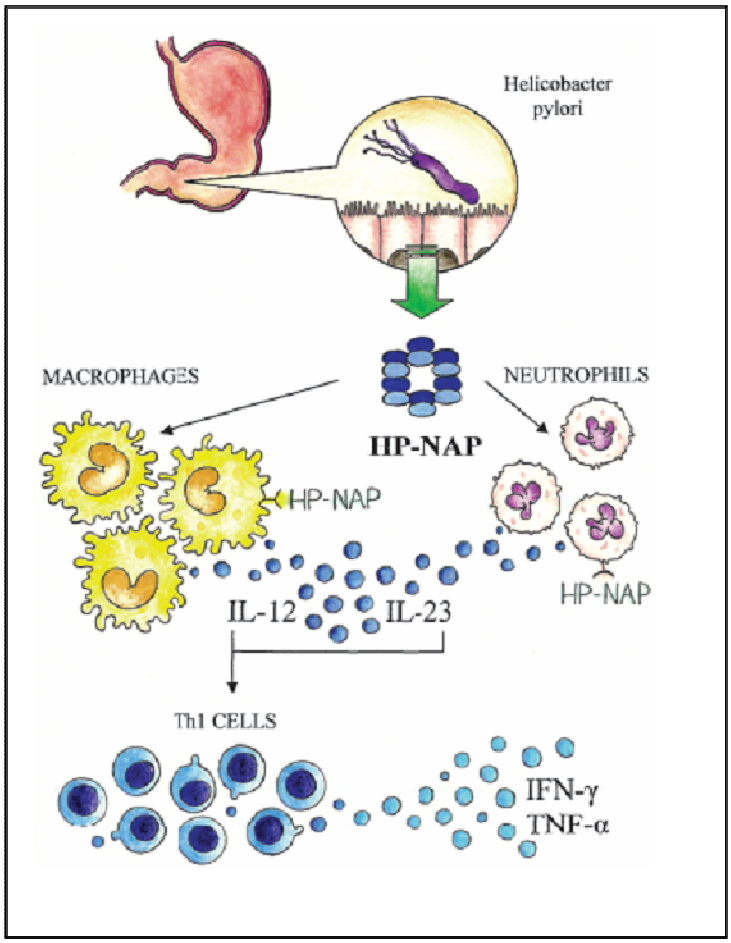


**Figure 1.14 Schematic representation of HP-NAP Th1-polarizing activities in *H. pylori* infection.** Following *H. pylori* infection of the gastric antrum, HP-NAP first attracts and activates neutrophils to produce IL-12 and IL-23 together with CXCL8, CCL3, and CCL4. HP-NAP also triggers macrophages to produce IL-12, IL-23, and other Th1-polarizing cytokines. This cytokine 'milieu', together with HP-NAP and other *H. pylori* factors, promotes the preferential development of *H. pylori*-specific Th1 cells secreting IFN-γ and TNF-α[97].

A strong long-lasting Th1 polarized response would lead to gastric immunopathology if not fine-tuned by appropriate regulatory mechanisms. On the other hand, in other infectious and noninfectious immunopathological conditions, an extreme polarization of Th2-cell responses is responsible for disease. These Th2-dominated diseases, such as helminthes infection or atopy, or conditions in which an effective Th1 response is desired (vaccinology and cancer immunotherapy), could benefit from a powerful Th1-polarizing signal, such as HP-NAP. This signal could boost the Th1-polarizing capacity of DCs and redirect

the predominant Th2-cell response into a balanced, less pathogenic mixed Th1/Th2 response[98].

### 1.6.3 Immunosuppression of Th2 responses by *Helicobacter pylori* neutrophil-activating protein

Recently it has been demonstrated that the develop of pathologies which elicit a Th2 response could be mitigated by agents able to induce a Th1 immune response. Epidemiological studies and experimental data provided evidence suggesting that infectious diseases can influence the development of allergic disorders[99]. Moreover an inverse correlation between the onset of allergic disorders and the incidence of infections[100] was observed. This phenomenon can be explained with the inhibition of the allergic Th2 inflammation by Th1 responses elicited by infectious agents, able to induce the production of IFN-γ, IL-12, IL-18 and IL-23[100,101]. This view is supported by studies showing that animals can be protected from developing asthma by using live or killed bacteria or their components, which induce Th1 responses[101,102].

The *Helicobacter pylori* neutrophil-activating protein (HP-NAP) produced by the Gram-negative bacterium *H. pylori*, by acting on both neutrophils and monocytes via toll-like receptor (TLR2) agonistic interaction, was demonstrated to induce significantly an IL-12 and IL-23-enriched milieu[103] that has the potential of driving the differentiation of antigen stimulated T cells towards a polarized Th1 phenotype[104,105]. Accordingly, addition in culture of HP-NAP to allergen-induced T cell lines resulted in a remarkable increase of IFN-γ-producing T cells and decrease of IL-4-secreting cells[103].

Recently it has been demonstrated that the protein HP-NAP could immunosuppress the Th2 responses during *Trichinella spiralis* infection. In this study groups of *T. spiralis*-infected BALB/c mice received i.p. HP-NAP treated mice showed less eosinophilia and had higher IL-12 and IFN-γ levels and lower IL-4 and IL-5 levels, providing evidence that HP-NAP enhances endogenus IL-12 and IFN-γ response and exerts a powerful anti Th2 activity *in vivo*, targeting both IL-5-induced eosinophilia and IL-4-mediated hyper-IgE responses induced by parasitic infection[106].

The ability of HP-NAP to down modulate the Th2 immune response by eliciting a Th1 responses was observed also in the development of ovalbumin (OVA)-induced asthma in mouse. In this model was demonstrated that both systemic and mucosal administration of HP-NAP strongly inhibit the development of airway eosinophilia and bronchial inflammation stimulated by OVA treatment. Likewise, HP-NAP treatment strongly affected the lung cytokine release, reducing the production of IL-4, IL-5 and Granulocyte-macrophage colony-stimulating factor (GM-CSF). These findings provide the indication that both systemic administration and mucosal administration of HP-NAP are effective in preventing allergic asthma.

For this reason, it has been suggested that HP-NAP may represent a novel immune modulating agent[97] and might be a possible new tool for therapeutic strategies aimed to redirect Th2 into a less aggressive Th1 response[102].

# 2. AIM OF THE PROJECT

There are several experimental data sustaining a central role of inflammatory chemokines and cytokines in the develop of alveolitis in interstitial lung diseases. These data are confirmed by influence that the hyper-expression of chemokines/cytokines or down-regulation of its receptors could have on regulation of lung inflammation or on modulation of lymphocyte T CD4+ Th1/Th2 type response. Recent studies demonstrated that the recruitment of Th1 or Th2 is dependent by the bioavailability in the inflammatory milieu of specific subsets of chemokines and respective receptors. The Th1 type inflammation shows a differential expression of CXCL9, CXCL10, CXCL11, CXCL16, MIP1α and CCR5, whereas chemokines and its receptors as TARC, MCP1, CCR3 and CCR4 are preferentially expressed during the Th2 type response. The chemokines are crucial during the evolution of ILD to fibrosis. It has been demonstrated that the expression of pro-fibrosis chemokines is locally up-regulated by the interaction epithelium-fibroblasts and matrix-inflammatory cell. The model mouse of inflammation and fibrosis induced by bleomycin is an valuable tool to understand the role of chemokines and cytokines involved in lung inflammatory response and the mechanism of its regulation. A particular interest for the signal transduction downstream to pro-inflammatory stimuli is recently emerged by the fact that some molecules, involved in the cell signaling cascade, resulted to be important regulator of inflammatory response. Particularly our attention focused on the GSK-3 kinase and HP-NAP protein.

The kinase GSK-3 is an important mediator in the signal transduction pathway downstream of inflammatory stimuli and could have a pivotal role also in

the pathogenesis of lung pro-inflammatory diseases. GSK-3 is constitutively expressed in several cell types, is involved in several signal transduction pathways, as the PI(3)K, stimulating the production of IL-10 and down-regulating contemporary the expression of pro-inflammatory cytokines as IL-1β, IL-12, IL-6, TNF, IFN-γ. Since in the model mouse of IPF induced by bleomycin, the inflammatory Th2 type response is activated through the regulation of transcription factors NF-kB, mediated by pro-inflammatory cytokines, it is possible that GSK-3 inhibition had an effect on pulmonary inflammation bleomycin-induced and particularly on regulation of pro-fibrotic chemo-cytokine milieu.

Recently it has been shown that the *Helicobacter pylori* neutrophil-activating protein (HP-NAP), produced by the Gram-negative bacterium *H. pylori*, by acting on both neutrophils and monocytes *via* toll-like receptor (TLR2) agonistic interaction, significantly contributes to induce an IL-12 and IL-23-enriched milieu that has the potential of driving the differentiation of antigen stimulated T cells towards a polarized Th1 phenotype. Moreover epidemiological studies and experimental data provided evidence that infectious diseases can influence the development of allergic disorders [99]. In fact it has been demonstrated an inverse correlation between the onset of allergic disorders and the incidence of infections[100]. This phenomenon can be explained with the inhibition of the allergic Th2 inflammation by Th1 responses elicited by infectious agents, able to induce the production of IFN-γ, IL-12, IL-18 and IL-23[100,101]. This view is also supported by studies showing that model mouse can be protected from developing asthma by using live or killed bacteria or their components, which induce Th1 responses[101] .

Taking advantage of these quoted findings and using the bleomycin-induced IPF model mouse, in this research project we studied the effect of pharmacologic GSK-3 inhibition and the effect of HP-NAP treatment on IPF development induced by bleomycin. Particularly our attention focused on:

- the evolution of the early phases of the bleomycin-induced inflammatory process in term of qualitative and quantitative determination of the different cell populations involved;
- the level of the cytokines and chemokines involved in the inflammatory network;
- the expression of transcriptional factors involved in the Th1/Th2 differentiation;
- extent and quality of pulmonary fibrosis.

# 3. MATERIALS AND METHODS

## 3.1. DRUGS

Betadine: povidone-iodine (PVPI) topical antiseptics (B/BRAUN, Milan, Italy).

Zoletil: combination of a dissociative anesthetic agent, tiletamine hypochloride, and a tranquilizer, zolazepam hypochloride (Virbac.srl, Milano, Italy). This drug is used for injection anaesthesia in dogs, cats, wild and zoo animals. It produces dose-dependent sedation to general anesthesia.

Bleomycin: glycopeptide antibiotic (Aventis Pharma SpA, Varese, Italy) produced by the bacterium *Streptomyces verticillus*. This drug acts by induction of DNA strand breaks and it is used in the treatment of several diseases, such as Hodgkin lymphoma (as a component of the ABVD regimen), squamous cell carcinomas, testicular cancer, pleurodesis as well as plantar warts.

SB216763: highly selective GSK-3 inhibitor (Sigma-Aldrich, St. Louis, MO, USA). This compound is an arylindolemaleimide that inhibits GSK-3 in an ATP competitive manner [3,107].

HP-NAP: the *Helicobacter pylori* neutrophil-activating protein, kindly provided by De Bernard M., PhD, University of Padua, (VIMM, Venetian Molecular Medicine Institute).

## 3.2. ANIMALS AND MODEL MOUSE DEVELOPMENT

In this study we used C57BL/6N female and male mice (12 weeks old, about 25-30gr of weight), purchased from Charles River (Charles River Laboratories

Inc., Milan Italy). Experimental protocols were reviewed and approved by the local Animal Care Committee of the University of Padova. In this project we developed a model mouse of pulmonary fibrosis by bleomycin instillation.

### 3.2.1 Bleomycin instillation

The animals were removed from the chamber, shaved, prepped with an betadine solution, and anaesthetized by intraperitoneally injection of 0.02ml of Zoletil 100 (4mg/ml). The intact trachea was exposed with blunt dissection, and a 1-cm length of trachea was elevated and supported intact. Bleomycin (0.125 U; 100µl of a 3.0 U/ml solution in sterile saline) was administered with a 23-gauge needle and a 1-ml syringe and injected directly into the tracheal lumen. The incision in the skin of the neck was closed with two to three wound clips.

### 3.2.2. SB216763 and HP-NAP administration

**SB216763 treatment**

The SB216763 (0.5mg; 25µl of a 20mg/ml solution in DMSO (Dimetilsulfosside, Sigma) 25%, PEG 400 (polietilen glicole 400, Fluka) 25% and sterile saline 50%) was intravenously administrated (i.v.) at day 0 and than intraperitoneally (i.p) twice at week until day 28.

SB216763 was administered to evaluated the effect on fibrosis of GSK-3 inhibition. Initially, to create survival curves sixty mouse were differently randomized to receive phosphate buffer solution (PBS), PBS plus SB216763 and DMSO as control, Bleomycin and Bleomycin plus SB216763. The treatment with

DMSO was performed to prove the appropriate control for the SB216763 instillation, since the DMSO is the vehicle of the SB216763 compound. The healthy status of the mice was followed for 28 days.

To study the effect on fibrosis development by GSK-3 inhibition with SB216763 treatment, the mice were differently randomised in 5 cohorts (n=16 for each cohort) to receive PBS, PBS plus SB216763 and DMSO as control, Bleomycin and Bleomycin plus SB216763 for the fibrosis develop investigation.

At day 0, day +2, day +7 and day +28, four mice belonging to each cohorts, were sacrificed by $CO_2$ inhalation for BALF evaluation and histological analysis. The experiment was repeat 3 times. Moreover to determine the effect of GSK-3 blockade on fibrosis after that the fibrotic phases was already established, we administered the inhibitor SB216763 at day +14 (late treatment) from the administration of bleomycin (20 mice, four for each treatment), and sacrificed at day +28. The experiment was repeated 3 times.

**HP-NAP treatment**

The HP-NAP (10μg in PBS solution) was intravenously administrated (i.v.) at day 0 and than intraperitoneally (i.p) twice at week until day 28. HP-NAP was administered to evaluated the effect on develop of bleomycin-induced fibrosis. Again, to create survival curves forty-eight mouse were differently randomized in 4 cohort to receive phosphate buffer solution (PBS) and HP-NAP as control, Bleomycin and Bleomycin plus HP-NAP. The healthy status of the mice was followed for 28 days.

Finally to study the effect on fibrosis development by HP-NAP treatment, the mice were differently randomised in 4 cohorts (n=16 for each cohort) to

receive PBS, PBS plus HP-NAP as control, Bleomycin and Bleomycin plus HP-NAP for the fibrosis develop investigation. At day 0, day +7, day +14 and day +28, mice, four mice belonging to each cohorts were sacrificed by $CO_2$ inhalation for BALF evaluation and histological analysis. The experiment was repeated 3 times.

### 3.3 BRONCHOALVEOLAR LAVAGE

Mice were anaesthetized and a soft cannula (23G) was inserted into the trachea. Bronchoalveolar lavage (BAL) was performed three times by the instillation and withdrawal of 0.3 ml of saline at various time points. The bronchoalveolar lavage fluid (BALF) was centrifuged at 400g for 10 min at 4°C, the pellet was resuspended in 1 ml of saline, red blood cells lysed and BALF cells were then microscopically scored on a Neubauer counting chamber. The cells were used for flow cytometry analysis.

### 3.4 PROCESSING OF THE LUNGS

Four weeks after intratracheal instillation, the mice were weighed, anesthetized, heparinised, and exsanguinated via the femoral artery. The heart and lungs were removed *en bloc*; the lungs were dissected away from the external vasculature and bronchi and sectioned parasagittally, superior to inferior. The left lungs were used for the histological analysis, whereas the right ones were used for the cell isolation and molecular analysis. Liver and kidneys were also explanted,

and all the specimens were fixed in buffered 4% paraformaldehyde for morphological studies.

### 3.4.1. Histology

Lung tissues were fixed in formalin, embedded in paraffin and dissectioned in 4-5μm slices. Subsequently they were stained with Hematoxylin&Eosin (H&E), to evaluate the degree of inflammatory cell infiltration and alveolar cuboidalization and stained with Masson's trichrome to evaluate the degree of interstitial fibrosis. The degree of inflammatory cell infiltration, interstitial fibrosis and alveolar cuboidalization was evaluated using a semiquantitative subjective scoring method (as percent of lung parenchyma involved as observed microscopically): mild 0 to 30%, moderate 30 to 50%, diffuse > 50%. Moreover, to precisely quantify fibrosis, formalin-fixed paraffin-embedded lung tissue were cut at 4-5μm slides and stained with H&E for the evaluation of inflammatory cell infiltration and the entity of alveolar cuboidalization and with Heidenheim Trichrome for the extension of interstitial fibrosis. Then, each section was scanned at X 40 magnification to identify at least 5 areas (hot spots) with the largest extension of fibrosis (Trichrome staining). Each hot spot was then examined at X 200 magnification (0.949 $mm^2$/field) and the fibrosis was quantified by using digital quantitative analysis (Image Pro Plus software version 4.1, Media Cybernetics, Silver Spring MD). The mean value of the five areas was taken as representative of the whole section.

### 3.4.2. Lung homogenates preparation

Mouse lungs were minced, digested at 37°C for 1 hour in a saline solution containing collagenase IV (Sigma-Aldrich), 2% FCS and 5mM EDTA, and then filtered. The cell suspension, obtained by the filtration, was washed in saline, centrifuged at 400g for 10 min at 4°C, resuspended in buffered 30% Percoll (Amersham Biosciences, Buckinghamshire, UK) and then stratified on buffered 60% Percoll. After centrifugation at 500g for 25 min, without brake, mononuclear cells were recovered from the interface between the 30% and 60% Percoll gradients (Figure 3.1) and washed three times with cold PBS by centrifugation at 400g for 8 min at 4°C . Total cell counts and viability were determined.

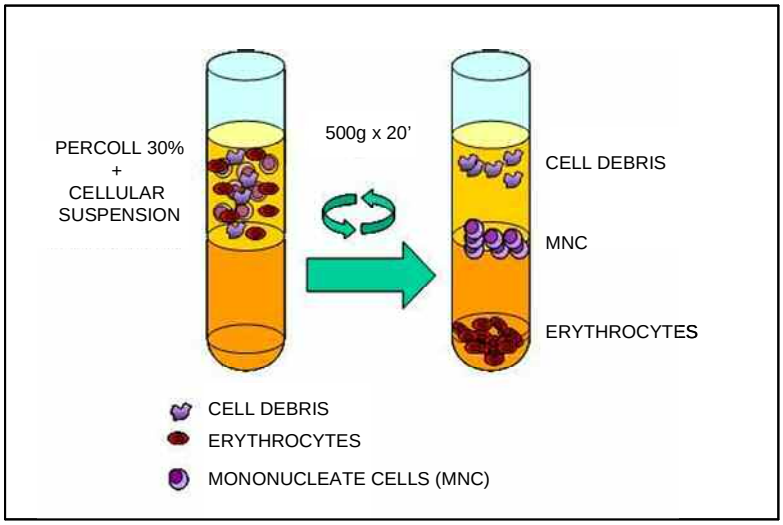


**Figure 3.1 Distribution of mononuclear cells, erythrocytes, and cell debris after treatment with Percoll of lung homogenates preparation.**

## 3.5 FLOW-CYTOMETRY ANALYSIS AND CELL SORTING OF LUNG CELLS

### 3.5.1 Flow-cytometry analysis

The surface antigens expression of cells recovered by the lung homogenates preparation of different treated mice groups, at the different time courses, were evaluated by flow-cytometry analysis.

Flow cytometry is a powerful and effective tool for analyzing the structural and functional characteristics of cells or particles in suspension. It allows simultaneous multiparametric analysis of the physical and/or chemical characteristics of single cells flowing through an optical and/or electronic detection apparatus. A tube containing a single cell suspension is placed on the instrument where the sample is pushed by air under pressure through tubing where it is injected into a nozzle. The nozzle, containing sheath fluid under pressure, hydrodynamically focuses the cells so that they exit the nozzle in single file down the center of the stream resulting in laminar flow. The flow rate can be controlled by adjusting the differential pressure between the sheath fluid and the sample injection pressure. Laser light is then focused onto the stream where each cell is excited as it passes through the laser beam. Photo multiplier tubes (PMT's) are detectors which collect the photon emissions from each "event" and convert them to analog voltages. The analog signals are then digitized by analog to digital converters (ADC's) and recorded as data files. Optical filters are placed before the detectors so that only wavelengths of light corresponding to specific fluorochrome emissions are collected by each detector (e.g. FITC emits in the green region

therefore a 30 nm bandpass filter centered at 520 nm could be used to collect light from this fluorochrome). Light scattered at the same wavelength and direction as the laser light, primarily from the surface of the cell, correlates with relative cell size (Forward Angle Light Scatter) while light scattered 90 degrees to the laser (Side Scatter) usually from internal structures, correlates with granularity. By correlating these two parameters, one can discriminate subpopulations of cells, for example, in peripheral blood samples. Signals corresponding to cell debris or cell aggregates can also be detected and excluded from analysis on the basis of forward and side scatter. Staining cells with multiple fluorochromes conjugated to antibodies or fluorochromes directed at other specific targets such as DNA, cytokines, or other proteins, distinguishes cell subpopulations which can be quantified. Data is displayed and analyzed using histograms or two-dimensional dot plots on a computer system.

In this study have been utilized as fluorochromes the fluorescein isothiocyanate (FITC) and the phycoerythrin (PE): both fluorochromes are excited at a wavelength of 488nm by the argon laser of cytofluorimetry. The spectrum emission for the FITC fluorochromes is the green light (530±30nm), instead the spectrum emission for the PE fluorochromes is the red light (585±42nm). The protocol requires a double direct staining: BALF cells were resuspended in FACS buffer (Sigma-Aldrich) and incubated with PE and FITC-conjugated anti-mouse monoclonal antibody (Ab) $CD3^+$, $CD4^+$, $CD8^+$, $Gr1^+$, $Mac1^+$ (BD PharMingen, San Diego, CA, USA) for 30 minutes at 4°C. After the incubation the samples were centrifuged at 500g for 10 minutes and the cells resuspended in saline. Flow cytometry was performed after gating on the lymphocyte population using a FACSCalibur analytical flow cytometer (Becton-Dickinson Immunocytometry

Systems, Mountain View, California, USA) and analyzed using CellQuest Pro software (BD bioscience, San Jose, CA). For each sample were acquired $1x10^4$ events.

### 3.5.2 Cell sorting

Subpopulations of cells or particles that have been resolved by fluorescence or physical parameters can be isolated for further experimentation by using the instrument's cell sorting capability. A pizo-electric quartz crystal connected to the nozzle causes the cell stream to oscillate and form droplets. The droplets are formed at a high enough frequency so that any given droplet will contain only one cell. When a cell meets the criteria defined by sort "windows", the sorting electronics system places a charge on the cell stream at exactly the time when the droplet containing the cell of interest is breaking off from the stream. The droplet passes between two metal plates that have a very high voltage. The resulting magnetic field forces the charged droplet to be deflected toward the plate with the opposite charge. By placing a collection vessel in the deflected droplet's path, cell populations up to 99% purity can be collected at rates of approximately one thousand per second. The current flow cytometer can sort two populations at the same time.

In this study T $CD4^+$ lymphocytes and $Mac1^+$ macrophages were double-labeled using mouse monoclonal Ab anti $CD4^+$ and $Mac1^+$ (BD Pharmingen) and FACS-sorted from the lung cells suspension by FACSAria cell sorter (BD Bioscience) according to the manufacturer’s instructions.

## 3.6 MOLECULAR ANALYSIS: REAL-TIME PCR (RT-PCR)

RT-PCR (reverse transcription-polymerase chain reaction) is a sensitive method for the detection of mRNA expression levels. Traditionally RT-PCR involves two steps: the reverse transcription (RT) reaction and PCR amplification. RNA is first extracted and reverse transcribed into cDNA using a reverse transcriptase, the resulting cDNA is than used as templates for subsequent PCR amplification using specific primers. The use of DNA-binding fluorescent dyes, such as SYBR® Green, to detect and quantitate the PCR product, allows quantitative PCR to be performed in real time. Real-time PCR, using labeled oligonucleotide probes, employs two different fluorescent reporters and relies on the transfer of energy from one reporter (the energy donor) to the second reporter (the energy acceptor) when the reporters are in close proximity. The second reporter can be a quencher or a fluor. If the second reporter is a fluor, the energy can be absorbed and re-emitted at another wavelength through fluorescent resonance energy transfer (FRET), and the progress of the reaction can be monitored by the decrease in fluorescence of the energy donor or the increase in fluorescence of the energy acceptor. During the exponential phase of PCR, the change in fluorescence is proportional to the accumulation of PCR product. To simplify quantitation, specially designed instruments perform both the thermal cycling steps to amplify the target and the fluorescence detection to monitor the change in fluorescence in real time during each PCR cycle so the progress of the reaction and accumulation of PCR product is monitored by the resulting increase in fluorescence. The amount of cDNA must be done where the amplification is logarithmic. In Real-Time PCR the cycle number at which the increase in

fluorescence (and therefore cDNA) is logarithmic is calculated (the threshold line) and the point at which the fluorescence crosses the threshold line is called the Ct. DNA-binding dyes are easy to use but do not differentiate between specific and nonspecific PCR products, for this reason, with this approach, preliminary experiments must be performed prior to the quantitation experiments to discriminate between the signal generated by the desired PCR product and the signal generated by the nonspecific amplification. The software plots the rate of change of relative fluorescence units (RFU) with time (T) (-d(RFU)/dT), and this will peak at the melting temperature (Tm). A nonspecific amplification would give a pick of fluorescence whit a different melting temperature with respect to PCR product of interest.

### 3.6.1 RNA Extraction

Total RNA was purified from total sorted T $CD4^+$ lymphocytes and $Mac1^+$ macrophages by the Rneasy Mini Kit Protocol QIAGEN. Following the procedure of the protocol:

- $<4x10^6$ cells were resuspended in lysis buffer (350µl of RTL buffer, 1% β mercaptoetanol 14,5M, Sigma) and homogenized by passing the lysate at least 5 times through a blunt 20-gauge needle fitted to an RNase-free syringe;
- to the lysate was added 1 volume of 70% ethanol and the mixture was mixed by pipetting, transferred to a RNeasy spin column placed in a collection tube and centrifuged for 1 minute at 11000 rpm. The flow-through was discarded and the collection tube was reused;

- to the spin column were added 700µl of RW1 buffer (wash buffer) and centrifuged for 1 minute at 11000 rpm to wash the spin column membrane. The flow-through was discarded and the collection tube was reused;
- to the spin column was added 80µl of DNA digestion solution (RDD buffer, 70µl, plus DNAse I, 10µl of a 2,7 kunits/µl solution in sterile saline, QIAGEN) and incubated for 30 minutes at room temperature to eliminate the genomic DNA;
- after the incubation, to the spin column were added 500µl of RPE buffer (wash buffer) and centrifuged for 1 minute at 11000 rpm to wash the spin column membrane. The flow-through was discarded and the collection tube was reused;
- to the spin column were added again 500µl of RPE buffer (wash buffer) and centrifuged for 2 minutes at 12800 rpm to wash the spin column membrane. The RNeasy spin column was placed in a new 1.5ml collection tube;
- to elute the RNA, 30µl of RNase free $H_2O$ were added to the spin column and centrifuged for 1 minute at 11000 rpm;

### 3.6.2 cDNA syntesis

The cDNA was synthesized from the extracted RNA (see 3.6.1) by the Reverse Transcription System Kit (Promega). This system is based on the use of random primers and the Avian Myeloblastosis Virus (AMV) Reverse-Transcriptase Activity[108]. This enzyme synthesizes single-stranded cDNA from total or poly(A)+ isolated RNA by its polymerase 5'-3' activity and its RNasi H

3’-5’ activity which degrades the RNA filament of the double RNA-DNA helix formed during the cDNA syntesis. Following the procedure of the protocol:

- a master mix was prepared and aliquotated in volumes of 20µl for each sample. The master mix is composed of MgCl2 25mM, buffer RT 10X, dNTPs mix 10mM, RNase inhibitor 40µg/µl, AMV reverse-transcriptase 25µg/µl, random primers (dT) 0,5µg/µl, RNA 0,2µg and RNase free $H_2O$ to volume;
- the samples were incubated for 15minutes at 42°C, for 5 minutes at 95°C and than cooled in ice to block the reaction;
- the cDNA obtained was conserved at -80°C or directly used for a PCR reaction (RT-PCR);

### 3.6.3 mRNA expression levels quantification by RT-PCR

In this study the cDNA obtained from the subcellular populations ($CD4^+$ and $Mac1^+$) of mice differently treated were quantified by RT-PCR. For each sample were amplified the genes of interest (T-bet, GATA3, IL-4, IFN-γ, TNF-α, IL10 and MCP1 for the T lymphocytes $CD4^+$, TNF-α and MCP-1 for the macrophages $Mac1^+$) and the housekeeping mouse gene β-actin as internal calibrator. The primers used in this project (Table 2), were designed with the program Primer Express (Applied Biosystem), so that they could discriminate between the cDNA and the genomic DNA to avoid amplification of contaminant genomic DNA. These primers amplified a PCR product between 150 and 300 bp, had a GC content >50% and an annealing temperature of 60°C.

**Table 2. Primers for RT-PCR.**

| | | | |
|---|---|---|---|
| **β-ACTIN** | | **IFN-γ** | |
| *Forward* | GAGAGGGAAATTCGTGCGTA | *Forward* | TTGCCAAGTTTGAGGTCAAA |
| *Reverse* | ACATCTGCTGGAAGGGTGGC | *Reverse* | CCTTTTCCGCTTCCTGAGG |
| **T-bet** | | **MCP-1** | |
| *Forward* | TGTGACCCAGATGATCGTCT | *Forward* | GCCAGCTCTCTCTTCCTCCAC |
| *Reverse* | CTGAGTGATCTCTGCGTTCTT | *Reverse* | GCGTTAACTGCATCTGGCTA |
| **GATA3** | | **IL-10** | |
| *Forward* | CTGTCGGCAGCAAGGAGAG | *Forward* | TAAGGGTTACTTGGGTTGCA |
| *Reverse* | CTCTAACCCATGGCGGTGAC | *Reverse* | TGCTCCACTGCCTTGCTCTT |
| **IL-4** | | **TNF-α** | |
| *Forward* | CAGCAACGAAGAACACCAG | *Forward* | TCTATGGCCCAGACCCTCAC |
| *Reverse* | GCATCGAAAAGCCCGAAAG | *Reverse* | GTTTGCTACGACGTGGGCTAC |

The protocol used for the amplification, requires, for each sample to be analyzed, a solution composed by SYBER GREEN (Invitrogen), PCR master mix 2X, primers forward and reverse (10pM/μl), $H_2O$ RNase-free, and cDNA to a final volume of 15μl. The RT-PCR was performed using the following conditions: UNG (uracil N-glycosilase, present in the master mix) activation at 50°C for 2min and Taq Gol Polymerase (Applied Biosystem) activation at 95°C for 10min, followed by 50 cycles of DNA denaturing at 95°C for 15 seconds, primers annealing at 60°C for 30 seconds and extension at 72°C for 1 minute. Each reaction of amplification was performed in duplicate and a negative control was included in each run.

### 3.6.4 Data analysis

Amplification, detection, and data analysis were performed using the ABI PRISM 7000 sequence detection system (Applied BioSystem, Foster City, CA). The quantification of mRNA levels was obtained by a method of relative quantification, the Delta-Delta Ct method (2-DDCt), following the instructions of the manufacturer (Applied Biosystems). The mice treated with saline or plus

SB216763 have been used as internal calibrator of the samples. Once set the threshold line and the baseline, the corrispective Ct values were calculated. For each sample were calculated:

1. $DCt_n = Ct_n(gene) - Ct_n$ (β-actin)
2. $DDCt_n = Ct_n(sample) - Ct_n$ (internal calibrator)
3. Relative Quantification= $2^{-DDCtn}$(sample)

In this way for each sample has been calculated a value which represents the relative genic quantification, compared to the sample used as internal calibrator and considered of value 1.

**3.7 TUNEL ASSAY**

The Tunel assay was performed on cells from lung biopsy. Following the procedure of the protocol:

1. single cells (1-2X$10^6$) were re-suspended in 500ul PBS;

2. a volume of 5ml 1% paraformaldehyde was added to the cell suspension and the mixture incubated on ice 15'; then the cells were pellet and the supernatant removed;

3. cells were washed for 2X in PBS (5ml) and re-suspend in 500ul PBS;

4. to cell suspension were added 5ml of ice cold 70% Ethanol. The samples were incubate on ice for 30'. (Cells may be stored in 70% Ethanol at –200C for several days.) The cells were pellet, washed 2X in wash buffer and pellet again;

5. cells were re-suspend in 50ul DNA Labeling Solution Reaction and incubated at 37ºC, 60'. Cells were vortex every 15' to re-suspend;

7. each tube of cells was washed 2X with 1.0ml Rinse buffer and pellet. Cell pellets was re-suspend in 100ul Antibody Solution Reaction and incubate at room temp., in the dark, 30';

8. PI/RNase Staining solution (900ul) was added and cells incubated in the dark, at room temp., 30';

9. the cells were analyze within 3 hours by flow cytometry.

**Reagents**

dH2O PBS, Ca++, Mg++-free

70% (v/v) Ethanol

1% (w/v) paraformaldehyde/PBS

APO-BRDUTM Apoptosis Kit – BD PharMingen Cat.# 6576KK

(Trademark of Phoenix Flow Systems, San Diego, CA) contains:

FITC labeled anti- BrdU mAb Reaction buffer

PI/RNase staining soln. Rinse buffer

Negative Control cells Wash buffer

Positive Control cells TdT enzyme

Br-dUTP

DNA Labeling Soln. Antibody Soln./1 reaction

TdT Reaction buffer 10.00ul FITC labeled anti- BrdU mAb 5.00ul

TdT enzyme 0.75ul Rinse buffer 95.00ul

Br-dUTP 8.00ul Total volume 100.00ul

dH2O 32.25ul

Total volume 51.00ul

## 3.8 CELL LINE CULTURE

A549 cells were cultured at in Dulbecco's modified Eagle's medium (Gibco) supplemented with and 20% fetal bovine serum (Gibco) at 37 °C, in a humidified incubator with an atmosphere of 5% $CO_2$. Cell were plated at concentration of $0.2x10^6$ cells/ml of medium at once at confluence were treated with bleomycin 5, 8 and 10 μM for 24, 48 and 72 hours for sequent zymography assay and p65 phosphorylation assay.

## 3.9 ZYMOGRAPHY ASSAY

Zimography is a electrophoretic technique that allows the measure of gelatinolytic activity of matrix metalloproteinases present in culture medium. The cell line A549 was incubated in DMEM, without FBS, alone or with bleomycin 5, 8 and 10 uM. After 24h the supernatant was collected and centrifuged to remove residual cells. The samples were resuspended in a sample buffer containing 62.5mM Tris-HCl (pH 6.8), 10% glycerol, 2% SDS, and 0.00625% (w/v) bromophenol blue, then were agitated for 20min at room temperature and loaded without boiling onto 7.5% acrylamide/bisacrylamide (29.2:0.8) separating gel containing 0.1% (w/v) gelatine (Sigma-Aldrich). Substrate gel zymography was performed with a Mini-Protein II apparatus from Bio-Rad (Hercules; CA) and electrophoresis was carried out at a constant voltage of 100V. After electrophoresis, the gels were soaked in 0.25% Triton X-100 (2×30min) at room temperature and rinsed in sterile water. The gels containing gelatine were incubated at 37°C for 16h in the incubation buffer containing 50mM Tris–HCl

(pH 7.6), 20mM NaCl, 5mM $CaCl_2$. The gels were then stained for 15–30min in 0.1% (w/v) Coomassie blue R-250 (Amersham Biosciences) in 30% methanol and 10% acetic acid, and destained in the same solution without the Coomassie blue dye. The clear bands on the blue background represent gelatin digestion by the MMP-9 present in the samples. The bands were quantified using the analysis system densitometry GelDoc 2000 - QuantityOne software (Bio-Rad).

### 3.10 p65 phosphorylation assay

Cells ($5x10^5$ for each assay) were prepared by cell lyses with Tris 20mM, NaCl 150mM, EDTA 2mM, EGTA 2mM, Triton X-100 0.5% supplemented with complete protease inhibitor cocktail (Roche; Mannheim, Germany) and sodium orthovanadate 1mM (Calbiochem; Gibbstown, NJ). Samples were then subjected to SDS/PAGE (10% gels), transferred to nitrocellulose membranes, and immunostained with anti-p65 monoclonal antibody (Upstate, Milan, Italy), anti-phospho p65 (Ser536) policlonal antibody (Upstate, Milan, Italy) and anti-β-actin monoclonal antibody (Sigma-Aldrich; Milano, Italy) using an enhanced chemiluminescent detection system (Amersham Biosciences; Buckinghamshire, UK).

### 3.11 STATISTICAL ANALYSIS

Data are expressed as means ± SD. Statistical significance was determined by one-way ANOVA test. For all analyses, $p < 0.05$ was accepted as statistically significant.

# 4. RESULTS

## 4.1 INVESTIGATION OF GSK-3 ROLE IN DEVELOPMENT OF ALVEOLITIS AND PULMONARY FIBROSIS IN A BLEOMYCIN-INDUCED IDIOPATHIC PULMONARY FIBROSIS MODEL MOUSE

In this first part of the project we evaluated the role of GSK-3 on alveolitis and fibrosis development in a bleomycin (BLM)-induced Idiopathic Pulmonary Fibrosis model mouse in order to better characterize this disorder and identify new therapeutic strategies. To this purpose, in the model mouse, we inhibited GSK-3 by the compound SB216763, a specific GSK-3 inhibitor ATP competitor. The effect of GSK-3 inhibition was evaluated by considering:

- the survival of treated mice;
- the evolution of the early phases of the inflammatory process in term of qualitative and quantitative determination of the different cell populations involved (T lymphocytes, neutrophils, macrophages);
- the level of the cytokines (IL-4, IL-10 and IFN-γ) and the transcriptional factors (T-bet and GATA3) involved in the Th1/Th2 differentiation;
- lung histopathological examination in terms of inflammation, epithelial cell cuboidalization and fibrosis;
- apoptosis of lung epithelial cells.

Some experiments were performed also *in vitro*, using the cell lines A549. In these experiments has been considered the MMP-9 realising by the cell line in the culture medium, since MMP-9 is a pivotal enzyme in the remodelling of lung during fibrosis establishment. We also evaluated the transcription factor p65, member of NF-κB family, for its important role in survival and proliferation after phosphorylation by GSK-3.

### 4.1.1 Effect of the *in vivo* administration of the GSK-3 inhibitor SB216763 in survival of mice treated with bleomycin intratracheal instillation

In this group of experiments we evaluated the putative *in vivo* toxicity of SB216763, the compound we used to inhibit GSK-3. Five different cohorts of C57BL6 mice were than randomized to receive intratracheal instillation of either saline (n=12), BLM (n=12), saline plus SB216763 (n=12), saline plus vehicle (n=12) or BLM plus SB216763 (n=12). The vehicle for SB216763 is the DMSO, that we used as internal control to eliminate the possibility that the effects on survival of GSK-3 inhibition could be dependent on DMSO itself and not on SB216763 activity. The health status of differently treated mice was followed for 28 days.

As it is possible to observe by survival curves (Figure 4.1), none of mice treated with saline or vehicle died. Four of 12 BLM treated mice (30%) died of respiratory distress between day +14 and day +17 after the treatment. On the contrary, none of the mice receiving saline plus SB216763 i.v. at day 0 and subsequently i.p. twice a week died, thus suggesting that *in vivo* administration of SB216763 is safe. Furthermore, the co-administration of BLM and SB216763

significantly improved the survival of BLM-treated mice ($p<0.05$), suggesting that SB216763 is protective against BLM-induced respiratory distress (Figure 4.1).

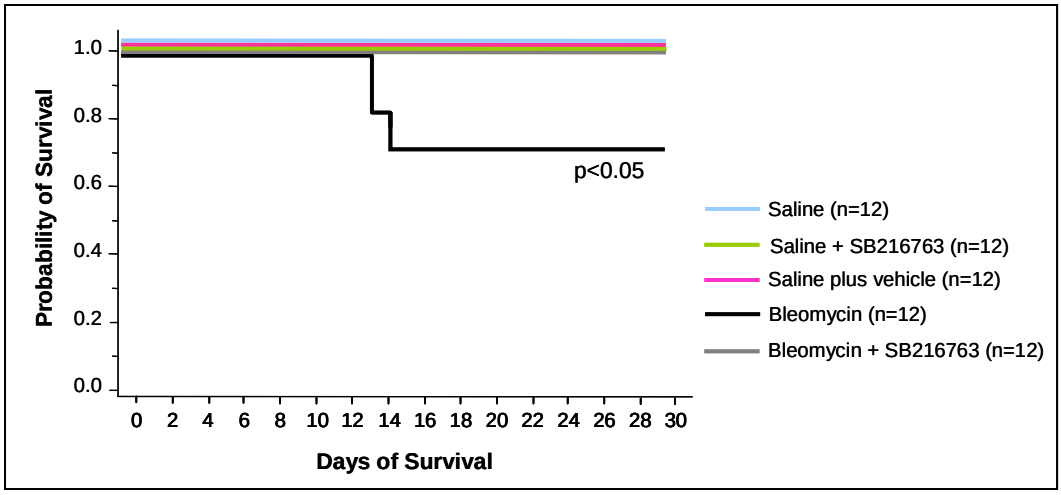


**Figure 4.1 Effect of SB216763 on the survival of BLM treated mice.** Sixty mice were differently randomized in five cohorts to receive intratracheal instillation of saline, BLM, saline plus SB216763, saline plus vehicle, BLM plus SB216763 and followed their health status for 28 days. Four of 12 BLM treated mice (30%) died of respiratory distress between day +14 and day +17 after the treatment. On the contrary, none of the mice receiving saline, saline plus vehicle, saline plus SB216763 or BLM plus SB216763 died, suggesting that SB216763 is safe and protective against BLM-induced respiratory distress ($p<0.05$).

### 4.1.2 GSK-3 modulates bleomycin-induced alveolitis

Once determined that SB216763 administration was safe, indeed it improved the survival of BLM-treated mice, we examined whether the blockade of GSK-3 could affect the dynamics of the evolution of the early phases of the inflammatory process taking place in the lung upon BLM exposure. To this aim, we analysed the bronchoalveolar lavage fluid (BALF) obtained from saline (n=4), saline plus vehicle (n=4), BLM (n=4), saline plus SB216763 (n=4) or BLM plus SB216763 (n=4) -treated mice at +2, +7 and +28 days after treatment. The experiment was repeated 3 times. We observed that BLM administration caused a marked alveolitis peaking at day +2

($8.3x10^6 \pm 2.51$), lasting up to day +7 ($5.7x10^6 \pm 2.1$ cells/ml of BAL) and to day +28, albeit gradual decrease ($2x10^6 \pm 0.8$ cells/ml of BAL), as demonstrated by the microscopic score of BALF total inflammatory cells (sum of macrophages, lymphocytes and neutrophils; Figure 4.2).

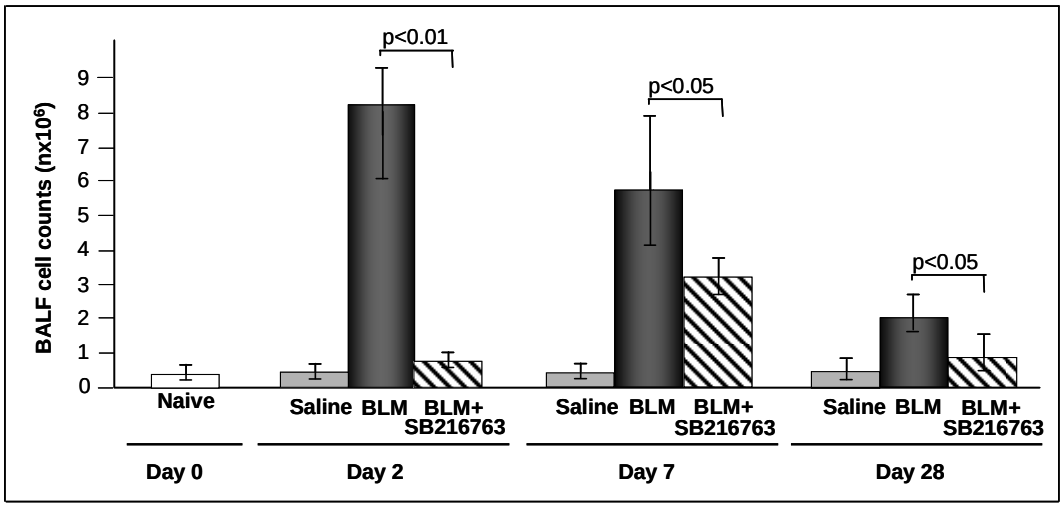


**Figure 4.2 SB216763 reduced the magnitude of BLM induced alveolitis.** Mice were treated with saline, saline plus vehicle, BML, saline plus SB216763 or BLM plus SB216763 (20mg/Kg), as described in materials and methods. We examined the broncho-alveolar lavage fluid (BALF) at day +2, +7 and +28 from the BLM instillation. We found a significant reduction of alveolitis, at day +2 ($p<0.01$), day +7 ($p<0.05$) and also day +28 ($p<0.05$), in mice treated with BLM plus SB216763 as compared to mice treated with the only BLM. Since we did not found differences between the count in the BALF of saline, saline plus vehicle and saline plus SB216763 –treated mice, in the figure are represented the results only of the saline treated group. Results represent mean ± SD of three separate experiments (n=4 *per* experiment).

Remarkably, mice randomised to receive BLM plus SB216763 showed a noteworthy reduction in the overall BALF cellularity at day +2 ($0.57 \pm 0.14$ cells/ml, $p<0.01$) which was confirmed at day +7 ($3.2x10^6 \pm 1.4$ cells/ml, $p<0.05$) and also at day + 28 ($1.05x10^6 \pm 0.6$ cells/ml, $p<0.05$). Furthermore the cytological analysis of BALF of the control groups (saline, saline plus vehicle or saline plus SB216763) did not reveal a significant alveolitis, neither at day +2 nor at day +7 and +28 ($<0.5x10^6 \pm 0.1$ cells/ml).

Then, flow cytometry analysis of BALFs allowed a qualitative determination of the different cell populations involved in BLM-induced

alveolitis, namely neutrophils ($Gr1^+/Mac1^-$ and $Gr1^+/Mac1^+$ cells), macrophages ($Mac1^+$ cells) and T-lymphocytes ($CD3^+/CD4^+$ and $CD3^+/CD8^+$ cells) (Figure 4.3).

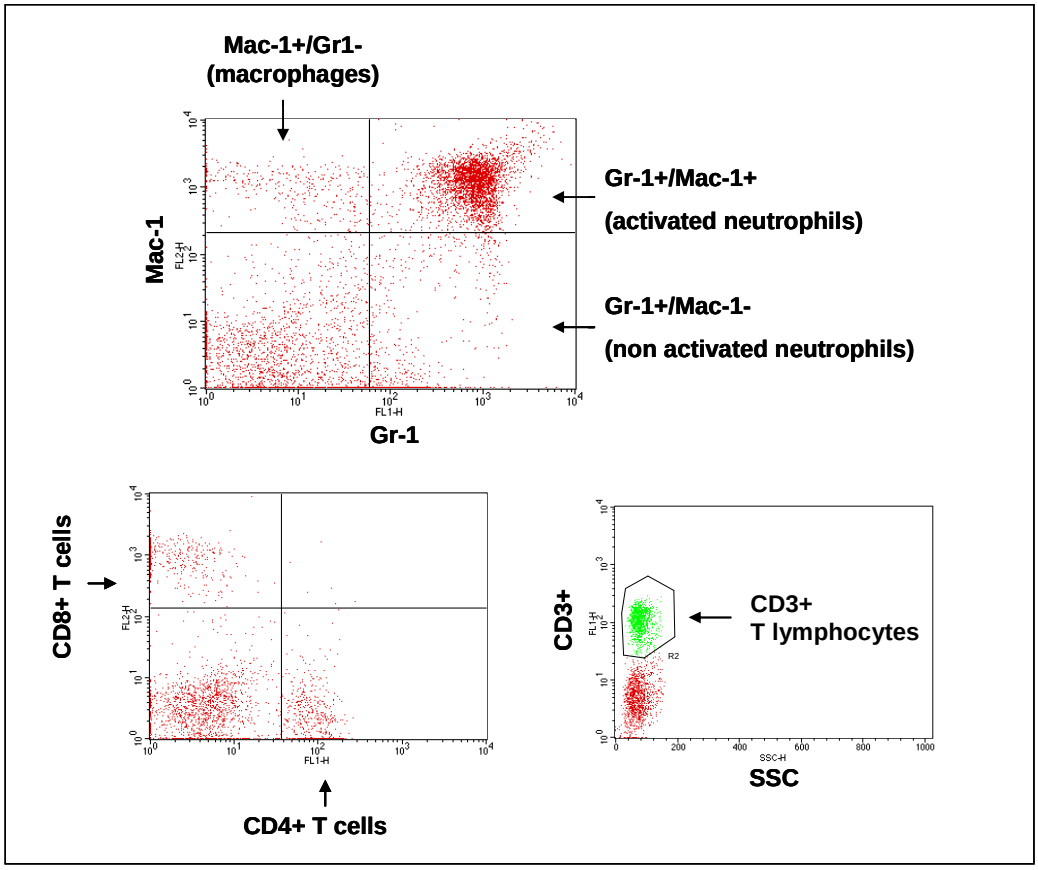


**Figure 4.3 Representative cytogram.** Cytofluorimtery analysis of BALs allowed qualitative and quantitative determination of BAL subpopulation (macrophages, total neutrophils, activated and non activated neutrophils, CD3+ T lymphocytes, CD4+ T lymphocytes and CD8+ T lymphocytes. In figure are reported the representative results of a BAL analysis of a BLM treated mouse sacrified at day +7.

Bleomycin treatment caused an important neutrophilic alveolitis as early as day +2 (66% ± 19). At day +7 the proportion of neutrophils decreased (42% ± 10) and then at day +28 increased again (72% ± 20). Anyway, comparable levels of the percentage of neutrophils in the BALFs of BLM-treated were observed in the BLM plus SB216763-treated mice at all the time-intervals analysed (day +2: 57% ± 29; day +7: 51% ± 27; day +28: 63% ± 5, Figure 4.4 A).

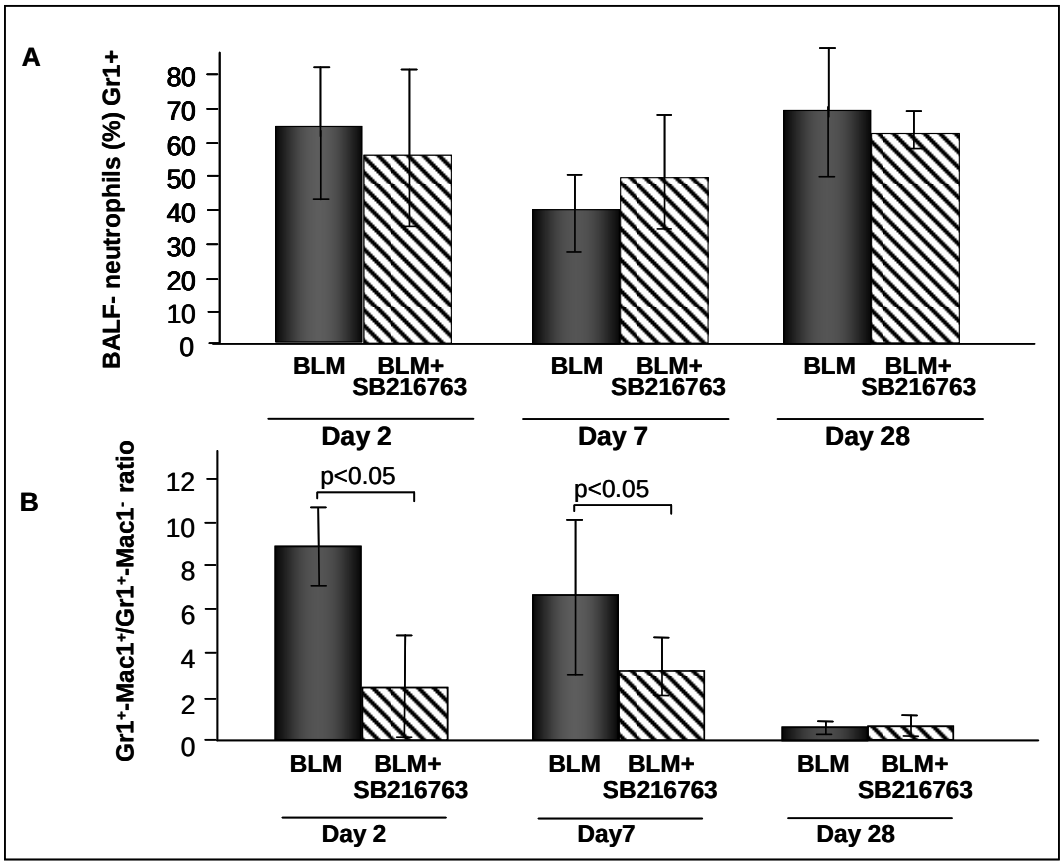


**Figure 4.4 SB216763 attenuated BLM induced alevolitis.** BALF-neutrophils ($Gr1^+$-$Mac^+$ and $Gr1^+$-$Mac^-$) were determined by flow cytometry. BLM challenge caused an important neutrophilic alveolitis at all the time-intervals analysed. Anyway, in the BLM plus SB216763-treated mice, the percentage of observed neutrophils were comparable to percentage of BLM-treated mice at all the time-intervals analysed (A). Remarkably the analysis of the ratio between activated ($Gr1^+$/$Mac1^+$) and non-activated neutrophils ($Gr1^+$/$Mac1^-$) revealed in the BLM treated mice the presence of a considerable lung infiltration of activated neutrophils at day +2 and at day +7 that gradually extinguished at day +28 (B). In fact, the ratio between activated ($Gr1^+$-$Mac1^+$) and non-activated ($Gr1^+$-$Mac1^-$) neutrophils was significantly reduced in the group of mice treated with BLM plus SB216763 compared to BLM treated mice at both day +2 and day +7 ($p<0.05$). Results represent mean ± SD of three separate experiments (n=4 *per* experiment).

However, the analysis of the ratio between activated ($Gr1^+$/$Mac1^+$) and non-activated neutrophils ($Gr1^+$/$Mac1^-$), was significantly reduced ($p<0.05$, Figure 4.4 B), at both day +2 and day +7, in the group of mice treated with BLM plus SB216763 ($Gr1^+$-$Mac1^+$/$Gr1^+$-$Mac1^-$ at day+2: 1.7 ± 1.7; at day+7: 2.8 ± 2) compared to the group of mice treated with the only BLM ($Gr1^+$-$Mac1^+$/$Gr1^+$-$Mac1^-$ at day +2: 8.6 ± 2.1; at day +7: 6.4 ± 3.9) revealing, in the BLM treated mice, the presence of a considerable lung infiltration of activated neutrophils at day +2 ($Gr1^+$-$Mac1^+$/$Gr1^+$-$Mac1^-$: 8.6 ± 2.1) that gradually extinguished giving

place to the prevalence of a non-activated population at day +7 ($Gr1^+$-$Mac1^+$/$Gr1^+$-$Mac1^-$: 6.4± 3.9) and at day +28 ($Gr1^+$-$Mac1^+$/$Gr1^+$-$Mac1^-$: 0.64 ± 0.12) (Figure 4.4 B).

In this cytofluorimetry analysis also the T $CD3^+$ percentage resulted altered in the different groups. In the BLM-treated group, as compared to saline-treated controls, a significant increase in the percentage of $CD3^+$ T lymphocytes at day +7 (58% ± 8.5) was observed and it lasted up to day +28 (63% ± 6, Figure 4.5 A).

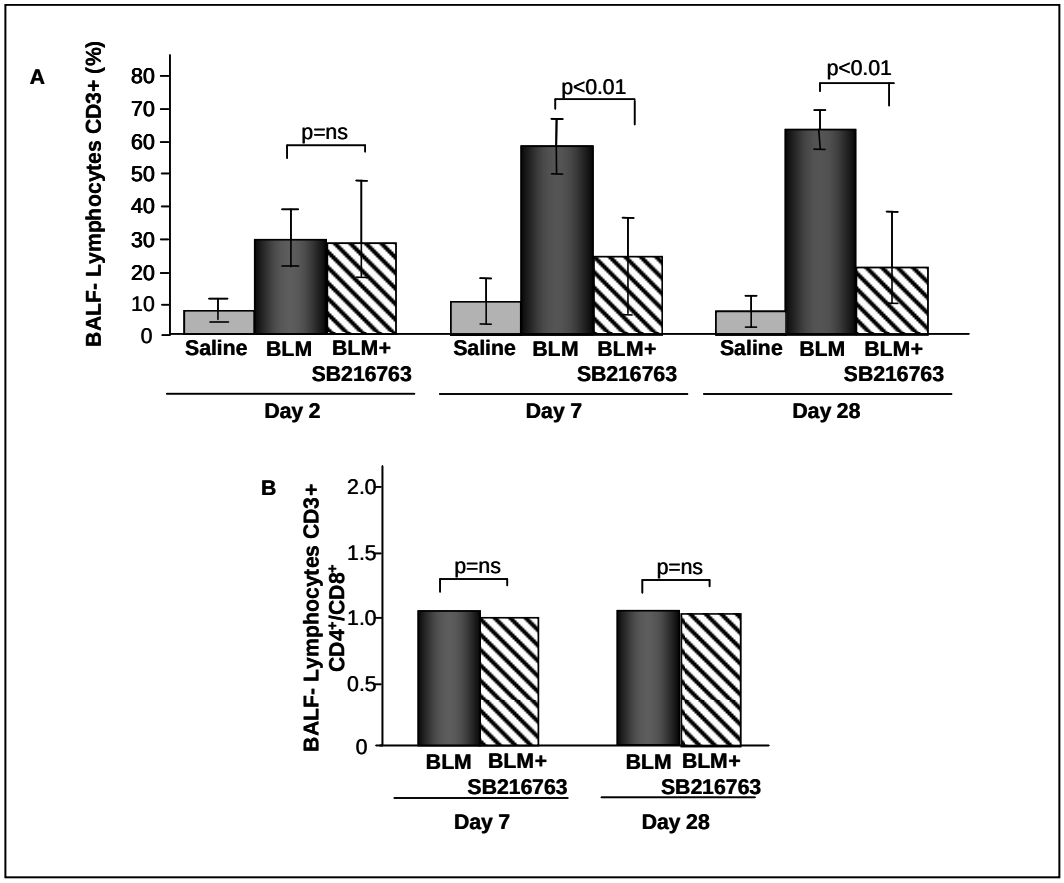


**Figura 4.5 SB216763 attenuated bleomycin induced T lymphocytes alveolitis. A)** The flow cytometry analysis of BALFs shows a significative increase of $CD3^+$ T lymphocytes at day +7 and day +28 in BLM treated mice. The co-administration of the inhibitor SB216763 reduced the level of CD3+ T lymphocytes both at day +7 and day +28 ($p<0.01$). **B)** Conversely the ratio CD4+/CD8+ did not show any differences between the group of mice treated with BLM plus SB216763 respect the group treated with the only BLM.

Bleomycin plus SB216763 administration, on the contrary, caused a clear and significant reduction in T lymphocyte percentage both at day +7 (26% ± 17,

$p<0.01$) and at day +28 (22% ± 14, $p<0.01$). No differences were observed between the two groups in terms of $CD3^+$ T lymphocyte $CD4^+$/ $CD8^+$ ratio (Figure 4.5 B). Finally, flow cytometry analysis of BALF at day +7 showed a similar increase in the percentage of $Mac1^+$ monocyte/macrophage cells in the BLM and BLM plus SB216763 groups (respectively 19% ± 12 *vs* 17% ± 8), followed by a gradual decline to baseline values at day +28.

### 4.1.3 GSK-3 modulates bleomycin-induced Th2 type inflammatory response

The role of GSK-3 in the modulation of Th2 type inflammatory response induced by BLM was evaluated by the analysis of mRNA expression levels of cytokines (IL-4, IL-10 and IFN-γ) and transcriptional factors (T-bet and GATA3) involved in the Th1/Th2 differentiation in T CD4+ cells, sorted by lungs of mice treated with saline, saline plus vehicle, saline plus SB216763, BLM and BLM plus SB216763. Each cohorts of mice (n=12) were evaluated at day +7 from the intratracheal administration of saline, SB216763, BLM and BLM plus SB216763.

In the group of BLM treated mice, with respect to the control group, the mRNA levels of IL-4 and IFN-γ showed a remarkable switch *versus* a Th2 response, as highlighted by the significant increase of IL-4/ IFN-γ ratio (6.6 ± 1.8, Figure 4.6 A).

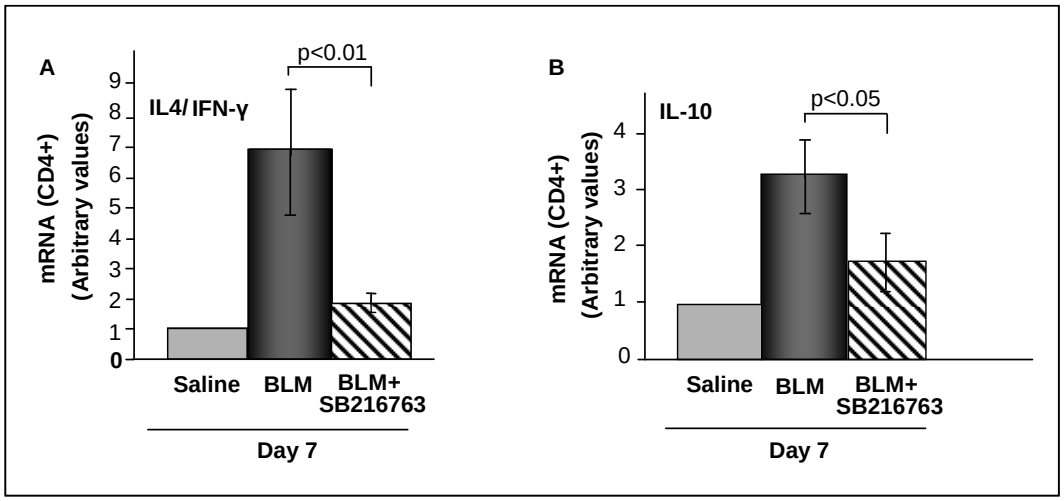


**Figure 4.6 SB216763 hampered bleomycin induced Th2 cytokine expression. A)** Evaluation by RT-PCR of IL-4 and IFN-γ expression levels in the $CD4^+$ cells sorted by lung of mice at day +7, showed a reduced IL-4/IFN-γ ratio in the BLM plus SB216763 treated mice ($p<0.05$) with respect to the mice treated with BLM alone. **B)** mRNA expression level of IL-10 was significantly reduced ($p<0.05$) at day +7 by the co-adminstration of bleomicyn and SB216763, with respect to group of mice treated with BLM alone. These results suggest that GSK-3 blockade inhibits the expression of Th2 cytokines induced by the treatment with BLM. Results represent mean ± SD of three separate experiments (n=4 *per experiment*).

No differences in the IL-4/ IFN-γ ratio was observed in the mice treated with saline, saline plus vehicle or saline plus SB216763. Remarkably, the T CD4+ lymphocytes in the mice treated with BLM plus SB216763, compared to the mice treated with only BLM, showed a significant decrease of IL-4/ IFN-γ ratio (1.78 ± 0.29, $p<0.05$, Fig.4.6 A). In agreements with these results, the mRNA expression levels of IL-10 in T CD4+ cells of mice treated with BLM plus SB216763 were significant reduced respect to the mice treated with the only BLM (1.7 ± 0.54 and 3.3 ± 0.6 respectively, $p<0.05$, Figure 4.6 B).

To support these results, also the GATA3/T-bet ratio, the transcriptional factors responsible of Th2 differentiation in the CD4+ lymphocytes exposed to BLM, resulted significantly increased in the lymphocytes of mice treated with BLM, with respect to mice treated with saline, and the co-administration of BLM plus SB216763 significantly reduced this ratio, supporting the role of GSK-3 in the Th1/Th2 switch (Figure 4.7).

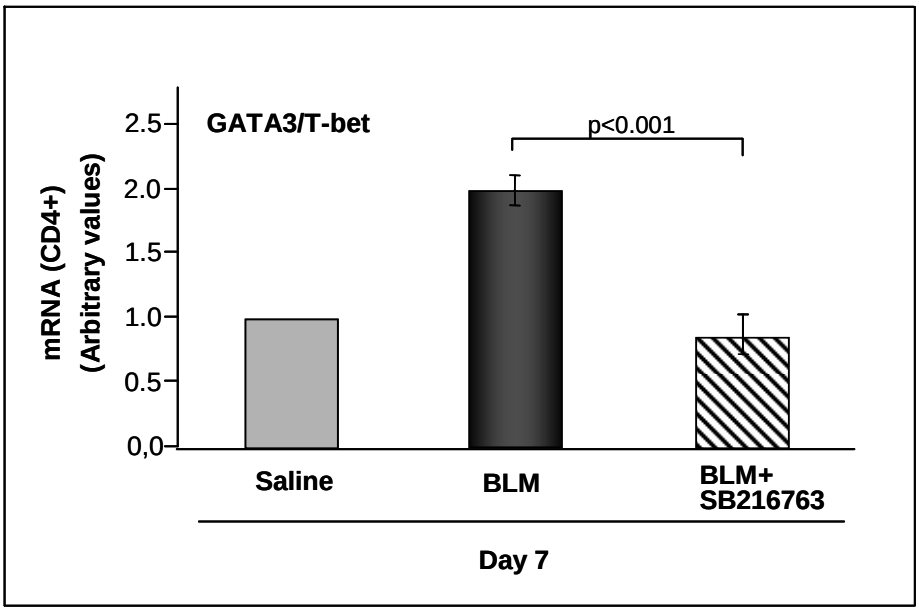


**Figure 4.7 SB216763 inhibits the expression of bleomycin-induced Th2 cytokines.** Expression level of GATA3 and T-bet, the transcriptional factors responsible of Th2 differentiation in $CD4^+$ lymphocytes exposed to BLM, were evaluated by RT-PCR. The co-administration of SB216763 and BLM significantly reduce the GATA3/T-bet ratio ($p<0.001$) in the $CD4^+$ lymphocytes respect the BLM treated mice. Results represent mean ± SD of three separate experiments (n=4 *per experiment*).

### 4.1.4 GSK-3 blockade inhibits BLM-induced macrophage inflammatory cytokine production

In order to assess the effects of GSK-3 blockade on pulmonary monocytes/macrophages exposed to BLM epithelial injury, we determined the gene expression levels of two macrophage-derived molecules, TNF-α and MCP1/CCL2, involved in the inflammatory profibrotic cascade. Analyses were performed at day +7 after BLM administration, on $Mac1^+$ monocytes/macrophages isolated from lungs of mice belonging to the various treated cohorts (n=12 for each cohort).

Administration of SB216763 to mice, exposed to BLM, consistently reduced the levels of TNF-α and MCP1/CCL2 detected in $Mac1^+$ lung cells

compared to mice treated with BLM alone ($p<0.05$ and $p<0.001$ respectively, Figure 4.8). No relevant differences were observed between mice treated with saline, saline plus vehicle or saline plus SB216763.

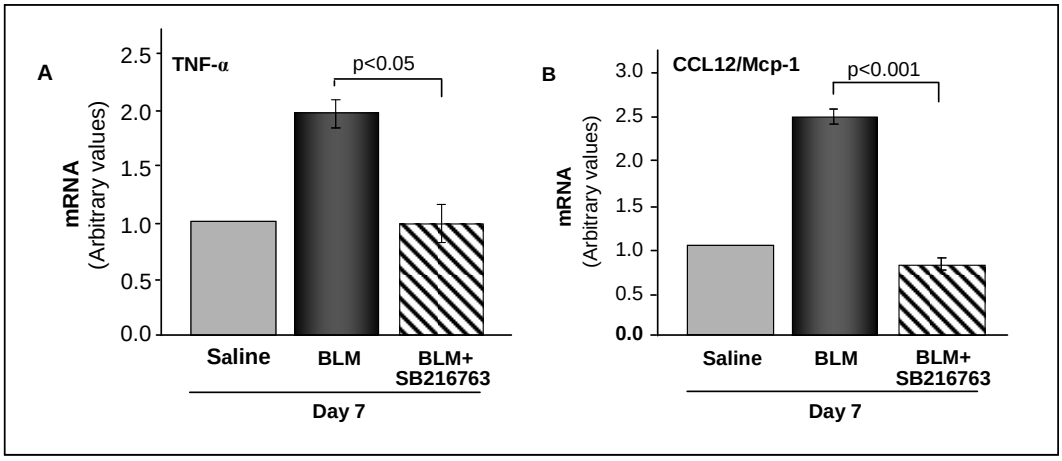


**Figure 4.8 SB216763 reduced bleomycin induced monocytes/macrophages inflammatory cytokine expression.** RT-PCR analysis of Mac1+/Gr1 -lung derived cells at day +7 following BLM stimulation showed an SB216763-mediated reduction in the expression levels of TNF-α (A, $p<0.05$) and MCP1/CCL12 ratio (B, $p<0.001$). Results represent mean ± SD of three separate experiments (n=4 *per experiment*).

### 4.1.5 GSK-3 blockade modulates bleomycin-induced lung fibrosis

The effect of GSK-3 inhibition in the lung fibrogenetic response to the bleomycin-induced damage, in collaboration of Prof. Calabrese's laboratory (University of Padua), was assessed by lung histological analysis of mice belonging to the different cohorts studied in this project (n=12 *per* cohorts). The mice were sacrificed at day +28, the lungs subjected to histopathological examination (in terms of inflammation, epithelial cell cuboidalization and fibrosis) and the antifibrotic effect of SB216763 was evaluated.

Histological evaluation of lungs from BLM-treated mice showed diffuse mononuclear cell infiltrates, epithelium cuboidalization and alveolar septa thickening associated with collagen deposition (Figure 4.9, A-B-C).

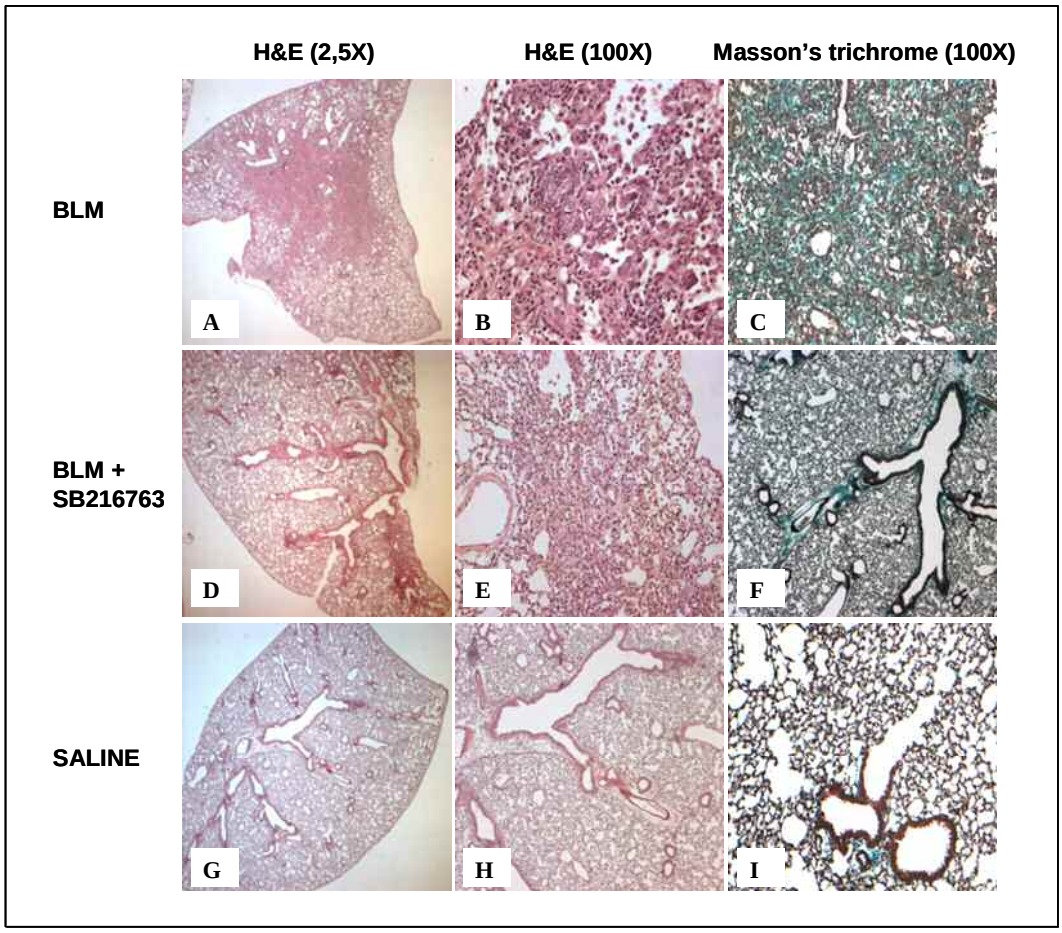


**Figure 4.9 Histological examination of the antifibrotic effects of SB216763 on bleomycin-induced pulmonary fibrosis.** Histological analysis was performed at day +28 by lung staining with Hematoxylin&Eosin (H&E), to evaluate the degree of inflammatory cell infiltration and alveolar cuboidalization and by Masson's trichrome to evaluate the degree of interstitial fibrosis. No alterations in the normal alveolar architecture were observed in saline-treated control groups (G, H, I). No differences were noticed in the saline, saline plus vehicle and saline plus SB216763 -treated mice (data not shown). As we can see, the BLM plus SB216763 –treated mice presented a consistent reduction of cell infiltrates, cuboidalization and fibrosis (B, E, H) as compared to the mice treated with BLM alone (A, D, G). Data are representative of three separate experiments.

On the contrary, lungs of mice in the BLM plus SB216763 treatment arm displayed a significant reduction in inflammatory infiltrates, epithelium cuboidalization, and fibrosis (Figure 4.9, D-E-F). No alterations in the normal alveolar architecture were observed in saline-treated control groups (Figure 4.9,

G-H-I.). Moreover, no microscopic degenerative changes were observed in the heart, liver and kidney of SB216763 treated mice (data not shown), thus excluding drug toxicity. The alterations observed by the microscopically analysis in the different experimental conditions were then scored through a pathological scoring system and represented as percent of lung parenchyma involved (Figure 4.10).

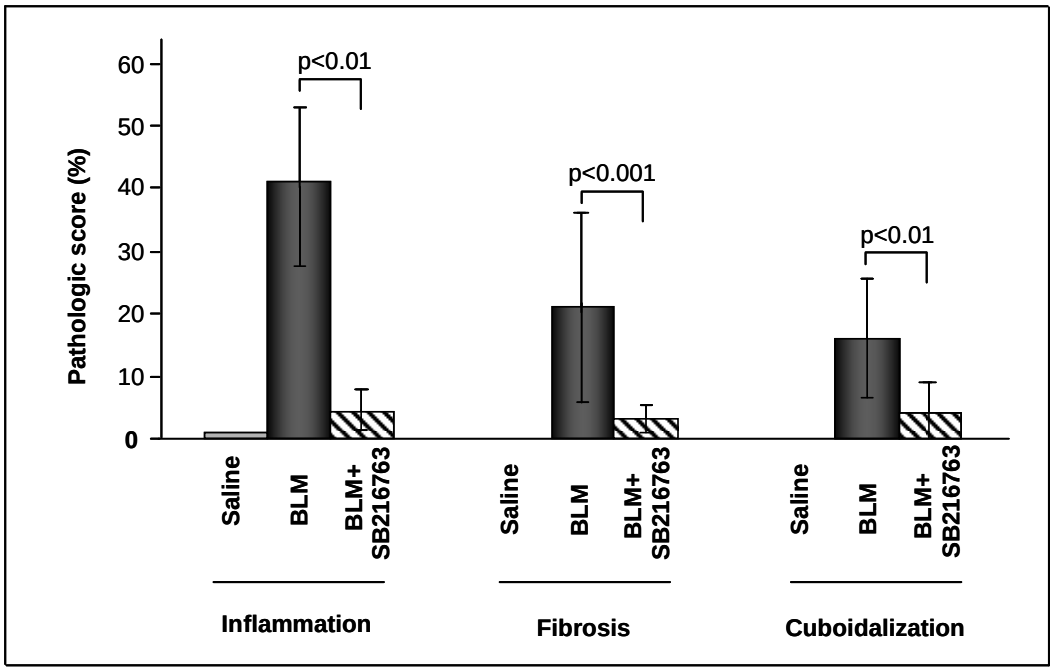


**Figure 4.10 Histologic quantification of the antifibrotic effects of SB216763.** Histological analysis of lungs from the different cohorts of treatment (saline, saline + SB216763, BLM and BLM + SB216763) demonstrated that SB216763 co-administrated with BLM, significantly reduced inflammatory cell infiltration, alveolar cells cuboidalization and fibrosis bleomycin-induced. Results represent mean ± SD of three separate experiments (n=4 *per experiment*).

Moreover, we set up a series of experiments in order to determine the effect of GSK-3 blockade on stabilization or reduction of fibrosis after that the fibrotic phase was already established as compared to the effects *ab initio*.

To this aim, mice were administered with BLM at day 0 and then the treatment with SB216763 was begun either at day 0 (early treatment) or at day +14 (late treatment), with subsequent twice a week administrations up to 28 days. In these experiments, to more precisely quantify the extent of fibrotic tissue, we utilized a semi-quantitative scoring system, as detailed in Materials and Methods.

As shown in Figure 4.11, we observed a considerable reduction of fibrosis in the group of mice treated with BLM plus SB216763 as compared to mice treated with BLM, and, remarkably, the antifibrotic effects present when SB216763 was administered after 14 days was comparable to that achieved with the administration of the inhibitor since day 0.

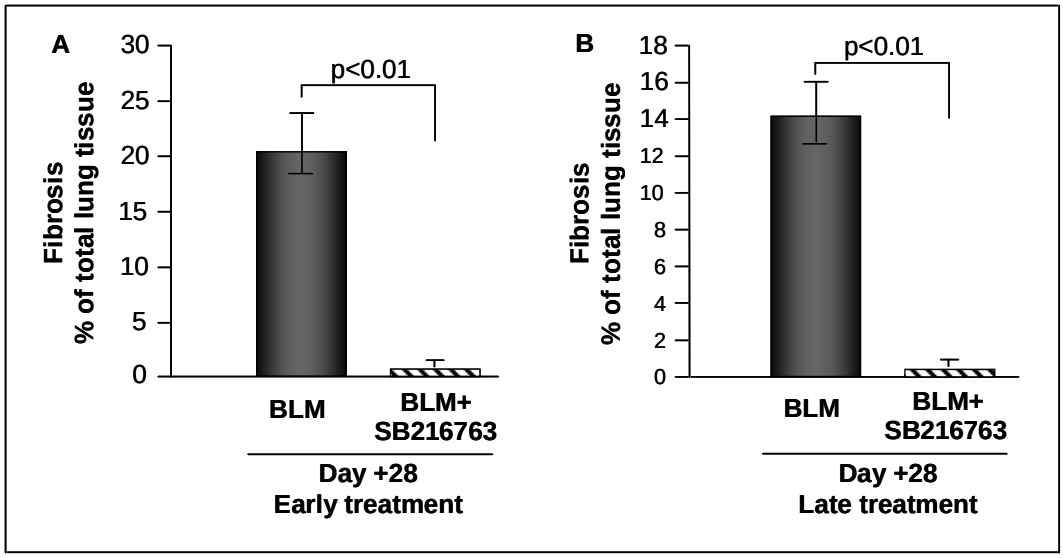


**Figure 4.11 Quantitative determination of fibrosis in the lungs.** To determine the effect of GSK-3 blockade on fibrosis after that the fibrotic phases was already established, we administered the inhibitor SB216763 at day +14 (late treatment) from the administration of BLM. We observed a considerable reduction of fibrosis in the late treatment **(B)**, reduction comparable to that achieved with the administration of the inhibitor since day 0 (early treatment, **A**).

### 4.1.6 GSK-3 blockade modulates bleomycin-induced epithelial cell lung apoptosis

Apoptosis of lung epithelial cell is found to be a key element during the establishment of pro-fibrotic inflammatory response. Hence, in order to evaluate the apoptosis in the epithelial lung cells of mice treated with BLM and BLM plus SB216763, in collaboration of Prof. Calabrese's laboratory (University of Padua), we used the TUNEL assay in the biopsies of mice sacrificed at day +28 of the treatment. In the mouse treated with BLM plus inhibitor SB216763 we observed a

drastic reduction of DNA fragmentation, that is of apoptosis, as compared to the mice treated with the only BLM. This reduction was confirmed with the early treatment, when the inhibitor was administered at day 0 with subsequent twice a week administrations, but also with the late treatment, when the inhibitor was administered at day +14 with subsequent twice a week administrations (Figure 4.12).

The results of histologic analysis, then revealed the important role of apoptosis in the epithelial lung cells during the pro-fibrotic inflammation, confirming that GSK-3 inhibition allowed to prevent the development of pulmonary fibrosis, probably modulating the epithelial damage induced by BLM.

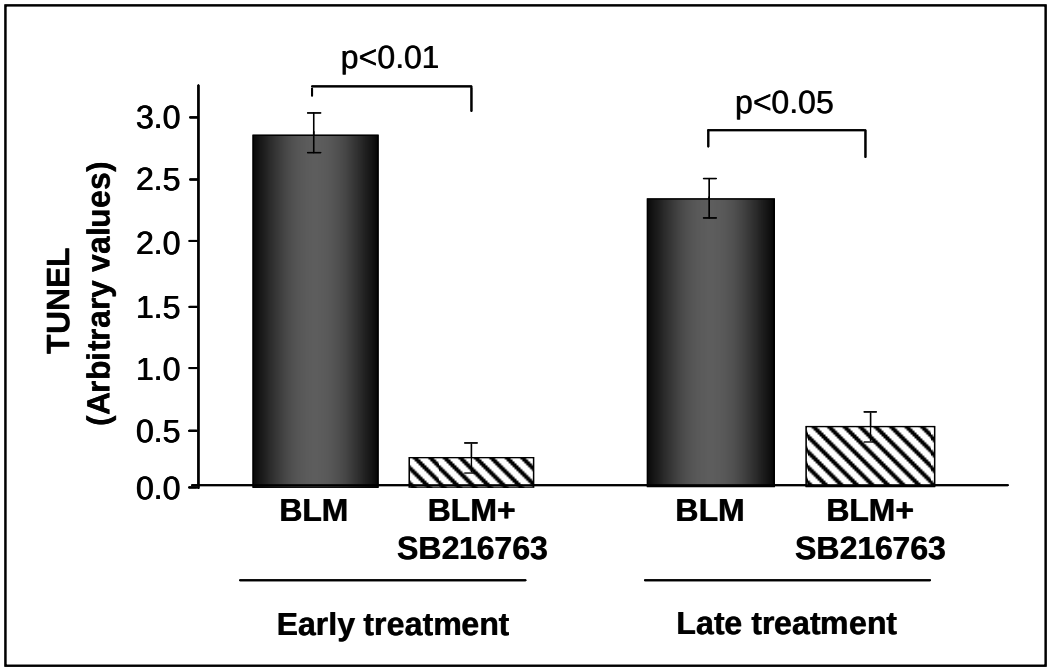


**Figure 4.12 Determination of apoptosis in the epithelial lung cells.** Apoptosis of epithelial lung cells was assessed, by TUNEL assay, in the biopsies of mice treated with BLM or BLM plus SB216763 and sacrificed at day +28. We found a significative reduction of apoptosis in group treated with BLM plus SB216763 as compared to group treated with only BLM. The reduction between the 2 groups was significant both in the early treatment ($p<0.01$) as in the late treatment ($p<0.05$).

### 4.1.7 Regulation by GSK-3 of MMP-9 release

The MMP-9 is a proteolytic enzyme that plays a pivotal role in the remodelling of extracellular matrix during fibrosis development[31,32]. To investigate if the release of MMP-9 during fibrosis establishment, induced by BLM, is regulated by GSK-3, we incubated the A549 cell line for 24h in the presence of the inhibitor SB216763.

We obtained a significative reduction of released MMP-9 already at BLM concentration of 5μM (0.55 ± 0.5, $p<0.01$, Figure 4.13), confirmed at 8 μM and 10 μM (respectively 0.37 ± 0.02 and 0.40 ± 0.04) as compared to control sample (used as calibrator).

This inhibition of MMP-9 release by SB216763, suggest that the inhibition of fibrosis develop in the model mouse could be mediated by GSK-3 inhibition through the downregulation of MMP-9 release.

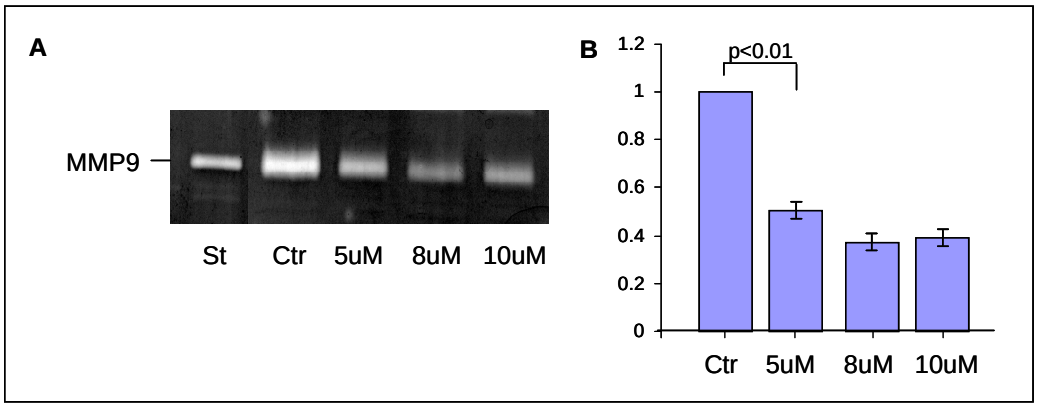


**Figure 4.13 The release of MMP-9 is downregulated by SB216763** The cell line A549 was incubated in presence of SB216763 for 24h. The release of MMP-9 in the culture medium was evaluated by Zimography assay. We obtained a significative reduction of the MMP-9 enzyme in the culture medium in the presence of increasing concentration of GSK-3 inhibitor. The result in the panel A is a representative experiment, whether in the panel B the results are the mean of 3 independent experiments.

### 4.1.8 Downregulation of p65 phosphorylation by GSK-3 inhibition

As already demonstrated, the compound SB216763 is able to inhibit the activity of GSK-3. A pivotal substrate of GSK-3 is the transcription factor p65, a important regulator for the expressions of genes involved in proliferation and cell survival. In this group of experiments we treated the cell line A549 with the GSK-3 inhibitor SB216763 to evaluate *in vitro* the phosphorylation levels of p65, since its activity is regulated through phosphorylation by GSK-3.

In the cell line A549, we found that the inhibition of GSK-3 by SB216763 decreased the phosphorylation level of p65 (Figure 4.14), suggesting that the activity of SB216763 could be explicated by the downregulation of GSK-3 also through the inhibition of p65 phosphorylation.

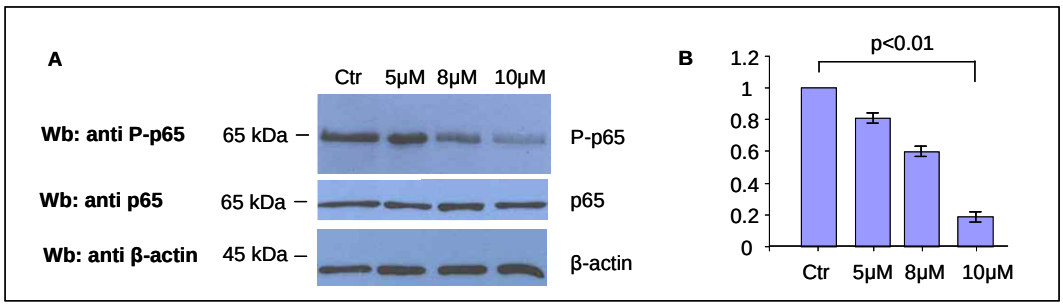


**Figure 4.14 Phosphorylation level of p65 in the cell line A549 before and after the treatment with SB216763.** In panel A is reported a representative of 3 experiments, whether in panel B are reported the results of 3 independent experiments. The cell line A549 was incubated with the inhibitor SB216763 and the phosphorylation level of p65 evaluated after 24h of incubation. As shown in figure we found a significative reduction of p65 phosphorylation after the treatment with SB216763 (0.80 ± 0.1, $p<0.05$ at 5 μM; 0.56 ± 0.15, $p<0.05$ at 8 μM; 0.28 ± 0.1, $p<0.01$ at 10 μM) as compared to untreated cells used as calibrator.

## 4.2 INVESTIGATION OF THE PROTEIN HP-NAP ABILITY TO MODULATE THE DEVELOPMENT OF PULMONARY FIBROSIS IN THE MODEL MOUSE BY PROMOTING A Th1 TYPE INFLAMMATORY RESPONSE

With this group of experiments we wanted to evaluate the ability of HP-NAP to inhibit, by stimulating a Th1 type inflammation, the development of pulmonary fibrosis, a disease mediated by a typical Th2 inflammatory response. The effect of HP-NAP administration was evaluated by considering:

- the survival of treated mice;
- the level of cytokines TNF-α, IL-4 and IFN-γ involved in Th1/Th2 differentiation;
- the evolution of the early phases of the inflammatory process in term of qualitative and quantitative determination of the different cell populations involved (lymphocytes, neutrophils, macrophages);
- lung histopathological examination in terms of inflammation, epithelial cell cuboidalization and fibrosis.

### 4.2.1 Effect of the *in vivo* administration of the protein HP-NAP on survival of mice treated with bleomycin intratracheal instillation.

As we did for the use of GSK-3 inhibitor SB216763, we evaluated the putative *in vivo* toxicity of HP-NAP. So, four different cohorts of C57BL6 mice were randomized to receive intratracheal instillation of either saline (n=12), BLM

(n=12), saline plus HP-NAP (n=12) or BLM plus HP-NAP (n=12), and followed their health status for 28 days.

We found that also the HP-NAP administration was protective against BLM-induced respiratory distress. Infact, as the previous survival experiments, we had about 30% of mortality in the group treated with BLM and we did not have deaths in the groups of mice treated with BLM plus HP-NAP ($p<0.05$, Figure 4.15). We confirmed that also the administration of HP-NAP is safe, infact none of the mice treated with saline plus HP-NAP died, moreover the HP-NAP coadministration with BLM resulted protective against respiratory distress caused by BLM because none of the treated mice died..

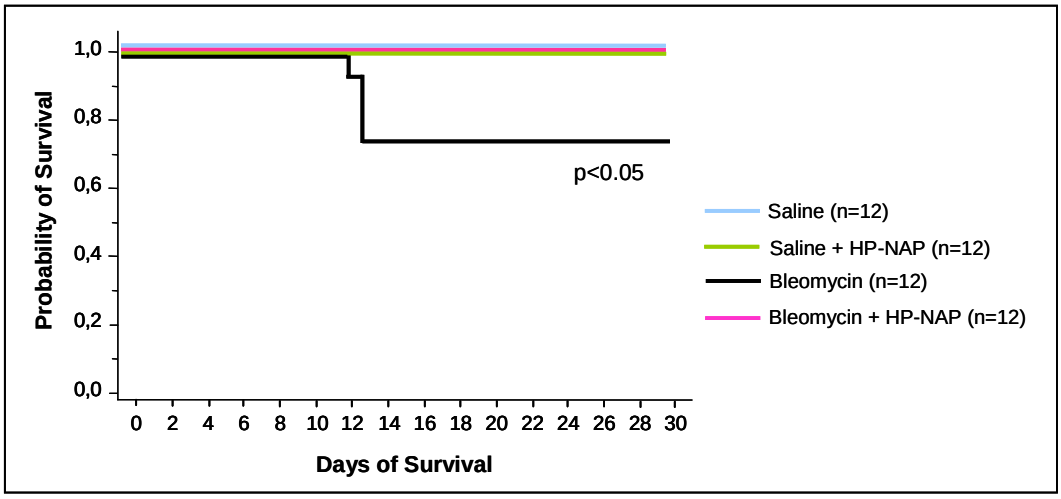


**Figure 4.15 Effect of HP-NAP protein administration on the survival of bleomycin treated mice.** Forty eight mice were differently randomized in four cohorts to receive intratracheal instillation of saline, BLM, saline plus HP-NAP, BLM plus HP-NAP and followed their health status for 28 days. The 30% of BLM treated mice died of respiratory distress between day +10 and day +12 after the treatment. On the contrary, none of the mice receiving saline, saline plus HP-NAP or BLM plus HP-NAP died, suggesting that HP-NAP, as we found for SB216763, is protective against BLM-induced respiratory distress ($p<0.05$).

### 4.2.2 HP-NAP administration modulates the Th2 immune response induced by bleomycin.

The role of HP-NAP in the stimulation of a Th1 type inflammatory response was evaluated by the analysis of mRNA expression levels of IFN-γ, a typical Th1 chemokine, and IL4, which is instead a typical Th2 chemokine. T CD4+ cells were sorted by lungs of mice treated with saline, saline plus HP-NAP, BLM and BLM plus HP-NAP. Each cohorts of mice (n=12), was evaluated at day +7 from the intratracheal administration of HP-NAP and BLM.

The treatment with HP-NAP, as expected, stimulated in the mouse the expression of IFN-γ, a Th1 chemokine (Figure 4.16 A, $p<0.05$ with compared to saline treated mice), whereas we did not observed an increasing of IL-4 level, a Th2 chemokine, between mice treated with saline or saline plus HP-NAP (Figure 4.16 B, p=ns).

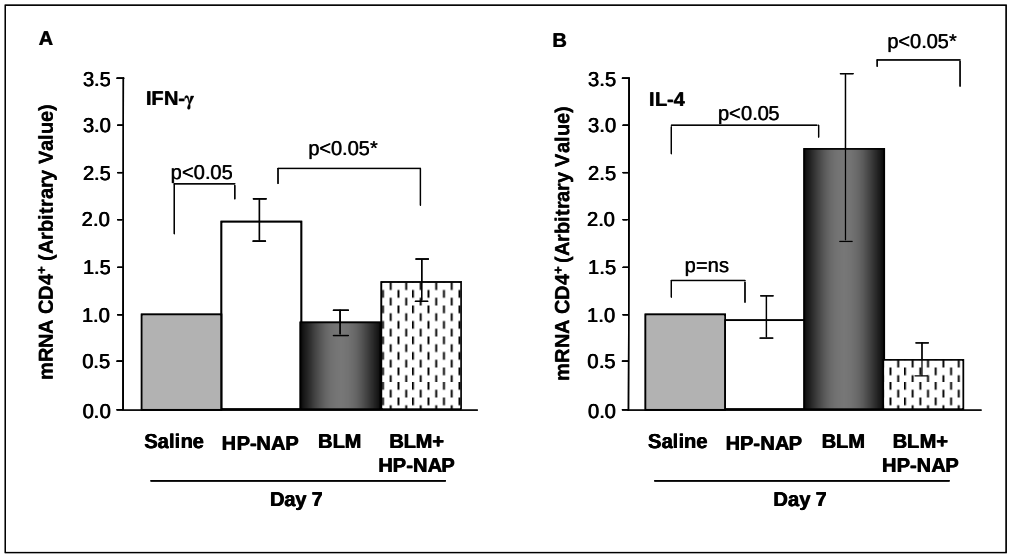


**Figure 4.16 HP-NAP administration modulates the Th2 immune response induced by bleomycin.** T CD4+ cells were sorted by BALs of mice scarified at day +7. The expression levels of IL-4 and IFN-γ were evaluated by RT-PCR. We found that expression levels of IL-4, increased by treatment with BLM, was reported to normal values ($p<0.05$) by co-administration of HP-NAP. Remarkably, the mRNA level of IFN-γ, increased by HP-NAP incubation, was significatively decreased ($p<0.05$) by the co-administration of HP-NAP and BLM. Results represent mean ± SD of three separate experiments (n=4 *per experiment*).

Whereas, as expected, BLM treatment caused a peak of IL-4 expression as compared to saline administration (Figure 4.16 B, $p<0.05$), increasing that, remarkably, was reduced to normal value by the co-administration of HP-NAP (Figure 4.16 B, $p<0.05$*). Moreover, the expression level of IFN-γ, that was increased by HP-NAP treatment (Figure 4.16 A, $p<0.05$), was reported to almost normal value by co-administration of BLM (Figure 4.16 A, $p<0.05$*)

These results suggested that HP-NAP contrasts the Th2 type immune response induced by BLM stimulating a Th1 type response. Infact the co-administration of BLM and HP-NAP reduced to normal values the expression levels of IL-4, increased by treatment with BLM, whereas IFN-γ, which expression was unaffected by BLM treatment, was increased by HP-NAP administration.

### 4.2.3 HP-NAP administration modulates bleomycin-induced alveolitis

We examined whether the administration of HP-NAP, by the stimulation of a Th1 inflammatory response, could affect the dynamics of the evolution of the early phases of the inflammatory process taking place in the lung upon BLM exposure. To this aim, we analysed the bronchoalveolar lavage fluid (BALF) obtained from saline (n=12), BLM (n=12), saline plus HP-NAP (n=12) or BLM plus HP-NAP (n=12) -treated mice at +7, +14 and +28 days after treatment. Bleomycin administration caused a marked alveolitis at day +7 ($2.2x10^6 \pm 0.93$), peaking at day +14 ($6.17x10^6 \pm 1.78$ cells/ml of BAL) and at day +28, albeit gradual decrease ($4.5x10^6 \pm 1.23$ cells/ml of BAL), as demonstrated by the

microscopic score of BALF total inflammatory cells (sum of macrophages, lymphocytes and neutrophils; Figure 4.17).

Remarkably, mice randomised to receive BLM plus HP-NAP showed a noteworthy reduction in the overall BALF cellularity at day +7 (1.4 ± 0.31 cells/ml, $p<0.01$) which was confirmed at day +14 ($3.95x10^6$ ± 1.81 cells/ml, $p<0.05$) and also at day + 28 ($2.25x10^6$ ± 1.5 cells/ml, $p<0.01$). Furthermore the cytological analysis of BALF of mice treated with saline plus HP-NAP showed only a slightly increased of cellularity (at day 7, 0.88 ± 0.21 ), confirmed at day +14 and +28, when compared to control group ($<0.5x10^6$ ± 0.1 cells/ml).

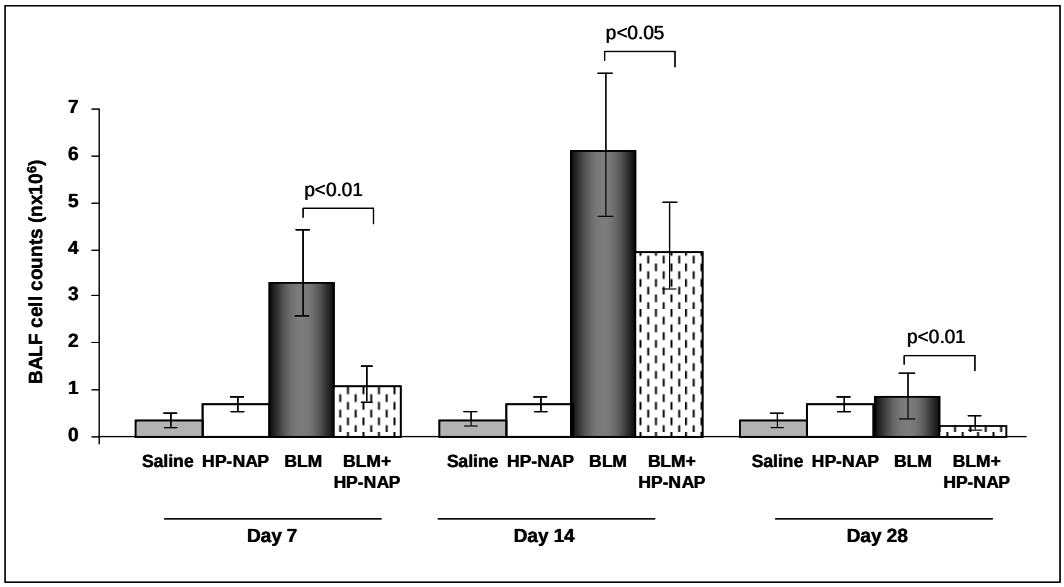


**Figure 4.17 HP-NAP reduced the magnitude of bleomycin induced alveolitis.** Mice were treated with saline, BML, saline plus HP-NAP or BLM plus HP-NAP (10 mg/mouse), as described in materials and methods. We examined the broncho-alveolar lavage fluid (BALF) at day +7, +14 and +28 from the BLM instillation. We found a significant reduction of alveolitis, at day +7 ($p<0.05$), day +14 ($p<0.01$) and also day +28 ($p<0.05$), in mice treated with BLM plus HP-NAP as compared to mice treated with the only BLM. Results represent mean ± SD of three separate experiments (n=4 *per experiment*).

Then, cytofluorimetry of BALFs allowed a qualitative determination of the different cell populations involved in BLM-induced alveolitis, namely neutrophils, macrophages ($Mac1^+$ cells) and T $CD3^+$ lymphocytes.

Bleomycin treatment caused an increased of neutrophils as early as day +7 (12% ± 4, $p<0.05$) as compared to control group (0.9 ± 0.1), lasting at day +14 (12% ± 5, $p<0.05$) and decreasing at day +28 (1.5% ± 0.2). Anyway comparable levels of the percentage of neutrophils in the BALF of BLM-treated were observed in the BLM plus HP-NAP-treated mice at all the time-intervals analysed (day +7: 14% ± 5; day +14: 14% ± 4; day +28: 3% ± 0.5, Figure 4.18).

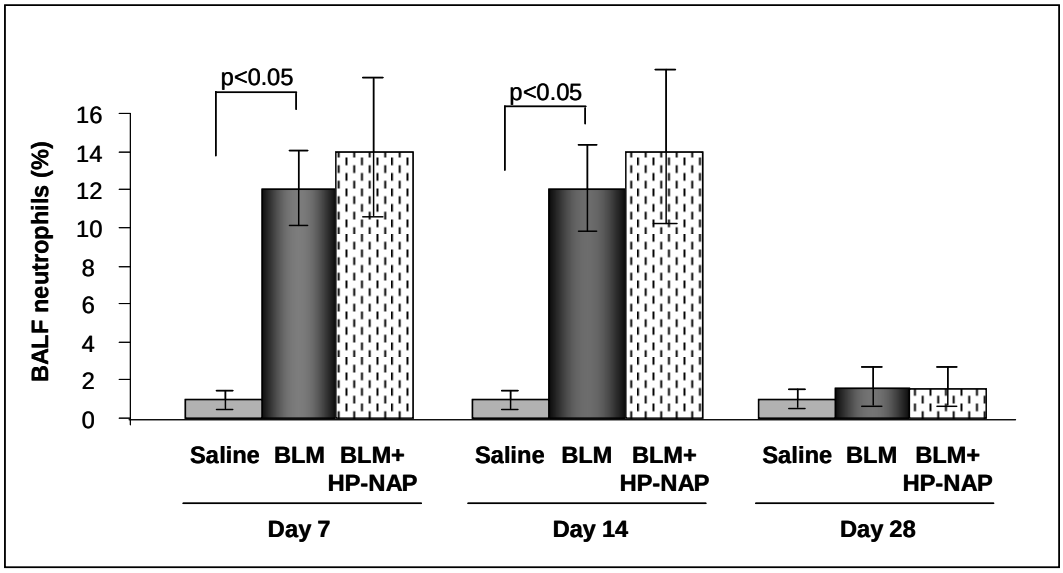


**Figure 4.18 Evaluation of neutrophils percentage in BALFs of HP-NAP treated mice.** Bleomycin challenge caused an neutrophilic alveolitis at all the time-intervals analysed. Anyway, in the BLM plus HP-NAP-treated mice, the percentage of observed neutrophils were comparable to percentage of BLM-treated mice at all the time-intervals analysed. Results represent mean ± SD of three separate experiments (n=4 *per experiment*).

Remarkably the were results of T $CD3^+$ lymphocytes evaluation. The BLM administration caused, at day +7, an important increased of lymphocytes (44% ± 7) as compared to controls group (saline or saline plus HP-NAP administration, 0.9% ± 0.1, Figure 4.19). The increased percentage was confirmed at day +14 (31% ± 8) and day +28 (39% ± 10).

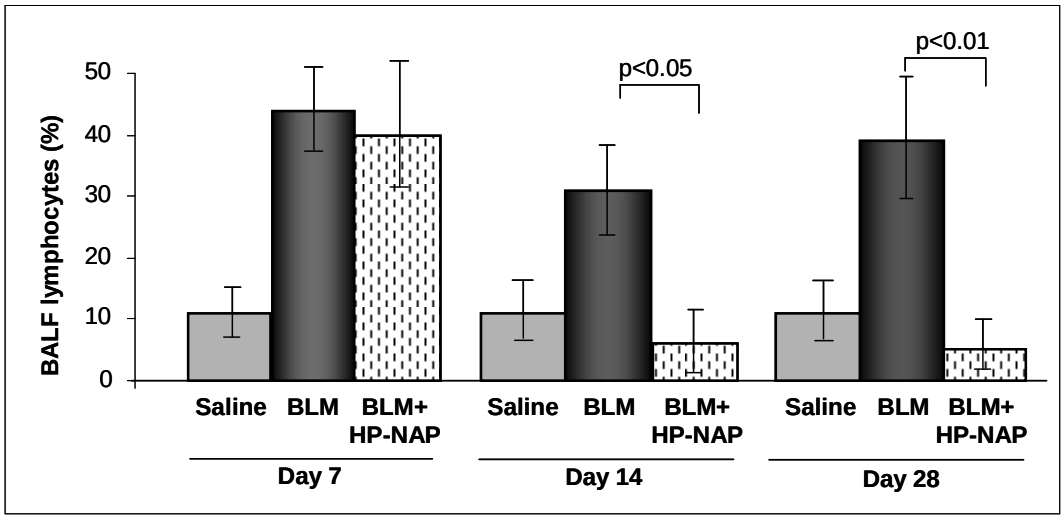


**Figure 4.19 Evaluation of lymphocytes percentage in BALFs of HP-NAP treated mice.** Bleomycin challenge caused an important increased of lymphocyte T $CD3^+$ percentage at all the time-intervals analysed. Moreover in the BLM plus HP-NAP-treated mice, the percentage of observed lymphocytes was reduced to normal values from day +14. Results represent mean ± SD of three separate experiments (n=4 *per experiment*).

As shown in Figure 4.19, since day 14 lasting to day 28, we observed a considerable reduction of lymphocytes percentage when HP-NAP was co-administered with BLM (respectively day 14: 6% ± 4, $p<0.05$ and day 28: 5.8 ± 4, $p<0.01$) as compared to only BLM treated group. These results suggest that HP-NAP administration could prevent the lymphocytosis induced by BLM.

The macrophages percentage resulted increased in BALs of HP-NAP-treated mice as compared to the BLM administration ( $p<0.01$ at day +7, Figure 4.20). This increased was prevented at day +7 by the co-administration of BLM, where we had comparable level between the BLM and BLM+HP-NAP groups. Anyway the co-administration was able to prevent the increasing of macrophages percentage only at day +7, in fact at day +14 and day +28 the difference between the two groups resulted statistically significant ($p<0.05$) (Figure 4.20). These results suggest that also the Th2 type response could be able to interfere, at least initially, with the HP-NAP-induced Th1 response develop.

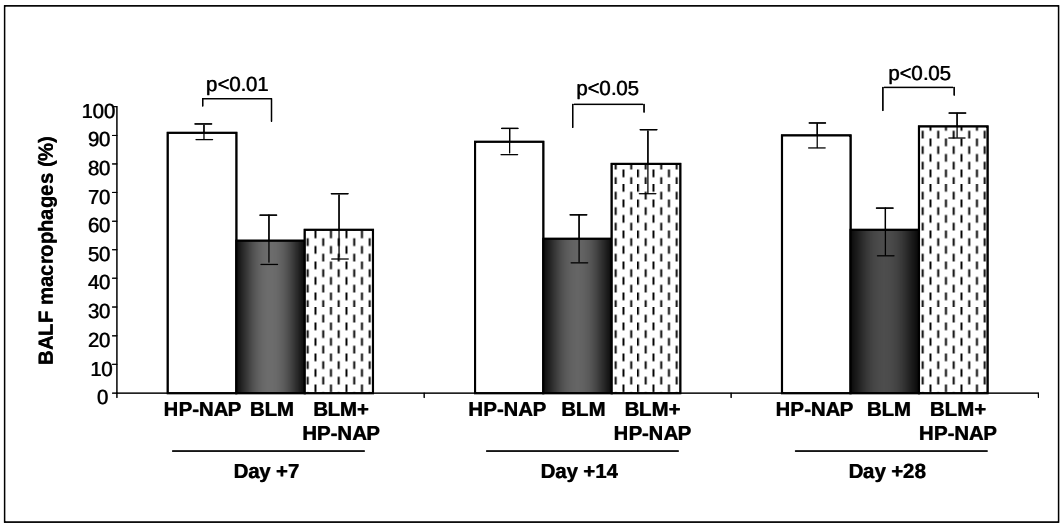


**Figure 4.20 Macrophages evaluation in BALFs of HP-NAP treated mice.** HP-NAP challenge caused at day +7 an important increased of macrophages percentage (91% ± 2, $p<0.01$) as compared to BLM treated group (53% ± 5), increased confirmed at day +14 and day +28. Remarkably the co-administration of HP-NAP increased significantly the percentage of macrophages with respect to group treated with only BLM. This increased was observed at day 14 (80% ± 19, $p<0.05$) and day +28 (93% ± 5, $p<0.05$). Results represent mean ± SD of three separate experiments (n=4 *per experiment*).

### 4.2.4 HP-NAP modulates BLM-induced lung fibrosis

The effect of HP-NAP in the lung fibrogenetic response to the BLM-induced damage was assessed by lung histological analysis of mice belonging to the different cohorts studied in this project (n=12 *per* cohorts). The mice were sacrificed at day +14 and +28, the lungs subjected to histopathological examination (in terms of inflammation, epithelial cell cuboidalization and fibrosis) and the antifibrotic effect of HP-NAP was evaluated (Figure 4.22).

Histological evaluation of lungs from BLM-treated mice showed diffuse mononuclear cell infiltrates, epithelium cuboidalization and alveolar septa thickening associated with collagen deposition. On the contrary, lungs of mice in the BLM plus HP-NAP treatment arm displayed a significant reduction in inflammatory infiltrates, epithelium cuboidalization, and fibrosis. No alterations in the normal alveolar architecture were observed in HP-NAP or saline-treated

control groups. Moreover, no microscopic degenerative changes were observed in the heart, liver and kidney of SB216763 treated mice, thus excluding drug toxicity.

The alterations observed by the microscopically analysis in the different experimental conditions were then scored through a pathological scoring system and represented as percent of lung parenchyma involved.

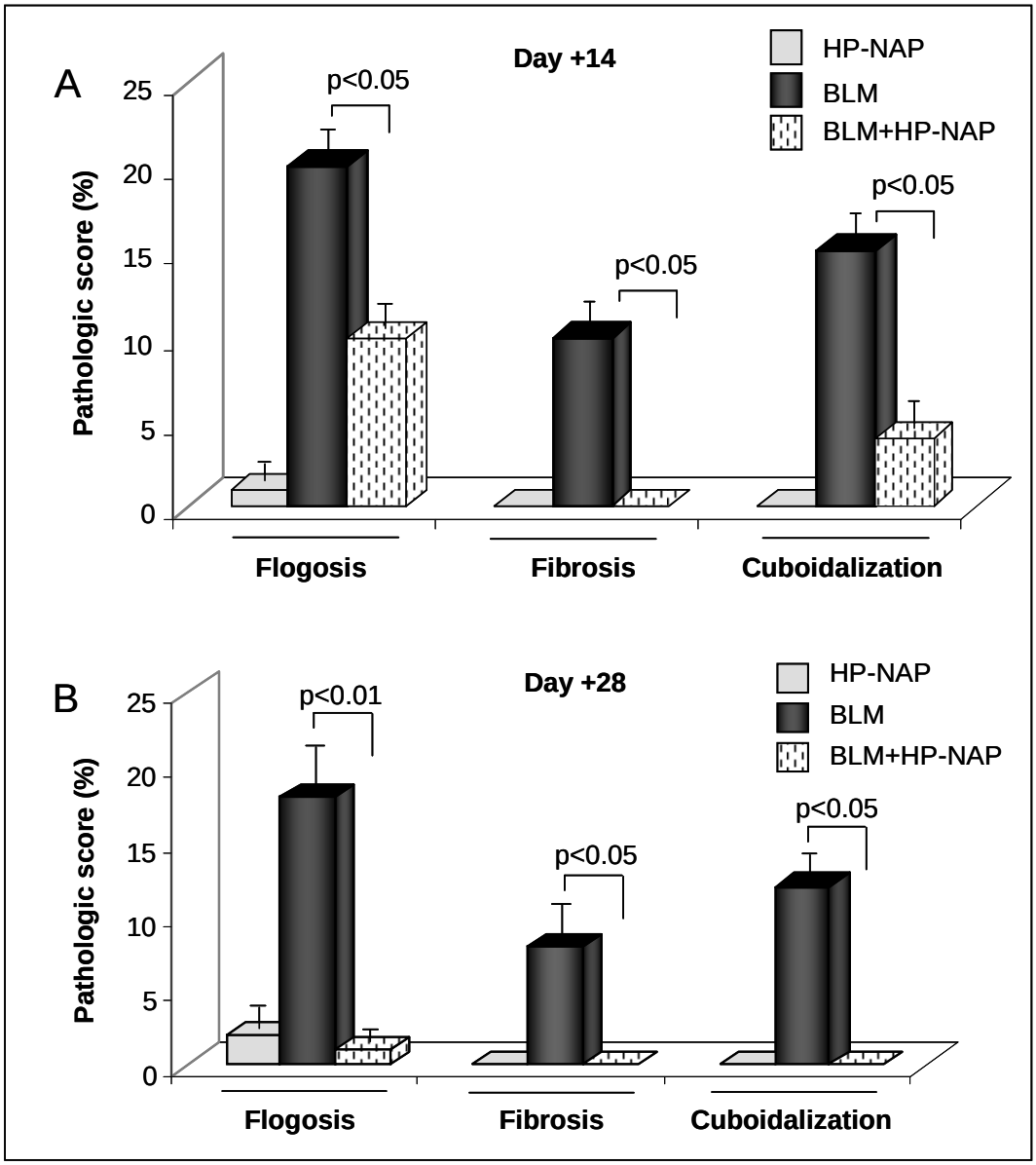


**Figure 4.22 Histologic quantification of the antifibrotic effects of HP-NAP.** Histological analysis of lungs from the different cohorts of treatment (saline, saline + HP-NAP, BLM and BLM + HP-NAP) demonstrates that HP-NAP co-administrated with BLM, significantly reduced inflammatory cell infiltration, alveolar cells cuboidalization and fibrosis BLM-induced, both at day+14 and +28. Results represent mean ± SD of three separate experiments (n=4 *per experiment*).

# DISCUSSION

We show in this research that chemical inhibition of GSK-3, with the synthetic compound SB216763, and HP-NAP administration can efficiently prevent the development of BLM-induced lung fibrosis in a model mouse, likely by modulating the BLM-triggered inflammatory lung epithelial-damage-dependent inflammatory response.

The most accepted view on IPF pathophysiology entails the hypothesis that a persistent injury to the lung alveolar epithelium results in an aberrant fibrogenetic response sustained by an anomalous balance between extracellular matrix production and reabsorption with consequent subversion of the normal lung parenchyma architecture[31,109]. However, the mechanisms underlying this exaggerated reparative response are unknown. A current view stresses the importance of genetic predisposition in developing IPF, and a number of genetic studies, aimed at identifying the precise molecular determinants[58,110], are currently ongoing. On the other hand, the role of chronic inflammatory response in IPF pathogenesis represents a subject of intense research by many years[1,39,111]. Yet, while animal models of pulmonary fibrosis clearly have shown that an inflammatory response precedes the development of fibrosis, the limited efficacy in the clinical setting of the therapeutic employment of anti-inflammatory drugs in the treatment of patients affected by IPF has led to the view that the inflammatory phase represents an associated phenomenon rather than the real cause of the development of fibrosis in IPF[31].

Our study substantiates a pathogenetic role for the inflammatory response in the BLM-model (a model that mimics most profibrogenetic diffuse lung

diseases), in fact both SB216763 and HP-NAP counteracted the fibrogenesis development down-modulating the inflammation induced by BLM treatment.

Noteworthy we found that the GSK-3 inhibition was accompanied by a significant containment of the inflammation, through the reduction in neutrophil activation and lymphocyte recruitment, and by an absent/reduced development of lung fibrosis. Moreover we have observed that the *in vivo* administration of GSK-3 inhibitor was associated with a reduction in the lymphocyte infiltrate and in neutrophil alveolar activation ($Gr1^+/Mac1^+$ cells) in the early phases of the inflammatory process. To the best of our knowledge, a role for GSK-3 in modulating the *in vivo* function of these two cell populations has not been previously described. Our evidence suggests that GKS-3 might regulate lymphocyte and neutrophil biological functions, such as cell activation, chemotaxis and the expression of surface molecules involved in cell-cell and cell-matrix interactions, downstream from inflammatory stimuli. Further experiments are therefore required to better understand the mechanism(s) involved in the down-modulation of these cell populations.

Inflammation is recognized to be a contributor also to the pathogenesis of pulmonary hypertension (PH)[19], that occurs to 80% of patients with IPF. Patients with PH have higher circulating levels and pulmonary expression of various inflammatory cytokines, including endothelin-1 (VOCE QUI) and chemokines[21,112]. The same four pathological processes are reported: vasoconstriction, inflammation, thrombosis and remodelling have been described in all types of Pulmonary Arterial Hypertension (PAH)[112]. In recent studies of patients with COPD, it was found that pulmonary artery pressure correlated positively with the circulating levels of two cytokines, namely, IL-6 and MCP-1[37].

Alltogether these results suggest that the control of inflammation, besides counteracting the development of IPF, would also prevent the establishment of pulmonary hypertension, thus improving symptoms and survival in the patients suffering from these ominous diseases.

The findings presented in this research, moreover, confirm recent data on the role of GSK-3 in regulating the production of pro-inflammatory cytokines in monocytes/macrophages[71]. In particular, our data demonstrate that the inhibition of GSK-3 modulates the macrophage production of TNFα and of CCL2/MCP1, molecules which are known to play a relevant role in the onset of the inflammatory/fibrogenetic process and in the recruitment of monocytes, respectively[52]. It is therefore tempting to speculate that upon simultaneous treatment with BLM and SB216763 the reduced activation of neutrophils and the decreased recruitment of lymphocytes that we observed represent the consequence of the perturbation of GSK-3-regulated macrophage functions. However, it should be noted that there are data implicating GSK-3 in the direct regulation of cell mobility[113]. In fact, in discrete subcellular compartments GSK-3 local inhibition is associated with the stimulation of cell movement[114,115], whereas global GSK-3 inhibition inside the cell is accompanied by a profound impairment of cell mobility[116].

The role of inflammation in fibrosis development was confirmed, in our experiments, also by treatment with HP-NAP. In BLM plus HP-NAP treated mice we observed a noteworthy reduction in BAL cellularity and lymphocyte percentage with respect to BLM treated mice. We found also that IL-4, stimulated by treatment with BLM, was reduced to normal value by co-administration of HP-

NAP, whereas HP-NAP treatment induced an over-expression of IFN-γ, whose level was unaffected by BLM.

These findings suggest that HP-NAP stimulates an inflammatory Th1 response and remarkably counteracts the Th2 inflammatory response stimulated by BLM treatment. Our results are in agreements with data recently published where epidemiological and experimental studies demonstrated that infectious diseases can influence the development of allergic disorders[99]. This phenomenon was explained with the inhibition of the allergic Th2 inflammation by Th1 responses elicited by infectious agents.

In this context, an intriguing fact emerging from our data regards the effect of SB216763 on lung T-helper lymphocytes. Compelling evidence suggests the existence of a Th2 microenvironment in fibrotic lungs[52,117], as demonstrated by *in situ* studies in the pulmonary tissue of human subjects with IPF as well as by the *in vivo* experiments in mice rendered deficient for various Th2 associated genes[118-120]. In our experimental model, the assessment of the degree of Th1/Th2 lymphocyte differentiation through the determination of the level of gene expression of Th1/Th2 cytokines demonstrated a Th2 skewed differentiation as early as days +7 after BLM treatment. Interestingly, SB216763 administration blocked the Th-2 differentiation, as shown by the lack of up-regulation of IL-4 and IL-10 expression in T-helper ($CD4^+$) lymphocytes in the lung. However, our data do not exclude the possibility that the reduced Th2 switch is due to the inhibition of the lung macrophage-dependent inflammatory response by SB216763. Whatever the mechanisms may be, we postulate that the blockade of Th2 formation causes a decreased bioavailability of important fibrogenic cytokines, such as IL-4 and IL-10, and therefore constitutes a crucial mechanism

by which SB216763 exerts its anti-fibrotic effect. This hypothesis is supported by our results with HP-NAP protein, where the fibrosis was prevented by blocking the Th2 differentiation, and also by results of other laboratories where HP-NAP treatment was shown to be effective in preventing allergic asthma by blocking again the Th2 phenotype of immune response. If the develop of a Th1 immune response, counteracting the develop of a Th2 response, could also improve the symptoms of pulmonary hypertension, is still under investigation and further experiments are to be performed.

These results, even though preliminary, suggest the possibility of using GSK-3 inhibitors and HP-NAP protein to modulate the inflammatory and fibrogenic response in the lung. The use of GSK-3 inhibitors has been speculated for metabolic diseases, including type II NIDDM, given the crucial role of GSK-3 downstream of insulin signalling, and some neurological conditions (bipolar disorder, Alzheimer disease, Parkinson disease, Huntington disease), since GSK-3 phosphorylates proteins playing an important pathogenetic role in these disorders. Very recently, a number of studies have demonstrated the potential usefulness of this approach in some inflammatory pathological conditions and in some connected pathologies as pulmonary hypertension. For instance, mice treated with SB216763 were protected by LPS-induced septic shock[71]. Another study showed that GSK-3 may regulate IL-10 production upon IFN-γ stimulation in macrophages and its inhibition leads to increased IL-10 levels and protection against the damage consequent to experimentally-induced arthritis and peritonitis[72]. Inflammatory chemokines, as IL-6, MCP1 and TGF-β, have been found overexpressed in ILDs[37,112]. Our study is the first to test the effects of GSK-3 inhibition on the development of lung inflammation and fibrosis in a mouse

model, demonstrating a protective effect of this treatment versus the fibrosis and perhaps the pulmonary hypertension, hypothesis that will be verified. Moreover our results candidate HP-NAP for novel strategies of prevention and treatment of allergic diseases, treatment aimed to redirect Th2 into Th1 response. Furthermore, the potential beneficial effect of HP-NAP for asthma treatment has been already tested in mice by using mucosal administration and in order to hamper the pathogenetic mechanism of allergy, most studies point at immune deviation from Th2 towards a less pathogenic Th1 response[121].

In conclusion, by demonstrating that GSK-3 kinase regulates the early phases of inflammatory cell activation and recruitment, as well as the generation of a specific Th2 skewed immune response, and by showing that HP-NAP is able to prevent the fibrosis blocking the Th2 immune response induced by BLM, the results of this PhD research work can contribute to increase the understanding of the molecular mechanisms underlying the pathogenesis of lung inflammation and fibrosis. The confirmation of the role of inflammation in IPF, suggest that inflammation itself could favour the established of pulmonary hypertension, that develops to 80% of patients with IPF. More importantly, the present data suggest that the modulation of GSK-3 and/or HP-NAP may represent novel ways to improve the therapeutic armamentarium of drugs that are able to block fibrogenesis in the lung of patients with most diffuse lung diseases.

# REFERENCES


1. Green FH. Overview of pulmonary fibrosis. Chest. 2002;122:334S-339S.
2. Katzenstein AL, Myers JL. Idiopathic pulmonary fibrosis: clinical relevance of pathologic classification. Am J Respir Crit Care Med. 1998;157:1301-1315.
3. Coghlan MP, Culbert AA, Cross DA, et al. Selective small molecule inhibitors of glycogen synthase kinase-3 modulate glycogen metabolism and gene transcription. Chem Biol. 2000;7:793-803.
4. Coultas DB, Zumwalt RE, Black WC, Sobonya RE. The epidemiology of interstitial lung diseases. Am J Respir Crit Care Med. 1994;150:967-972.
5. Hansell A, Hollowell J, Nichols T, McNiece R, Strachan D. Use of the General Practice Research Database (GPRD) for respiratory epidemiology: a comparison with the 4th Morbidity Survey in General Practice (MSGP4). Thorax. 1999;54:413-419.
6. Gribbin J, Hubbard RB, Le Jeune I, Smith CJ, West J, Tata LJ. Incidence and mortality of idiopathic pulmonary fibrosis and sarcoidosis in the UK. Thorax. 2006;61:980-985.
7. Garcia CK, Raghu G. Inherited interstitial lung disease. Clin Chest Med. 2004;25:421-433, v.
8. Marshall RP, Puddicombe A, Cookson WO, Laurent GJ. Adult familial cryptogenic fibrosing alveolitis in the United Kingdom. Thorax. 2000;55:143-146.
9. Itoh T, Nagaya N, Ishibashi-Ueda H, et al. Increased plasma monocyte chemoattractant protein-1 level in idiopathic pulmonary arterial hypertension. Respirology. 2006;11:158-163.
10. Raghu G, Freudenberger TD, Yang S, et al. High prevalence of abnormal acid gastro-oesophageal reflux in idiopathic pulmonary fibrosis. Eur Respir J. 2006;27:136-142.
11. Kim DS, Collard HR, King TE, Jr. Classification and natural history of the idiopathic interstitial pneumonias. Proc Am Thorac Soc. 2006;3:285-292.
12. Collard HR, King TE, Jr., Bartelson BB, Vourlekis JS, Schwarz MI, Brown KK. Changes in clinical and physiologic variables predict survival in idiopathic pulmonary fibrosis. Am J Respir Crit Care Med. 2003;168:538-542.
13. Flaherty KR, Mumford JA, Murray S, et al. Prognostic implications of physiologic and radiographic changes in idiopathic interstitial pneumonia. Am J Respir Crit Care Med. 2003;168:543-548.
14. Latsi PI, du Bois RM, Nicholson AG, et al. Fibrotic idiopathic interstitial pneumonia: the prognostic value of longitudinal functional trends. Am J Respir Crit Care Med. 2003;168:531-537.
15. Bjoraker JA, Ryu JH, Edwin MK, et al. Prognostic significance of histopathologic subsets in idiopathic pulmonary fibrosis. Am J Respir Crit Care Med. 1998;157:199-203.
16. Azuma A, Nukiwa T, Tsuboi E, et al. Double-blind, placebo-controlled trial of pirfenidone in patients with idiopathic pulmonary fibrosis. Am J Respir Crit Care Med. 2005;171:1040-1047.
17. Raghu G, Brown KK, Bradford WZ, et al. A placebo-controlled trial of interferon gamma-1b in patients with idiopathic pulmonary fibrosis. N Engl J Med. 2004;350:125-133.

18. Demedts M, Behr J, Buhl R, et al. High-dose acetylcysteine in idiopathic pulmonary fibrosis. N Engl J Med. 2005;353:2229-2242.
19. Nathan SD, Noble PW, Tuder RM. Idiopathic pulmonary fibrosis and pulmonary hypertension: connecting the dots. Am J Respir Crit Care Med. 2007;175:875-880.
20. Lettieri CJ, Nathan SD, Barnett SD, Ahmad S, Shorr AF. Prevalence and outcomes of pulmonary arterial hypertension in advanced idiopathic pulmonary fibrosis. Chest. 2006;129:746-752.
21. Nadrous HF, Pellikka PA, Krowka MJ, et al. Pulmonary hypertension in patients with idiopathic pulmonary fibrosis. Chest. 2005;128:2393-2399.
22. Kawut SM, O'Shea MK, Bartels MN, Wilt JS, Sonett JR, Arcasoy SM. Exercise testing determines survival in patients with diffuse parenchymal lung disease evaluated for lung transplantation. Respir Med. 2005;99:1431-1439.
23. Nathan SD, Shlobin OA, Ahmad S, Urbanek S, Barnett SD. Pulmonary hypertension and pulmonary function testing in idiopathic pulmonary fibrosis. Chest. 2007;131:657-663.
24. Taskar VS, Coultas DB. Is idiopathic pulmonary fibrosis an environmental disease? Proc Am Thorac Soc. 2006;3:293-298.
25. Steele MP, Speer MC, Loyd JE, et al. Clinical and pathologic features of familial interstitial pneumonia. Am J Respir Crit Care Med. 2005;172:1146-1152.
26. Egan JJ, Stewart JP, Hasleton PS, Arrand JR, Carroll KB, Woodcock AA. Epstein-Barr virus replication within pulmonary epithelial cells in cryptogenic fibrosing alveolitis. Thorax. 1995;50:1234-1239.
27. Piccinelli AL, Salazar De Ariza J, Miranda RV, Mora SQ, Aquino R, Rastrelli L. Three new furostanol saponins from the leaves of Lycianthes synanthera ("Chomte"), an edible Mesoamerican plant. J Agric Food Chem. 2005;53:289-294.
28. Irving WL, Day S, Johnston ID. Idiopathic pulmonary fibrosis and hepatitis C virus infection. Am Rev Respir Dis. 1993;148:1683-1684.
29. Kuwano K, Nomoto Y, Kunitake R, et al. Detection of adenovirus E1A DNA in pulmonary fibrosis using nested polymerase chain reaction. Eur Respir J. 1997;10:1445-1449.
30. Maher TM, Wells AU, Laurent GJ. Idiopathic pulmonary fibrosis: multiple causes and multiple mechanisms? Eur Respir J. 2007;30:835-839.
31. Selman M, Pardo A. Idiopathic pulmonary fibrosis: an epithelial/fibroblastic cross-talk disorder. Respir Res. 2002;3:3.
32. Wynn TA. Cellular and molecular mechanisms of fibrosis. J Pathol. 2008;214:199-210.
33. Dorfmuller P, Perros F, Balabanian K, Humbert M. Inflammation in pulmonary arterial hypertension. Eur Respir J. 2003;22:358-363.
34. Humbert M, Monti G, Brenot F, et al. Increased interleukin-1 and interleukin-6 serum concentrations in severe primary pulmonary hypertension. Am J Respir Crit Care Med. 1995;151:1628-1631.
35. Sanchez O, Marcos E, Perros F, et al. Role of endothelium-derived CC chemokine ligand 2 in idiopathic pulmonary arterial hypertension. Am J Respir Crit Care Med. 2007;176:1041-1047.
36. Eddahibi S, Chaouat A, Tu L, et al. Interleukin-6 gene polymorphism confers susceptibility to pulmonary hypertension in chronic obstructive pulmonary disease. Proc Am Thorac Soc. 2006;3:475-476.

37. Savale L, Tu L, Rideau D, et al. Impact of interleukin-6 on hypoxia-induced pulmonary hypertension and lung inflammation in mice. Respir Res. 2009;10:6.
38. Dunsmore SE, Shapiro SD. The bone marrow leaves its scar: new concepts in pulmonary fibrosis. J Clin Invest. 2004;113:180-182.
39. Wynn TA. Fibrotic disease and the T(H)1/T(H)2 paradigm. Nat Rev Immunol. 2004;4:583-594.
40. Mowen KA, Glimcher LH. Signaling pathways in Th2 development. Immunol Rev. 2004;202:203-222.
41. Theofilopoulos AN, Koundouris S, Kono DH, Lawson BR. The role of IFN-gamma in systemic lupus erythematosus: a challenge to the Th1/Th2 paradigm in autoimmunity. Arthritis Res. 2001;3:136-141.
42. Liew FY. T(H)1 and T(H)2 cells: a historical perspective. Nat Rev Immunol. 2002;2:55-60.
43. Colonna M. Can we apply the TH1-TH2 paradigm to all lymphocytes? Nat Immunol. 2001;2:899-900.
44. Chakir H, Wang H, Lefebvre DE, Webb J, Scott FW. T-bet/GATA-3 ratio as a measure of the Th1/Th2 cytokine profile in mixed cell populations: predominant role of GATA-3. J Immunol Methods. 2003;278:157-169.
45. Meneghin A, Hogaboam CM. Infectious disease, the innate immune response, and fibrosis. J Clin Invest. 2007;117:530-538.
46. Zhu Z, Homer RJ, Wang Z, et al. Pulmonary expression of interleukin-13 causes inflammation, mucus hypersecretion, subepithelial fibrosis, physiologic abnormalities, and eotaxin production. J Clin Invest. 1999;103:779-788.
47. Huaux F, Liu T, McGarry B, Ullenbruch M, Phan SH. Dual roles of IL-4 in lung injury and fibrosis. J Immunol. 2003;170:2083-2092.
48. Jiang D, Liang J, Hodge J, et al. Regulation of pulmonary fibrosis by chemokine receptor CXCR3. J Clin Invest. 2004;114:291-299.
49. Keane MP, Belperio JA, Burdick MD, Strieter RM. IL-12 attenuates bleomycin-induced pulmonary fibrosis. Am J Physiol Lung Cell Mol Physiol. 2001;281:L92-97.
50. Luster AD. Chemokines--chemotactic cytokines that mediate inflammation. N Engl J Med. 1998;338:436-445.
51. Moser B, Loetscher P. Lymphocyte traffic control by chemokines. Nat Immunol. 2001;2:123-128.
52. Agostini C, Gurrieri C. Chemokine/cytokine cocktail in idiopathic pulmonary fibrosis. Proc Am Thorac Soc. 2006;3:357-363.
53. Gharaee-Kermani M, Denholm EM, Phan SH. Costimulation of fibroblast collagen and transforming growth factor beta1 gene expression by monocyte chemoattractant protein-1 via specific receptors. J Biol Chem. 1996;271:17779-17784.
54. Chung KF, Barnes PJ. Cytokines in asthma. Thorax. 1999;54:825-857.
55. Liu JY, Brass DM, Hoyle GW, Brody AR. TNF-alpha receptor knockout mice are protected from the fibroproliferative effects of inhaled asbestos fibers. Am J Pathol. 1998;153:1839-1847.
56. Kolb M, Margetts PJ, Anthony DC, Pitossi F, Gauldie J. Transient expression of IL-1beta induces acute lung injury and chronic repair leading to pulmonary fibrosis. J Clin Invest. 2001;107:1529-1536.

57. Piguet PF, Vesin C, Grau GE, Thompson RC. Interleukin 1 receptor antagonist (IL-1ra) prevents or cures pulmonary fibrosis elicited in mice by bleomycin or silica. Cytokine. 1993;5:57-61.
58. Whyte MK. Genetic factors in idiopathic pulmonary fibrosis: transforming growth factor-beta implicated at last. Am J Respir Crit Care Med. 2003;168:410-411.
59. Umezawa H, Maeda K, Takeuchi T, Okami Y. New antibiotics, bleomycin A and B. J Antibiot (Tokyo). 1966;19:200-209.
60. Razonable RR, Henault M, Paya CV. Stimulation of toll-like receptor 2 with bleomycin results in cellular activation and secretion of pro-inflammatory cytokines and chemokines. Toxicol Appl Pharmacol. 2006;210:181-189.
61. Embi N, Rylatt DB, Cohen P. Glycogen synthase kinase-3 from rabbit skeletal muscle. Separation from cyclic-AMP-dependent protein kinase and phosphorylase kinase. Eur J Biochem. 1980;107:519-527.
62. Frame S, Cohen P. GSK3 takes centre stage more than 20 years after its discovery. Biochem J. 2001;359:1-16.
63. Doble BW, Woodgett JR. GSK-3: tricks of the trade for a multi-tasking kinase. J Cell Sci. 2003;116:1175-1186.
64. Wang QM, Park IK, Fiol CJ, Roach PJ, DePaoli-Roach AA. Isoform differences in substrate recognition by glycogen synthase kinases 3 alpha and 3 beta in the phosphorylation of phosphatase inhibitor 2. Biochemistry. 1994;33:143-147.
65. Miller JR. The Wnts. Genome Biol. 2002;3:REVIEWS3001.
66. Cohen P, Frame S. The renaissance of GSK3. Nat Rev Mol Cell Biol. 2001;2:769-776.
67. Hoeflich KP, Luo J, Rubie EA, Tsao MS, Jin O, Woodgett JR. Requirement for glycogen synthase kinase-3beta in cell survival and NF-kappaB activation. Nature. 2000;406:86-90.
68. Richmond A. Nf-kappa B, chemokine gene transcription and tumour growth. Nat Rev Immunol. 2002;2:664-674.
69. Ali A, Hoeflich KP, Woodgett JR. Glycogen synthase kinase-3: properties, functions, and regulation. Chem Rev. 2001;101:2527-2540.
70. Steinbrecher KA, Wilson W, 3rd, Cogswell PC, Baldwin AS. Glycogen synthase kinase 3beta functions to specify gene-specific, NF-kappaB-dependent transcription. Mol Cell Biol. 2005;25:8444-8455.
71. Martin M, Rehani K, Jope RS, Michalek SM. Toll-like receptor-mediated cytokine production is differentially regulated by glycogen synthase kinase 3. Nat Immunol. 2005;6:777-784.
72. Hu X, Paik PK, Chen J, et al. IFN-gamma suppresses IL-10 production and synergizes with TLR2 by regulating GSK3 and CREB/AP-1 proteins. Immunity. 2006;24:563-574.
73. Stambolic V, Ruel L, Woodgett JR. Lithium inhibits glycogen synthase kinase-3 activity and mimics wingless signalling in intact cells. Curr Biol. 1996;6:1664-1668.
74. Ilouz R, Kaidanovich O, Gurwitz D, Eldar-Finkelman H. Inhibition of glycogen synthase kinase-3beta by bivalent zinc ions: insight into the insulin-mimetic action of zinc. Biochem Biophys Res Commun. 2002;295:102-106.
75. Ryves WJ, Dajani R, Pearl L, Harwood AJ. Glycogen synthase kinase-3 inhibition by lithium and beryllium suggests the presence of two magnesium binding sites. Biochem Biophys Res Commun. 2002;290:967-972.

76. Meijer L, Flajolet M, Greengard P. Pharmacological inhibitors of glycogen synthase kinase 3. Trends Pharmacol Sci. 2004;25:471-480.
77. Cover TL, Tummuru MK, Cao P, Thompson SA, Blaser MJ. Divergence of genetic sequences for the vacuolating cytotoxin among Helicobacter pylori strains. J Biol Chem. 1994;269:10566-10573.
78. Graham DY. Helicobacter pylori: its epidemiology and its role in duodenal ulcer disease. J Gastroenterol Hepatol. 1991;6:105-113.
79. Megraud F, Lamouliatte H. Helicobacter pylori and duodenal ulcer. Evidence suggesting causation. Dig Dis Sci. 1992;37:769-772.
80. Parsonnet J, Friedman GD, Vandersteen DP, et al. Helicobacter pylori infection and the risk of gastric carcinoma. N Engl J Med. 1991;325:1127-1131.
81. Wick MJ, Madara JL, Fields BN, Normark SJ. Molecular cross talk between epithelial cells and pathogenic microorganisms. Cell. 1991;67:651-659.
82. Mai UE, Perez-Perez GI, Allen JB, Wahl SM, Blaser MJ, Smith PD. Surface proteins from Helicobacter pylori exhibit chemotactic activity for human leukocytes and are present in gastric mucosa. J Exp Med. 1992;175:517-525.
83. Mai UE, Perez-Perez GI, Wahl LM, Wahl SM, Blaser MJ, Smith PD. Soluble surface proteins from Helicobacter pylori activate monocytes/macrophages by lipopolysaccharide-independent mechanism. J Clin Invest. 1991;87:894-900.
84. Kurose I, Granger DN, Evans DJ, Jr., et al. Helicobacter pylori-induced microvascular protein leakage in rats: role of neutrophils, mast cells, and platelets. Gastroenterology. 1994;107:70-79.
85. Olivieri R, Bugnoli M, Armellini D, et al. Growth of Helicobacter pylori in media containing cyclodextrins. J Clin Microbiol. 1993;31:160-162.
86. Weitzman SA, Gordon LI. Inflammation and cancer: role of phagocyte-generated oxidants in carcinogenesis. Blood. 1990;76:655-663.
87. Wotherspoon AC, Doglioni C, Diss TC, et al. Regression of primary low-grade B-cell gastric lymphoma of mucosa-associated lymphoid tissue type after eradication of Helicobacter pylori. Lancet. 1993;342:575-577.
88. Yoshida N, Granger DN, Evans DJ, Jr., et al. Mechanisms involved in Helicobacter pylori-induced inflammation. Gastroenterology. 1993;105:1431-1440.
89. Evans DJ, Jr., Evans DG, Takemura T, et al. Characterization of a Helicobacter pylori neutrophil-activating protein. Infect Immun. 1995;63:2213-2220.
90. Menegazzi R, Zabucchi G, Zuccato P, Cramer R, Piccinini C, Patriarca P. Oxidation of homovanillic acid as a selective assay for eosinophil peroxidase in eosinophil peroxidase-myeloperoxidase mixtures and its use in the detection of human eosinophil peroxidase deficiency. J Immunol Methods. 1991;137:55-63.
91. Namavar F, Sparrius M, Veerman EC, Appelmelk BJ, Vandenbroucke-Grauls CM. Neutrophil-activating protein mediates adhesion of Helicobacter pylori to sulfated carbohydrates on high-molecular-weight salivary mucin. Infect Immun. 1998;66:444-447.
92. Phadnis SH, Parlow MH, Levy M, et al. Surface localization of Helicobacter pylori urease and a heat shock protein homolog requires bacterial autolysis. Infect Immun. 1996;64:905-912.
93. Teneberg S, Miller-Podraza H, Lampert HC, et al. Carbohydrate binding specificity of the neutrophil-activating protein of Helicobacter pylori. J Biol Chem. 1997;272:19067-19071.

94. Grant RA, Filman DJ, Finkel SE, Kolter R, Hogle JM. The crystal structure of Dps, a ferritin homolog that binds and protects DNA. Nat Struct Biol. 1998;5:294-303.
95. Peitsch MC, Wells TN, Stampf DR, Sussman JL. The Swiss-3DImage collection and PDB-Browser on the World-Wide Web. Trends Biochem Sci. 1995;20:82-84.
96. Tonello F, Dundon WG, Satin B, et al. The Helicobacter pylori neutrophil-activating protein is an iron-binding protein with dodecameric structure. Mol Microbiol. 1999;34:238-246.
97. D'Elios MM, Amedei A, Cappon A, Del Prete G, de Bernard M. The neutrophil-activating protein of Helicobacter pylori (HP-NAP) as an immune modulating agent. FEMS Immunol Med Microbiol. 2007;50:157-164.
98. Satin B, Del Giudice G, Della Bianca V, et al. The neutrophil-activating protein (HP-NAP) of Helicobacter pylori is a protective antigen and a major virulence factor. J Exp Med. 2000;191:1467-1476.
99. Strachan DP. Hay fever, hygiene, and household size. Bmj. 1989;299:1259-1260.
100. Herz U, Lacy P, Renz H, Erb K. The influence of infections on the development and severity of allergic disorders. Curr Opin Immunol. 2000;12:632-640.
101. Wohlleben G, Erb KJ. Atopic disorders: a vaccine around the corner? Trends Immunol. 2001;22:618-626.
102. Codolo G, Mazzi P, Amedei A, et al. The neutrophil-activating protein of Helicobacter pylori down-modulates Th2 inflammation in ovalbumin-induced allergic asthma. Cell Microbiol. 2008;10:2355-2363.
103. Amedei A, Cappon A, Codolo G, et al. The neutrophil-activating protein of Helicobacter pylori promotes Th1 immune responses. J Clin Invest. 2006;116:1092-1101.
104. Oppmann B, Lesley R, Blom B, et al. Novel p19 protein engages IL-12p40 to form a cytokine, IL-23, with biological activities similar as well as distinct from IL-12. Immunity. 2000;13:715-725.
105. Trinchieri G. Interleukin-12 and the regulation of innate resistance and adaptive immunity. Nat Rev Immunol. 2003;3:133-146.
106. Del Prete G, Chiumiento L, Amedei A, et al. Immunosuppression of TH2 responses in Trichinella spiralis infection by Helicobacter pylori neutrophil-activating protein. J Allergy Clin Immunol. 2008;122:908-913 e905.
107. Smith DG, Buffet M, Fenwick AE, et al. 3-Anilino-4-arylmaleimides: potent and selective inhibitors of glycogen synthase kinase-3 (GSK-3). Bioorg Med Chem Lett. 2001;11:635-639.
108. Goodman HMaM, R.J. . Cloning of hormone genes from a mixture of cDNA molecules. Meth Enzymol. 1979;68:75–90.
109. Chapman HA. Disorders of lung matrix remodeling. J Clin Invest. 2004;113:148-157.
110. Reynolds HY, Gail DB, Kiley JP. Interstitial lung diseases--where we started from and are now going. Sarcoidosis Vasc Diffuse Lung Dis. 2005;22:5-12.
111. Shen AS, Haslett C, Feldsien DC, Henson PM, Cherniack RM. The intensity of chronic lung inflammation and fibrosis after bleomycin is directly related to the severity of acute injury. Am Rev Respir Dis. 1988;137:564-571.

112. Ryu JH, Krowka MJ, Pellikka PA, Swanson KL, McGoon MD. Pulmonary hypertension in patients with interstitial lung diseases. Mayo Clin Proc. 2007;82:342-350.
113. Etienne-Manneville S, Hall A. Cdc42 regulates GSK-3beta and adenomatous polyposis coli to control cell polarity. Nature. 2003;421:753-756.
114. Eickholt BJ, Walsh FS, Doherty P. An inactive pool of GSK-3 at the leading edge of growth cones is implicated in Semaphorin 3A signaling. J Cell Biol. 2002;157:211-217.
115. Bazzoni G, Tonetti P, Manzi L, Cera MR, Balconi G, Dejana E. Expression of junctional adhesion molecule-A prevents spontaneous and random motility. J Cell Sci. 2005;118:623-632. Epub 2005 Jan 2018. Write to the Help Desk NCBI | NLM | NIH Department of Health & Human Services Privacy Statement | Freedom of Information Act | Disclaimer Sep 2005 2006 2008:2010:2000.
116. Farooqui R, Zhu S, Fenteany G. Glycogen synthase kinase-3 acts upstream of ADP-ribosylation factor 6 and Rac1 to regulate epithelial cell migration. Exp Cell Res. 2006;312:1514-1525.
117. Coker RK, Laurent GJ. Pulmonary fibrosis: cytokines in the balance. Eur Respir J. 1998;11:1218-1221.
118. Wallace WA, Ramage EA, Lamb D, Howie SE. A type 2 (Th2-like) pattern of immune response predominates in the pulmonary interstitium of patients with cryptogenic fibrosing alveolitis (CFA). Clin Exp Immunol. 1995;101:436-441.
119. Furuie H, Yamasaki H, Suga M, Ando M. Altered accessory cell function of alveolar macrophages: a possible mechanism for induction of Th2 secretory profile in idiopathic pulmonary fibrosis. Eur Respir J. 1997;10:787-794.
120. Majumdar S, Li D, Ansari T, et al. Different cytokine profiles in cryptogenic fibrosing alveolitis and fibrosing alveolitis associated with systemic sclerosis: a quantitative study of open lung biopsies. Eur Respir J. 1999;14:251-257.
121. Till SJ, Francis JN, Nouri-Aria K, Durham SR. Mechanisms of immunotherapy. J Allergy Clin Immunol. 2004;113:1025-1034; quiz 1035.